D-MEM
PhD-UNIMI

Doctorate program
Milan
EXPERIMENTAL
MEDICINE

Università degli Studi di Milano

PhD Course in
Experimental Medicine

CYCLE XXXIV

PhD thesis

Hedgehog/HDAC6 inhibition and chemotherapy: assessment of new drug combination in acute myeloid leukemia

---

Candidate: **Dr. Alex Pezzotta**

Matr. R12198

Tutor: **Prof./Dr. Anna Pistocchi**

Supervisor (if available): **Dr. Alberto Rissone**

Director: **Prof. Nicoletta Landsberger**

Academic Year 2021-2022

Summary

ABSTRACT

In Acute Myeloid Leukemia (AML), the dysregulation of the *Hh* signaling is involved in the development and expansion of leukemic cancer cells and influences the response to therapeutic agents. Notably, the FDA approved only one *Hh* inhibitor (glasdegib) as a therapeutic strategy for AML treatment, and the majority of patients eventually relapse, underlying the urgency of discovering new therapeutic targets. One characteristic of the *Hh* pathway is its localization on the primary cilium membrane (PC), a microtubule-based organelle expressed by almost all non-proliferating mammalian cells. Indeed, centrosomes participate in a mutually exclusive manner in the formation of PC or mitotic spindle. Cancer cells, including AML cell lines, are characterized by a high rate of proliferation and fail to present the PC on their surface. Novel approaches to restore the PC on the surface of cancer cells are emerging, and most of them target the histone deacetylase HDAC6. Indeed, HDAC6 inhibition prevents the reabsorption of the PC and blocks cell proliferation. Since HDAC6 inhibitors (i.e., TubastatinA) are already used to treat other tumors, they might also be promising in AML treatment. In this work, analyzing the blood samples of 36 adult AML patients, we demonstrated that *Hh* target genes (*GLI1, PTCH1*), *HDAC6*, and the Multi-Drug-Resistant genes (*MDRs*) *ABCC1* and *ASXL1* were more expressed than in healthy donors (HD). In addition, through *in silico* analyses, we verified that in AML patients the expression of *Hh/HDAC6* and *MDRs* genes were positively correlated. We also detected the same genetic regulation in *in vitro* models of AML, as cell lines with higher *Hh* expression (U937 and THP-1) showed higher levels of *HDAC6* and *MDRs* than cell lines with low *Hh* expression (NB-4 and OCI-AML2). We generated a zebrafish model with *Hh* hyperactivation through the injection of the *shh* mRNA to functionally investigate the effect of *Hh/HDAC6* dysregulation, and we confirmed the increased expression of *hdac6* and *MDRs*.

Moreover, in the zebrafish reporter line for the hematopoietic stem precursor cells (HSPCs) the *Tg(CD41:GFP)* line, we found that *Hh* hyperactivation induces the hyperproliferation and expansion of the HSPCs in the caudal hematopoietic tissue, a phenotype that resembles the expansion of leukemic blast of AML patients. Interestingly, we rescued this hematopoietic defect by treating the embryos with the HDAC6 inhibitor TubastatinA but not with the *Hh* inhibitor cyclopamine. By the generation of a zebrafish model carrying the overexpression of the human *HDAC6* mRNA, we demonstrated that HDAC6 alone can induce the hyperproliferation of the HSPCs population and that this phenotype is specific as, through its inhibition, we rescued the hematopoietic defect. Since we observed that an increased proliferation rate elicited the expansion of HSPCs, we hypothesized an implication

of the PC. Indeed, we demonstrated that zebrafish HSPCs present the PC, therefore suggesting that HDAC6 controls HSPCs proliferation, through PC's stabilization on their surface. For the first time, we described a role for HDAC6 in HSPCs expansion and identified it as a promising target for AML patients. Indeed, HDAC6 inhibition was also efficient in reducing the viability of leukemic cell lines and HSPCs expansion in well-established AML zebrafish models, carrying the overexpression of genes frequently mutated in AML patients: *NPMc+* and *FLT3-ITD*. Moreover, in these zebrafish models, we demonstrated the efficacy of combination therapy with the standard chemotherapeutic agent cytarabine and HDAC6 inhibition.

In conclusion, we identified a positive correlation between the *Hh* signaling, *HDAC6* and the *MDR* genes in AML patients. In the zebrafish model, we reported that both *Hh* or *HDAC6* overexpression drive the hyperproliferation of the HSPCs population, a phenotype that is rescued only through HDAC6 inhibition. HSPCs hyperproliferation and the rescue through the specific HDAC6 inhibition, might be explained by alteration in the PC, that we described to present in the HSPCs. As reporter for *Hh* inhibition, we demonstrated that also HDAC6 inhibition efficiently reduces the expression of *MDR* genes. Therefore, we hypothesize the use of HDAC6 inhibitor to counteract AML resistance mechanisms. Finally, we described that HDAC6 inhibition shows high potency in specific AML condition, and that can be a suitable target for the assessment of new combination therapies with standard chemotherapic agents.

DISCLOSURE OF RESEARCH INTEGRITY

We performed the experimental plan under the fundamental principles of research integrity (reliability, honesty, respect, accountability) in a context (University of Milan) which promotes the knowledge and the divulgation of the European Code of Conduct for Research Integrity. Dr. Alex Pezzotta and other researchers involved in the experimental procedures have been carefully informed on the basic principle of research integrity and received the proper training. Dr. Alex Pezzotta's supervisors and senior researchers mentor him and all the other team members, offering specific guidance and training to develop research activity following the culture of research integrity properly. The experimental designs and the methodological procedure have been clearly defined before the onset of the experiments accordingly to the state of art, to avoid the waste of public funding and the unnecessary use of biological samples.

We handled human and *in vitro* research samples with respect and care under National and International Guidance. Indeed, we used the *in vivo* zebrafish model system according to the national guidelines (Italian decree March 4, 2014, n. 26). Similarly, patients' material was collected after obtaining informed consent (protocol ASGMA-052A approved on May 8th, 2012 by Azienda San Gerardo) and was handled according to the Declaration of Helsinki.

We used all the collected data to generate a paper that we have submitted to a peer-review open access journal. Also, preliminary results not shown in the thesis were included and fruitfully revised in the discussion section.

All the decisions have been taken according to legal, ethical, and scientific understanding, carefully considering the implication of the research activity on the scientific community and society.

ABBREVIATIONS

AGM: aorta-gonad-mesonephric

AIRTUM: Associazione Italiana registro Tumori

ALM: anterior lateral mesoderm

AML: Acute Myeloid Leukemia

ATO: Arsenic trioxide

BCC: Basal cell carcinoma

CD: Catalytic domain

cebp1: CCAAT/enhancer binding protein 1

CHT: Caudal hematopoietic tissue

CLL: Chronic lymphocytic leukemia

CYLD: cylindromatosis

DHh: Desert hedgehog

DISP: Dispatched

ER: endoplasmic reticulum

etsrp: ETS-related protein

FAB: French-American-British

GBM: Glioblastoma

GLI-A: Glioma associated oncogenes active form

Gli-R: Glioma associated oncogenes repressive form

GLI: Glioma associated oncogenes

GPCRs: G-coupled receptors

HAAT: O-acyltransferase

HAT: Histone acetyltransferases

HDAC: Histone deacetylase

HDACi: HDAC inhibitors

Hh: Hedgehog

HhC: C-terminal Hog domain

HhN: N-terminal Hedge domain

HSPC: Hematopoietic and progenitor stem cells

ICM: intermediate cell mass

IDH: Isocitrate dehydrogenase

IHh: Indian hedgehog

LC: leukemic cancer cells

lmo2: LIM domain only 2

MB: Medulloblastoma

MDR: Multi-drug-resistance

MM: Multiple myeloma

mpeg1: macrophage-expressed 1

NES: nuclear export sequence

NLS: nuclear localization signal

NPM1: Nucleophosmin1

PC: Primary cilium

PDAC: pancreatic adenocarcinoma

PkA: Protein kinase A

PLM: posterior lateral mesoderm

PTCH: Patched

RBI: Rostral blood island

SE14: Serine/glutamate-rich repeat motif

SHh: Sonic hedgehog

SMO: Smoothened

SUFU: Suppressor of fused

TAD: transactivation domain

TF: Transcription factors

WHO: Word Health Organization

ZnF-UBP: ubiquitin zinc-dependent domain

ZNF: zinc-finger

INTRODUCTION

1 THE HEDGEHOG SIGNALING

1.1 *Hedgehog* signaling pathway: a general overview

The *Hedgehog* (*Hh*) signaling pathway was firstly described in *Drosophila melanogaster* and, at least of some differences, is conserved among vertebrates (1).

During normal development the *Hh* pathway plays pivotal roles in different processes controlling the expression of genes involved in cell cycle and proliferation, apoptosis and stem cell renewal (2). The abnormal activation of the *Hh* signaling has been linked to the development of different cancer forms such as medulloblastoma (MB), rhabdomyosarcoma, melanoma, basal cell carcinoma (BCC), glioblastoma (GBM), and breast, lung, liver, stomach, prostate, and pancreatic tumors (3) (4) (5). Moreover, as the *Hh* signaling is an important modulator of nervous system development, it is not surprising its link with the development of neurodegenerative disorders (6).

Several mutations are responsible for the pathogenicity of these disease: loss-of-function mutations are mainly found in neurodegenerative disorders while those of overexpression are causative of tumors (7). However, the significance of these mutations in terms of silencing or upregulation of the *Hh* signaling, depends on which component of the *Hh* pathway is affected by the mutation. Indeed, differently from other molecular mechanisms, the pathway is composed of a series of inhibitory events (8) (Fig.1). When *Hh* ligands are not present, the transmembrane receptor Patched (PTCH) sustains the inhibition of the signaling by suppressing the activity of the *G-coupled-receptor* (GPCR) Smoothened (SMO). In this condition, the Suppressor of Fused (SUFU) and the protein kinase A (PkA) block the processing of the full-length form of the *glioma associated oncogenes* Gli2/3 transcription factors (referred as GLI-fl) into their active forms (GLI-A). Once the *Hh* ligands bind to the receptor these inhibitory reactions are abrogated, promoting the formation of the GLI-A proteins that enter the nucleus and drive the transcription of target genes (9).

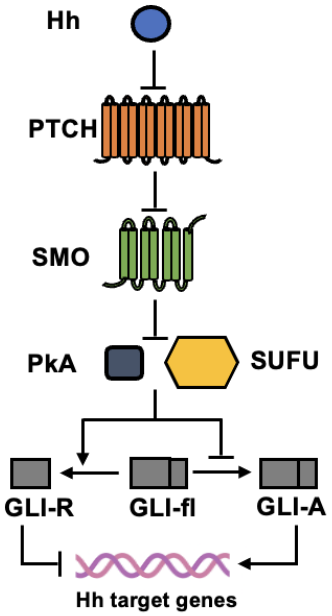

Fig.1: Overview of the *Hh* signaling pathway. When the *Hh* ligands did not bind the Patched (PTCH) receptors, the full-length form of the GLI family of transcription factors is processed and converted into the repressive forms (GLI-R) to inhibit the transcription of target genes. The binding of the *Hh* proteins PTCH relieves the Smoothened (SMO) inhibition, the signaling is transmitted toward the cells, and the proteins kinase A (PkA) and SUFU, are blocked. GLI transcription factors are not processed and, in their active forms (GLI-A) enter the nucleus and drive the transcription of target genes.

Given the role of the *Hh* signaling pathway in both normal and pathological conditions, and because of the complexity of its signaling transduction, it becomes crucial to focus on its components and its regulation.

1.2 Synthesis and secretion of the *Hh* ligands

The activation of the *Hh* signaling pathway in *D. melanogaster* is mediated by the action of one secreted ligand while in vertebrates, three *Hh* proteins, named Desert Hh (DHh), Indian Hh (IHh), and Sonic Hh (SHh), drive the transmission of the signaling (10). SHh is the most studied among the vertebrate's ligands, as it is involved in the morphogenesis and patterning of different organs (11). For instance, during embryogenesis, SHh controls the patterning of the left-right and dorso-ventral axis of the embryo, and the formation of the distal elements of the limbs (12).

The synthesis of the *Hh* ligands starts with the production of a 45 KDa precursor composed of two major domains: a secreted N-terminal Hedge domain (HhN) and a C-terminal Hog domain (HhC). The last shares features with the Inteins Family of protein and shows autocatalytic properties that are essential during the ligands' maturation (13). Indeed, once synthetized, the *Hh* proteins are transported into the endoplasmic reticulum (ER) and Golgi apparatus, becoming the substrates of proteolytic processes and post-translational modification (13) (Fig.2). Into the ER, after removal of the signal peptide, the *Hh* proteins undergo to an autocleavage mediated by the HhC domain. The HhN domain results in a C-terminus with an ester-linked cholesterol moiety and an N-terminus subsequently modified by the ER membrane-bound O-acyltransferase HAAT through the attachment of palmitate (14) (Fig.2). Together, these modifications generate dually lipidated and mature *Hh* ligands and are essential to ensure their correct transport inside and outside the cells and their signaling activity (15). However, these modifications increase the molecules' hydrophobic properties indicating that *Hh* proteins do not simply cross the plasma membrane but are transported in a process mediated by membrane-associated proteins (Fig2). Indeed, the 12-pass membrane protein Dispatched (DISP), and the Scube family of proteins cooperate to accomplish *Hh* secretion, recognizing different parts of the cholesterol moiety (9). Other mechanisms have been proposed to explain the *Hh* release ranging from lipoprotein or exosome-mediated release to multimers formation (9) (Fig.2).

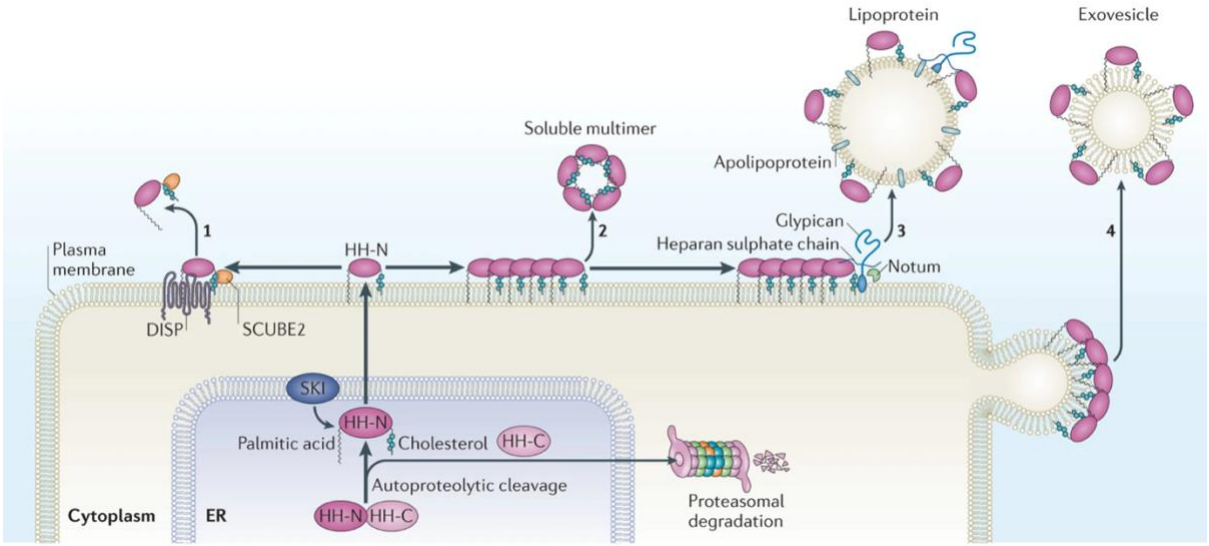

Fig.2: Synthesis and release of the Hh ligands. The 45 KDa precursor of the *Hh* ligands is transported into the ER where the HhC domain mediates the cleavage of the protein. The HhN domain is released, attached to a cholesterol moiety and subsequently modified by the

HAAT enzyme through the bind of palmitate. The HhC domain is then proteolytically degraded via proteasome while the modified HhN domain reaches the plasma membrane where can be secreted through different mechanisms. 1) The ligands are release by the cooperative action of the transmembrane protein Dispatched (DISP) and SCUBE. 2) HhN monomers can associate to form soluble multimers that are then secreted by the cell. 3) HhN oligomers, which form spontaneously, can interact with the glypican inserted into the plasma membrane and assembled into lipoparticles. 4) HhN can be released through the exosomes. Modified from Briscoe et al (9).

2 THE PRIMARY CILIUM

2.1 The primary cilium structure and function

The primary cilium (PC) is a subtle organelle found on the surface of almost all cell types. This structure is formed mainly in quiescent or non-proliferating cells (typically G0 or G1 phase) (16). The cilium is anchored to the plasma membrane by the basal body, a structure derived from the mother centriole of the centrosome (17). Therefore, due to the role of the centrosome in the formation of the mitotic spindle, there is an inverse correlation between the presence of the PC and cell division (18). The basal body, composed of 9 triplets of γmicrotubules, is the scaffold for the axoneme of the PC. Within the axoneme, α/β microtubules form a radial array of 9 doublets. Differently from motile cilia, the axoneme of the PC lacks the central pair of microtubules and the dynein motors, conferring to the structure its immobility (19).

2.2 The *Hh* signaling transduction within the PC

The PC in vertebrates sustains the *Hh* signaling transduction, as in the ciliary membrane are located all the components involved in the transmission of the signaling (20). The role of the PC in the *Hh* signaling transduction is reflected by the dynamic repositioning of the *Hh* components within the ciliary membrane. Indeed, in the absence of the *Hh* ligands, the PTCH receptors mainly localize in the membrane of the PC, SMO is retained in cytoplasmatic endosomes and the GLI transcription factors are converted into their repressive forms (9) (Fig.3). The 3D structure of the protein has clarified the molecular mechanism by which PTCH inhibits the signaling transduction. Cryo-electron microscopy sections revealed that PTCH contains a sterol-sensing-domain (SSD) that shares homology with proteins involved in the transport of cholesterol (21). Mutations in the SSD domain

completely abrogate the PTCH-mediated repression of SMO, suggesting that PTCH might inhibit the *Hh* signaling transduction modulating the abundance of sterol derivatives SMO activators (22). However, unlike other G-coupled receptors (GPCR), no ligand-binding function has been described for SMO even if some sterol-like molecules bind to its transmembrane domain, influencing its activity and stability (22). Cholesterol has been proposed as the putative SMO activator even if more detailed studies must be conducted. A different mechanism of inhibition suggests that PTCH might influence the movement of the endosomes through which SMO is trafficked or control the endosomes composition (13). Upon PTCH-mediated SMO inhibition, the entire pathway is kept-off and in the cytoplasm, the GLI transcription factors are post-translational modified by the action of different kinases. Indeed, when the *Hh* ligands are not present, the PkA is activated and, together with GSK3β and CKI, triggers the phosphorylation of the full-length form of the GLI transcription factors (TF; GLI-fl) (23). These phosphorylation events generate a binding site for the βTrCP protein which recruits the E3 ubiquitin ligase complex that, in turn, mediates the processing of the GLI-fl into their repressive forms (24). The relationship between PkA and *Hh* signaling is well established as the increase of PkA activity inhibits the signaling transduction while its downregulation exerts the opposite effect (25). In vertebrates, GPCR receptors regulate PKA activity. For instance, GPCR161 localizes into the PC membrane in the absence of the *Hh* ligands and stimulates the production of the cAMP, the main regulator of PkA activity (26). Another mechanism by which cells keep *Hh* signaling off is through the action of the Sufu protein. When the *Hh* ligands are not present, Sufu binds to GLI-fl proteins and sequesters them in a complex with the cilium kinesin-associated protein KIF7 (27), facilitating the phosphorylations exerted by the PkA. Moreover, SUFU competes with Importin-β1 for the binding of the eventually present GLI-A forms, interfering with their transport into the nucleus (28). Interestingly, SUFU can also recruit the HDAC corepressor complexes inhibiting the transcription of *Hh* target genes (29).

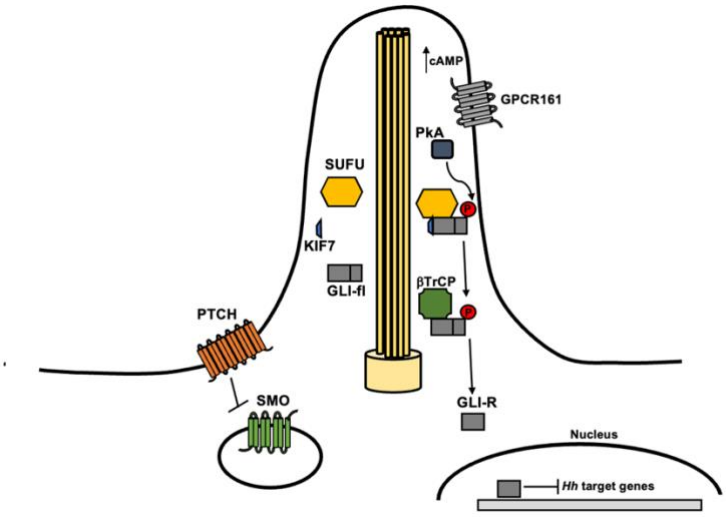

Fig.3: Inhibition of the *Hh* signaling. In the absence of *Hh* ligands, Patched (PTCH) is inserted in the PC membrane and inhibits Smoothened (SMO), which is found in endosomes. GLI transcription factors (GLI-fl), anchored to the anterograde kinesin-like motor protein KIF7 are transported to SUFU and phosphorylated by the protein kinase A (PkA) and other kinases. GPCR161 receptor increases the production of cAMP at the primary cilia resulting in the activation of PkA. Once phosphorylated, GLI-fl are partially degraded by the βTrCP complex into their repressive forms (GLI-R).

Once bound by the *Hh* ligands, the cell undergoes to a redistribution of the *Hh* component within the PC (Fig.4), starting with the transport of PTCH into endosome and its degradation (30). The internalization and degradation of PTCH is an event mediated by glypicans as they enhance the stability of the *Hh* ligands. Indeed, mutations in these membrane components reduced *Hh* signaling potency (9). Interestingly, *Hh* ligands can also modulate PTCH activity without inducing its degradation (31). This dual regulation relies on structural evidence that indicates the ability of *Hh* proteins to bind simultaneously to two PTCH receptors, inducing their removal from the ciliary membrane and the degradation of one of them, whit the consequent block of the sterol transposing function of the second (30). The presence of a multimolecular complex also facilitates the binding of the *Hh* ligands to PTCH receptors. Indeed, in vertebrates, it has been demonstrated that this complex, which includes the Cam-related/downregulated by oncogenes (CDO), the brother of CDO (BOC) and GA1 (growth arrest specific 1), increases the affinity of the *Hh*/PTCH interface (32). As PTCH is removed from the membrane of the PC, the G-protein coupled receptor SMO translocates into the ciliary membrane and drives the transmission of the signaling toward the cell (Fig.4). The

real mechanism of SMO activation is not entirely understood, even if evidence suggests that the active form of SMO is able to counteract PkA activity. This is accomplished through the Smo-mediated extrusion from the PC of the GPCR161 (33) (Fig.4). However, more detailed studies must be conducted to determine how SMO mediates the removal of GPCR16 from the ciliary membrane.

Following *Hh* stimulation, the SUFU-GLI complexes moved to the tip of the PC where they dissociate, with the consequent release of the GLI-fl. Moreover, given its important regulatory role, SUFU is ubiquitinated and degraded via proteasome (34). With SMO activation, the GLI proteins, not phosphorylated by PkA and not processed by the βTrCP complex, enter the nucleus and drive the transcription of *Hh* target genes.

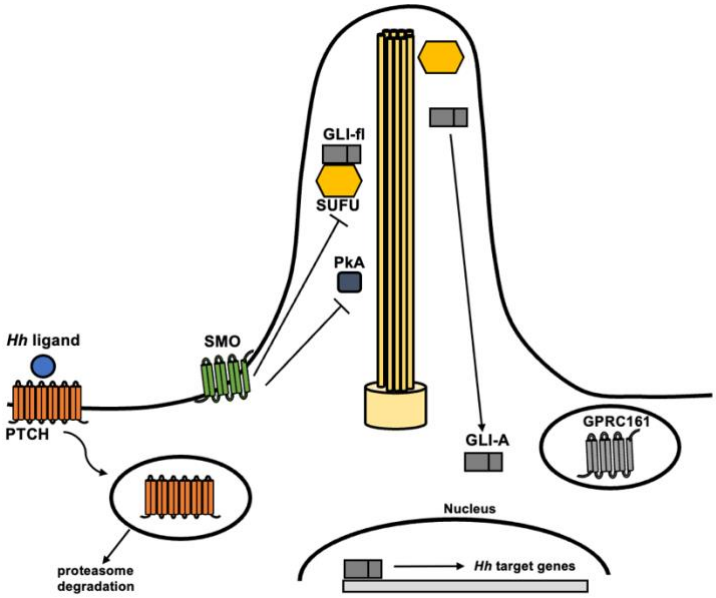

Fig.4: Activation of the *Hh* signaling. Once bound by the *Hh* ligands, the Patched (PTCH) receptor is internalized and degraded, while Smoothened (SMO) translocates in the cilium and counteracts PkA and SUFU activity. At the same time, the GPCR161 receptor is internalized with consequent reduction of the PkA activity. At the tip of the cilium, GLI-fl dissociates from SUFU and can enter the nucleus in its active form, driving the transcription of *Hh* target genes.

Ultimately, the *Hh* signaling transduction regulates the GLI protein activity, changing the balance between the activator and repressor forms. GLI proteins belong to the GLI-Kruppel family of zinc-finger (ZNF) containing transcription factors (35). In vertebrates, three GLI proteins (GLI 1, GLI 2, GLI 3) have been identified and, although the DNA binding site shows

high similarity, they activate target genes in a context-dependent manner. For instance, epigenetic changes in the regulatory regions of target genes might affect the transcriptional output (36). All GLI TFs contain a nuclear export sequence (NES) and a nuclear localization signal (NLS) that mediate their nucleo-cytoplasmic shuttling (8) and a C-terminal transactivation domain (TAD). They also possess a SUFU-interacting domain responsible for SUFU-mediated cytoplasmic retention. GLI2 and GLI3 contain a second SUFU-interacting site required to inhibit GLI transcriptional activity in the nucleus and a N-terminal repressor domain that allows them to function as both transcriptional activators and repressors, depending on the cellular context (12). Differently, GLI1 functions only as an activator, instituting, therefore a positive feedback-loop (13).

2.3 Non canonical *Hh* signaling

Besides the classical canonical ligand-PTCH-SMO axis, non-canonical mechanisms, which lead to the transcription of the *Hh* target genes independently to SMO, have been proposed. These mechanisms mainly derive from the activation of different oncogenic signaling, such as the *RAS-RAF-MEK-ERK* signaling pathways (37). Indeed, constitutive activation of MEK1 increases the activity of GLI1 with consequent up-regulation of *Hh* target genes. This positive feedback depends on a region within the GLI1 proteins, able to sense the status of the *ERK1/2* signaling (38). Moreover, a putative consensus site for MEK was identified in the N-terminus of GLI2/3 (39). The link between the non-canonical *Hh* and the RAS signaling pathways has been identified in different cancer forms. For instance, in human pancreatic adenocarcinoma (PDAC) cells, oncogenic kRAS increases GLI1 protein levels and activity, independently to the canonical *Hh* pathway (40). Similarly, the RAS pathway increases *GLI1* and *GLI2* mRNA and protein levels in colon cancer cells (41).

Also, the *PI3K-AKT-mTOR* signaling can enhance the *Hh* signaling transduction independently to SMO activation. Indeed, activation of *PI3K-AKT* signaling enhances GLI1 protein stability in pancreatic and ovarian cancer and in anaplastic large cell lymphoma (ALCL), blocking GLI1 phosphorylation and degradation (42). In addition, this signaling increases GLI1 transcriptional activity and nuclear translocation in melanoma and prostate cancer, and glioma cells (37).

3 ACUTE MYELOID LEUKEMIA

3.1 Acute myeloid leukemia: general features

Acute Myeloid Leukemia (AML) comprises a group of hematological disorders characterized by the presence of genetic and epigenetic alterations in the hematopoietic and progenitor stem cells (HSPC) (43). These events lead to the accumulation of undifferentiated myeloid cells, named leukemic blasts, defective in their proliferation and differentiation processes (44). Despite the achievement of complete remission, most patients develop resistance to standard chemotherapies and relapse.

AML can evolve in patients with hematological disorders (i.e., myeloid dysplastic syndrome) even though most cases appear *de novo* in healthy individuals (45).

Depending on the etiology, genetics, immune-phenotype, and blasts morphology, there are different classification systems for AML. The last edition of the World Health Organization (WHO) classification published in 2017, classified AML into six categories: AML with recurrent genetic abnormalities; AML with myelodysplasia-related changes; therapy-related myeloid neoplasms; AML, not otherwise specified; myeloid sarcoma; and AML linked to Down syndrome (46). The genetic profile of AML blasts allows the stratification of patients into three classes according to favorable, intermediate, and unfavorable prognosis. Indeed, patients with t(8;21) (q22;q22) [RUNX1/RUNX1T1], inv(16)(p13q22) [CBFB/MYH11] and t(15;17)(q24;q21) [PML/RARA] show a good response to chemotherapy treatment with the achievement of complete remissions (47). On the contrary, patients with t(6;9)(p23;q34) [DEK/NUP214], inv(3)(q21q26) [RPN1/EVI1] and t(1;22)(p13;q13) [RBM15/MKL1] are poor responders to common chemotherapy agents, with consequent unfavorable prognosis (47). The advances in the next generation sequencing (NGS) identified mutations in new genes with a high impact on the prognosis of patients characterized by normal karyotypes, such as somatic mutation in the *FLT3* and the *NPM1* genes (48). *FLT3* and *NPM1* mutations are late-occurring events in the development of AML and can be considered as markers for *de novo* AML (49). Nucleophosmin1 (NPM1) is a ubiquitously expressed phosphoprotein that primarily localized at the nucleoli with continuous shuttling between the nucleus and cytoplasm (50). AML-associated *NPM1* mutations result in the aberrant cytoplasmic translocation of the protein (NPMc+) (51). The *FLT3* gene encodes for a tyrosine kinase receptor that, during hematopoiesis, regulates several processes, including cell division and apoptosis (52). Normally inactive, in the presence of mutation, mainly the internal tandem duplication (ITD) in the juxtamembrane domain, the receptor is constitutively activated and drives the transmission of the *STAT5* signaling, therefore, enhancing the expression of

genes that sustain cell proliferation such as *Cyclin D1*, *c- MYC* and *p21* (53). Generally, the presence of the *FLT3-ITD* mutation is linked to poor prognosis, especially for younger (<60 years) and female patients (54). In Italy, based on data published by AIRTUM (Associazione Italiana registro Tumori), it is possible to estimate over 2000 new cases of AML in adults (55). Worldwide, AML is only in 35-40% of patients under 60 years of age and only in 5–15% of patients older than 60 years due to the appearance of multi-drug-resistance (MDR) mechanisms (56). Indeed, nearly 60% of elderly patients failed in inducing chemotherapy due to recurrence, and >85% of patients failed in treatment (56).

3.2 *Hh* signaling in AML

In hematological cancers, such as leukemia, *Hh* signaling drives the development and the expansion of leukemic cancer cells (LCs), sustaining their survival and proliferation (56). The presence of LCs is a significant problem in cancer management as they drive the emergence of resistance clones leading to disease recurrence (58). Increased expression of *Hh* signaling has been reported in AML cell line, and upregulation of *Hh* target genes (*GLI1*, *PTCH1*) and *SMO* has been observed in AML patients (59).

Therefore, inhibition of the *Hh* signaling pathway may represent an attractive strategy for AML patients, and initial promising results have been obtained in *in-vitro* studies. Indeed, the SMO inhibitor cyclopamine sensitizes chemoresistant CD34+ cells to cytarabine, one of the chemotherapy agents currently in use (60). However, cyclopamine has poor solubility, low potency, and off-target effects, making it unsuitable for clinical use (61). For this reason, researchers are developing cyclopamine derivative, which use is currently under investigation (62). Promising results have been obtained in preclinical studies where new SMO inhibitors showed the ability to induce LCs differentiation by promoting cell-cycle progression from dormancy (63). However, in a phase IIb clinical trial, the treatment with the cyclopamine derivative vismodegib did not block disease progression (64). Other SMO inhibitors are currently tested in different clinical trials with interesting primary results.

On the contrary, the use of GLI inhibitors has been tested only in preclinical studies, and their use in clinical trial has not been yet investigated (65). SMO inhibitor resistance mechanisms might be attributed to several causes ranging from acquired *SMO* mutations to SMO-independent GLI1 activation through the non-canonical *Hh* signaling (66). In the first case, mutations can both change the inhibitors-binding sites or induce allosteric changes in the SMO that lead to the constitutive activation of the protein (67). In the second case, various mechanisms sustain the SMO-independent GLI1 activation, such as atypical protein

kinases, the regulation of transcriptional activity, and the forced Gli1 nuclear localization (67). Whether *Hh* inhibition may be effectively used in the treatment of AML is under investigation. Only one *Hh* inhibitor (glasdegib) has been approved by the FDA as a therapeutic strategy to counteract AML progression in combination with low doses of cytarabine (63). Therefore, the discovery of new therapeutic targets able to modulate the *Hh* signaling might improve the treatment of AML patients.

One attractive structure to be targeted for the treatment of different tumors is the PC. Indeed, cancer cells, including AML cell lines failed to express the PC on their surface and present a high proliferation rate (68). Novel therapeutic approaches to restore PC on the surface of cancer cells, the so-called "ciliotherapy", are now emerging. One of the key players in PC destabilization is HDAC6, a class IIb member of histone deacetylase (HDAC) family of proteins. The HDAC6-mediated deacetylation of α-tubulin leads to PC disassembly by destabilizing axonemal stability and increasing the polymerization of the actin filaments (69). Interestingly, HDAC6 is overexpressed in several tumors such as GBM, multiple myeloma (MM), melanoma and colon cancers (70), and drugs to selectively prevent HDAC6 activity (i.e. TubastatinA) are currently in use (71). However, *HDAC6* expression and its relationship with *Hh* signaling in AML has never been investigated so far.

4 HISTONE DEACETYLASE FAMILY OF ENZYME

4.1 HDAC family of proteins

In mammals, the histone deacetylase (HDAC) family of proteins comprises 18 members grouped into four classes based on phylogenetic analyses and sequence homology to yeast protein orthologues (72). Class I (HDAC1, 2, 3, 8), class IIa (HDAC4, 5, 7, 9), and IIb (HDAC6, 10) and class IV (HDAC11) exert a Zn^{2+} dependent deacetylase activity (73). Instead, HDACs belonging from class III (Sirtuins 1-7) adopt a NAD^{+} dependent mechanism of action (72).

The state of interaction between histones and DNA influences gene expression. This process in eukaryotes is modulated by the activity of both HDACs and histone acetyltransferases (HAT). As histone deacetylases enzymes, HDACs negatively modulate gene expression obstructing the access of the transcriptional machinery. Indeed, the HDAC-mediated removal of the acetyl group recovers the positive charge on the lysine chains and restores the chromatin in a close conformation preventing the access of RNA polymerases and decreasing gene expression(74) (Fig.5).

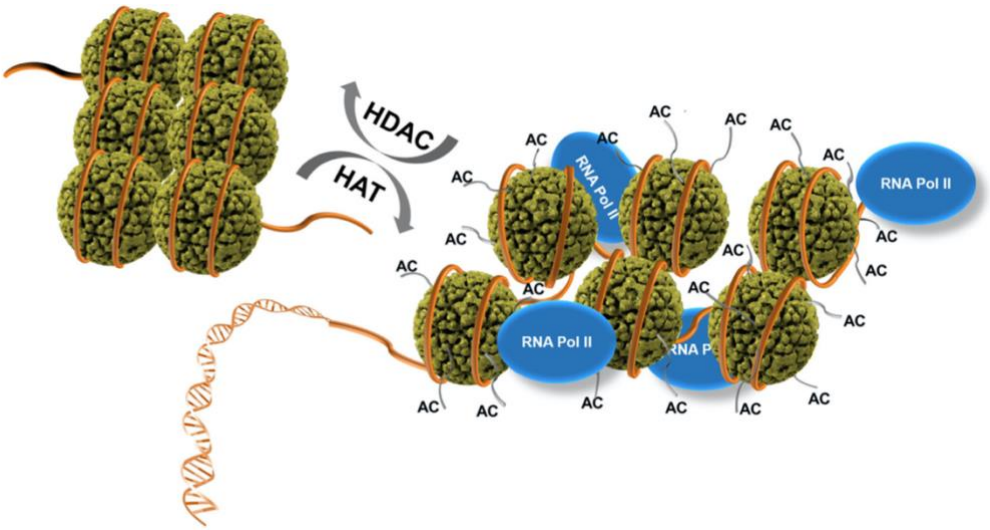

Fig.5: Epigenetic control of gene expression. The acetylation (AC) of histone lysine by HAT, opens the chromatin structure and enables the binding of RNA polymerase II (RNA Pol II). On the contrary, the HDAC-mediated lysine deacetylation restores the closed chromatin conformation (left). Histones: dark green spheres; DNA: orange; lysine residues: gray tails. Modified from Zhang et al. 2021.

Through this fine-tuned regulation, HDACs exert epigenetic control of gene expression. Alterations in the balance between HAT and HDAC activities result in the aberrant expression of specific genes and leads to the instability of the chromatin structure with the development of different human disease (72). Indeed, by altering the acetylated state of the chromatin, HDACs mainly influence the transcription of oncogenes and tumor suppressor genes (75). However, different human pathological conditions arise from an altered equilibrium between cytoplasmatic acetylated/non-acetylated proteins. Indeed, HDACs also regulate the deacetylation of different cytoplasmatic proteins, thereby influencing different biological processes and controlling cellular homeostasis (76).

4.2 HDAC6 structure

The *HDAC6* gene (Xp11.23), codifies for the largest HDAC protein, with 1215 aminoacids rearranged in a structure that makes HDAC6 unique among all the other HDACs. Indeed, HDAC6 contains two catalytic domains, the CD1 and CD2, located at the N-terminal and the central region, respectively, and a ubiquitin zinc-dependent domain (ZnF-UBP) at the C-terminus, which mediate the binding of ubiquitinated proteins (77) (Fig.6). Besides, HDAC6 shows nuclear export signals (NES) and a serine/glutamate-rich repeat motif at the C

terminus, both responsible of the preferentially cytoplasmatic localization of the protein (77) (Fig.6). In this cellular compartment, HDAC6 mainly targets non-histone substrates, including α-tubulin, protein tau, cortactin, heat shock protein (HSP90), and peroxiredoxin (78). Therefore, HDAC6 plays a role in several biological processes such as cell movement, autophagy, apoptosis, and protein transport and degradation, which alterations have been linked to the development of different human diseases (79).

Fig.6: HDAC6 domain organization. NES: nuclear export signal; CD: catalytic domain; SE14: serine/glutamate motif; ZnF-UBP: ubiquitin zinc-dependent domain.

4.3 Major molecular processes regulated by HDAC6

HDAC6 is the only deacetylase enzyme that preferentially resides into the cytoplasm and deacetylases different non-histone proteins therefore modulating a variety of biological processes.

The α-tubulin was the first described HDAC6 substrate and through its deacetylation HDAC6 regulates microtubules' stability and function and impacts on cell movement and migration. Indeed, the deacetylation of α-tubulin by HDAC6 reduces microtubules stabilization and promotes cell migration (80). In line with this, the HDAC6 specific inhibition restores α-tubulin acetylation and reduces cell motility, while its overexpression in mammalian cells leads to tubulin hypoacetylation and promotes chemotactic cell movement (81). Interestingly, HDAC6 controls cell motility, also deacetylating the F-binding protein cortactin. Indeed, HDAC6 translocates to actin-enriched membrane ruffles where deacetylates cortactin and enables the polymerization of the actin filaments, favoring cell migration (82). On the other side, HDAC6 specific inhibition blocks the HDAC6 peripheral translocation and its binding with cortactin, reducing cell motility (82).

Through its α-tubulin deacetylase activity, HDAC6 controls tubulin's binding with interacting partners such as the tumor suppressor cylindromatosis (CYLD) protein. CYLD regulates cell growth and division through its tubulin-mediated associations with microtubules. HDAC6, through the α-tubulin deacetylation, prevents CYLD activation and promotes cell division (83).

Notably, through the deacetylation of the α-tubulin and cortactin HDAC6 drives the disassembly and the resorption of the primary cilium (PC), therefore controlling *Hh* signaling transduction towards the cells and cell proliferation (84).

HSP90 is another well-characterized HDAC6 substrate that modulates the recycling of misfolded protein. Indeed, HSP90 HDAC6-mediated deacetylation drives the activation of HSF1 and promotes the induction of molecular chaperone heat shock genes, including the gene-encoding HSP90 (85). Through this mechanism, HDAC6 acts as a pro-survival protein, protecting cells from apoptosis after stress induced by misfolded proteins.

Interestingly, HDAC6 also plays a direct role in the degradation of misfolded proteins through the proteasome (UPS) or autophagic process (86). The degradation pathway of the polyubiquitinated proteins depends on the balance between HDAC6 and p97/VCP. Indeed, an excess of p97/VCP over HDAC6 promotes the dissociation of the polyubiquitinated proteins from HDAC6, ensuring their degradation through the proteasome system. On the contrary, an excess of HDAC6 drives their clearance through autophagy (87). Moreover, HDAC6 modulates the transport, microtubules-mediated, of the autophagosomes to the lysozymes and their fusion, recruiting and deacetylating the cytoplasmatic protein cortactin (88).

4.4 HDAC6 inhibition in AML

The use of the HDAC inhibitors (HDACi) for the treatment of different cancers relies on their ability to regulate gene expression through the induction of the acetylation of histone or non-histone proteins that control cell cycle progression, apoptosis, and differentiation (75). However, most of the HDACi lack specificity for specific isoforms leading to off-target effects (89). For this reason, in recent years, scientists are currently testing the use of new therapeutic agents able to target specific HDAC isoform to reduce the development of adverse side effects. The generation of these new compounds is suitable for HDAC isoforms for which the crystal structure of the catalytic domain is available, such as HDAC6. However, little is known about the contribution of HDAC6 in the development or in the progression of AML. In 2005, expression analyses performed on AML samples showed that the expression levels of *HDAC6* are at or around that of immature myeloid progenitor/blast cells (90).

Moreover, the specific inhibition of HDAC6 with the selective ST80 inhibitor reduced the proliferation of patients' blast and AML cell lines (91) In a combination setting with common therapeutic agents, another HDAC6 selective inhibitor named MPT0G211 reduced tumor growth affecting cell proliferation and induced cell death via apoptosis (92). These data

suggest that HDAC6 might play a role in the development or in the progression of AML and could represent an attractive target to be exploited.

5 THE ZEBRAFISH (*Danio rerio)* MODEL

5.1 Zebrafish hematopoiesis

In vertebrates, hematopoiesis occurs in two distinct phases, defined as primitive and definitive hematopoiesis (93). The first is responsible for the generation of primitive erythrocytes and macrophages, while the second establishes self-renewal hematopoietic stem cells (HSCs), which give rise to all the hematopoietic lineages (94). In zebrafish, despite differences in the anatomical sites, the molecular mechanisms governing hematopoiesis are highly conserved, making it suitable for the study of the hematopoietic development both in physiological and pathological conditions (95).

The anatomical sites of primitive hematopoiesis form during early embryonic development in two bilateral stripes of the lateral mesoderm: the rostral blood island (RBI) in the anterior lateral mesoderm (ALM) and the intermediate cell mass (ICM) blood islands which origin from the posterior lateral mesoderm (PLM) (Fig.7). The ICM locates nearly the notochord and is considered the zebrafish counterpart of the mammals' extra-embryonic yolk sack blood islands. Around 10.5 hours post fertilization (hpf) the expression of the bHLH transcription factor stem cell leukemia (*scl/tal1*) in the PLM indicates the beginning of the primitive hematopoiesis (96). At the same time, cells of the RBI region start to express the *ETS-related protein* (*etsrp/etv2*), *scl* and the myeloid marker *spi1b* (97). Shortly after, *etsrp/etv2* expression is detected in the PLM together with the expression of other hematopoietic genes such as *LIM domain only 2* (l*mo2*), the vascular genes including *GATA binding protein 2a* (*gata2a*) and the ETS family member *fli1a/b* (97). From the stage of 12 hpf, in the newly formed ICM, cells are progressively specified to the myeloid or erythroid fate, whit the expression of the *spi1b* and *gata1a,* respectively (98). Around 18 hpf, the cells of the RBI express the pan-leukocyte marker *l-plastin* (99) and myeloid markers, including both *interferon regulatory factor 8* (*irf8*) (100) and the *granulocyte progenitor marker CCAAT/enhancer-binding protein 1* (*cebp1*) (101). By 19 hpf, overlapping expression of the granulocyte marker *myeloid peroxidase* (*mpx*) and *gata1a* in cells within the PLM and later within the ICM may indicate a primitive myeloid-erythroid cell population (102). Finally, from the stage of 21.5 hpf, RBI-derived macrophages begin the expression of the *colony-stimulating factor receptor 1a* (*csf1ra/fms*), the *macrophage-expressed 1* (*mpeg1*), and other macrophage markers. At 24 hpf, granulocyte progenitors begin to differentiate, expressing

lysozyme C (*lyz*) and *mpx* (102). These last events represent the end of primitive hematopoiesis.

The appearance of hematopoietic stem and progenitor cells (HSPCs) indicates the beginning of the definitive hematopoiesis, and in zebrafish, HSPCs are identified by the expression of the hematopoietic stem cell markers *cmyb* and *runx1*. These HSPCs arise from the ventral wall of the dorsal aorta, considered the anatomical counterpart of the mammal aorta-gonad-mesonephric (AGM) from the stage of 26 hours post fertilization (hpf) (95) (Fig.7). *runx1* is the earliest marker of this cell population as embryos knocked-out for *runx1* lack the formation of HSPCs (103). On the contrary, *cmyb* is believed to act downstream of *runx1,* and in its absence, HSPCs are correctly formed and specified but cannot exit from the ventral wall of the dorsal aorta (104). The induction of Runx1 and the formation of the first HSPCs depends on the activation of the Notch signaling. Indeed, in the Notch *mindbomb* mutants and in embryos treated with the γ-secretase inhibitor DAPT, HSPCs are not formed (105). In line with this, transient activation of Notch signaling by induction of the Notch intracellular domain leads to the upregulation of HSPCs budding from the AGM (105). Also, through the Wnt16 ligand, the Wnt signaling controls the formation of the HSPCs, as it drives the Notch ligands dC and dD expression in the somites surrounding the dorsal aorta (106). Once formed, through their budding from the wall of the arterial vessel, HSPCs enter the circulation via the axial vein and colonize different organs: the caudal hematopoietic tissue (CHT) by 2 days post fertilization (dpf), the thymus by 3 dpf and the kidney marrow at 4 dpf (102) (Fig.7). The transcription factor Scl mainly mediates the budding of HSPCs. Indeed, *scl* expression is required in the AGM to initiate the epithelial-to mesenchymal transition (107). Once reached the CHT, HSPCs give rise mainly to embryonic macrophages, neutrophile and monocytes. From the kidney marrow, considered the anatomical counterpart of the mammal bone marrow, myeloid and erythroid cells, thrombocytes, and B-lymphoid cells originate. The thymus is instead responsible for the maturation of T lymphoid cells (102).

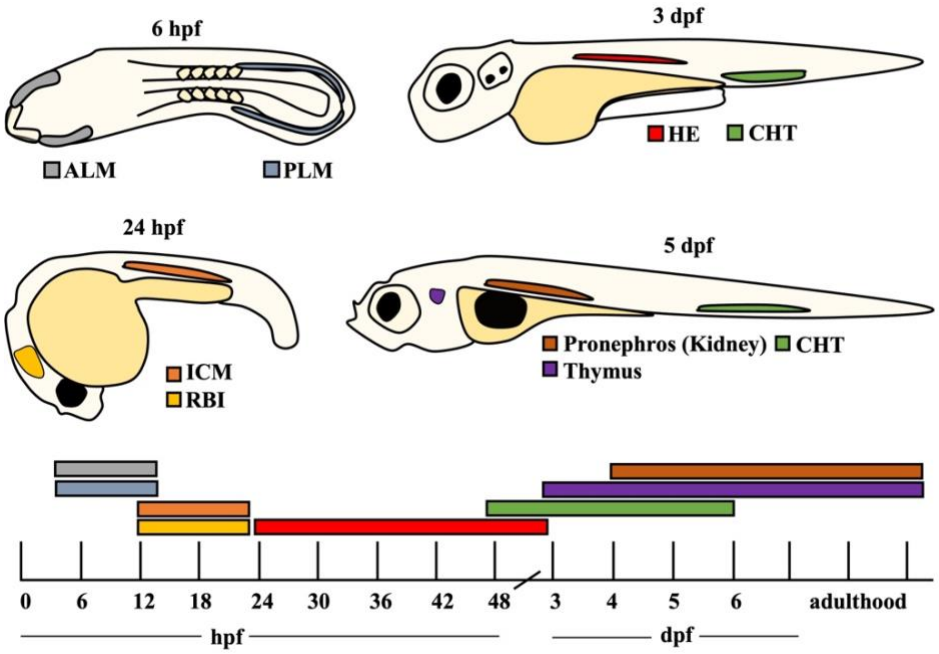

Fig.7: Anatomical sites of zebrafish primitive and definitive hematopoiesis. On the top, representative stages of zebrafish embryos in which are labelled the anatomical sites of hematopoiesis. On the bottom, a timescale indicating the stage at which the anatomical sites are active during hematopoiesis. ALM: anterior lateral mesoderm; PLM: posterior lateral mesoderm; ICM: inner cell mass; RBI: rostral blood island; HE: hemogenic endothelium; CHT: caudal hematopoietic tissue; hpf: hours post fertilization; dpf: days post fertilization.

5.2 Zebrafish as a model for AML

The dynamic processes underlying hematopoiesis are well conserved in zebrafish, and it is not surprising that mutations in the zebrafish hematopoietic genes at the basis of human disorders successfully phenocopy the human disease phenotypes. Different models have been described concerning the zebrafish as a model for the study of AML. For instance, the overexpression of the *AML1-ETO* mRNA causes alteration in both erythropoiesis and granulopoiesis, a phenotype found in AML patients (108). In addition, the specific overexpression of *NUP98-HOXA9* mRNA specifically in the myeloid compartment leads to the hyperproliferation of HSPCs and myeloid cells (109,110). Overexpression of the mutant form of *NUCLEOPHSOMIN* (*NPMc+)* in zebrafish embryos led to the expansion of primitive early myeloid cells, which was significantly enhanced in the absence of functional p53 (110). Similarly, in zebrafish embryos, overexpression of mRNAs expressing human *FLT3-ITD* or *FLT3* with a mutation in the tyrosine kinase domain (*FLT3-TKD*) resulted in expansion and clustering of myeloid cells through activation of downstream signaling pathways (111).

Approximately 30% of cytogenetically normal AML cells carry mutations in the *isocitrate dehydrogenase 1 and 2* (*IDH1/2*) genes (112). Also, for this mutation, the zebrafish model with forced expression of *IDH* genes shows increased myeloid progenitor cells and reduced myeloid differentiation (113).

The zebrafish model helped in understanding the role of the main hematopoietic genes during definitive hematopoiesis. Indeed, loss-of-function mutations in *RUNX1* are found in almost 10% of AML patients, and unfortunately, are associated with poor outcome (114). A zebrafish line harboring a truncated allele of *runx1* (*runx1*^{W84X}) is characterized by the block of definitive hematopoiesis, and the 20% of the embryos that reach the adult life showed a significant reduction of myeloid progenitor cells (115). In AML patients, also loss-of-function mutations in *SPI1* (*PU.1)* has been associated with the onset and progression of the disease and in adult zebrafish carrying the hypomorphic *pu.1* allele (*pu.1*^{G242D}), there is an expansion of immature myeloid cells in the kidney marrow (116). Therefore, zebrafish AML models confirm the evolutionary conservation of molecular mechanisms behind definitive hematopoiesis, and prompted out the pathogenetic role of some genes (i.e. *RUNX1* and *PU.1)* in AML development and progression.

As described above, the clonal expansion of leukemic blast is also driven by the serial acquisition of different mutations. In line with this, in zebrafish, the forced expression of the fusion gene *MOZ-TIF2*, showed a low incidence of leukemic phenotype, indicating that additional mutations are needed to the development of AML in patients carrying the inv(8)(p11q13) chromosomal rearrangement (117).

AIM OF THE THESIS

With this work we aim to decipher the *Hh/HDAC6/MDR* interplay in the field of acute myeloid leukemia (AML) to investigate if HDAC6 might represent a suitable therapeutic alternative for the treatment of AML patients.

-We addressed this point starting with the characterization of the *Hh/HDAC/MDR* interplay in a cohort of adult AML samples.

-We then moved to the generation of *in vivo* zebrafish models with *Hh* or *HDAC6* overexpression to decipher the molecular mechanism governing hematopoietic stem and progenitor cells (HSPCs) development.

-We also isolated the HSPCs from zebrafish embryos to identify if this cell population present the PC as recently described for human bone marrow cells. Indeed, this structure could be responsible for the HSPCS expansion following *Hh*/HDAC6 hyperactivation in zebrafish and could be a suitable target for HDAC6 inhibition.

-We performed *Hh* and HDAC6 specific inhibition in zebrafish embryos with *Hh* and HDAC6 overexpression and in zebrafish models of AML carrying the overexpression of the *NPMc+* and *FLT-ITD* transcripts. We also demonstrated in human AML cell lines the potentiality of HDAC6 inhibition.

-Finally, as combination therapies based on the co-administration of HDAC inhibitors and chemotherapic agents are currently under investigation, we tested this combination setting administrating the chemotherapic agent cytarabine and the HDAC6 inhibitor in the zebrafish models of AML.

MATERIAL AND METHODS

Patients

All human material and derived data were used in accordance with the Declaration of Helsinki. The genetic profile of AML specimens, previously characterized for molecular aberrancies in accordance with specific clinical protocol requirements, is listed in the table below (table 1). Patients enrolled belong to different French-American-British (FAB) classification systems (118), excluding M3, therefore all patients were negative for translocation t(15;17). Bone marrows of healthy individuals were collected as control for gene expression assays, upon appropriate Informed Consent ASG-MA-052A approved by Azienda San Gerardo on may 8th 2012.

Supplementary Table S1. Clinical Features of patients' cohort.

	AGE AT ONSET	KARYOTYPE	FAB CLASSIFICATION	NPM	FLT3-ITD	CEBPA	ckit	JAK2	t(9;22)	t(8;21)	inv(16)
1	47	46,XX,t(10;11)(p11;p15)[20]	M0	NEG	NEG	nk	nk	nk	NEG	NEG	NEG
2	49	46,XY[20]	M0/M1	NEG	NEG	NEG	nk	nk	NEG	NEG	NEG
3	48	46,XX[20]	M1	NEG	NEG	NEG	nk	nk	NEG	NEG	NEG
4	70	45,X,-Y,t(8;21)(q22;q22)[5]/46,XY[5]	M2	NEG	NEG	nk	NEG	nk	NEG	POS	NEG
5	72	47,XY,+mar[10]/46,XY[10]	M2	NEG	NEG	nk	nk	nk	NEG	NEG	NEG
6	47	45-46,XY,del(3)(q?22q?26),der(4)t(?1;4)(p36;p16),add(11)(p14),-12,del(12)(p11),add(21)(q22)[cp13]/46,XY[7]	nk	NEG	NEG	nk	nk	nk	nk	NEG	NEG
7	37	43,XY,?del(2)(q?33),-4,der(6)t(?4;6)(q?22;q21),i(11)(q10),-17,-18[19]/46,XY[2]	M1	NEG	NEG	nk	nk	nk	NEG	nk	nk
8	59	46,XY[20]		NEG	POS	nk	nk	nk	NEG	NEG	NEG
9	33	46,XY[15]	M1	NEG	POS	nk	nk	nk	NEG	NEG	NEG
10	30	46,XY[20]	M5	NEG	POS	nk	nk	nk	nk	NEG	NEG
11	20	46,XY,t(8;21)(q22;q22)[21]/46,XY[1]	nk	NEG	POS	nk	NEG	nk	nk	POS	NEG
12	58	46,XY,inv(16)(p13q22)[20]	M4	NEG	POS	nk	nk	nk	nk	NEG	POS
13	76	nk	M5	NEG	POS	nk	POS ex17	nk	nk	NEG	NEG
14	78	46,XX[27]	M4	NEG	POS	nk	nk	nk	nk	NEG	NEG
15	53	46,XY[22]	M4	NEG	POS	nk	nk	nk	nk	NEG	NEG
16	64	46,XX[20]	M5	NEG	POS	nk	nk	nk	nk	NEG	NEG
17	75	46,XY[26]	M4	NEG	POS	nk	nk	nk	nk	NEG	NEG
18	39	46,XY[20]	M1	POS (A)	NEG	nk	nk	nk	NEG	NEG	NEG
19	47	46,XX[20]	M5	POS (A)	NEG	nk	nk	NEG	NEG	NEG	NEG
20	58	46,XY/47,XY,+8[7/10]	nk	POS (QM)	NEG	nk	nk	nk	nk	NEG	NEG
21	50	46,XX[20]	M4	POS (A)	NEG	nk	nk	nk	nk	NEG	NEG
22	77	46,XY[20]	nk	POS (A)	NEG	nk	nk	nk	nk	NEG	NEG
23	54	46,XX,t(9;22)(q34;q11)[14]/46,XX[6]	M4	POS (A)	NEG	nk	nk	NEG	POS	NEG	NEG
24	60	46,XX[6]	nk	POS	NEG	nk	nk	nk	nk	NEG	NEG
25	62	46,XX[25]	M5	POS (A)	NEG ITD/POS D835/D836	nk	nk	nk	nk	NEG	NEG
26	58	46,XX[20]	nk	POS (A)	NEG	nk	nk	nk	nk	NEG	NEG
27	48	46,XX[20]	M4	POS (A)	POS	nk	nk	nk	NEG	NEG	NEG
28	51	46,XX[20]	M5	POS (A)	POS	nk	nk	nk	NEG	NEG	NEG
29	68	46,XX[20]	M4	POS (A)	POS ITD/POS D835/D836	nk	nk	nk	NEG	NEG	NEG
30	46	46,XY[20]	M2	POS	POS	nk	nk	nk	NEG	NEG	NEG
31	39	46,XX[22]	M1	POS (A)	POS	nk	nk	nk	nk	NEG	NEG
32	58	46,XY	M5	POS (A)	POS	nk	nk	nk	nk	NEG	NEG
33	35	46,XY,?r(18)(?)[16]/47,idem,+8[3]/46,XY[1]	nk	POS (B)	POS	nk	nk	nk	nk	NEG	NEG
34	58	46,XY[24]	M1	POS (A)	POS	nk	nk	nk	nk	NEG	NEG
35	70	46,XY[20]	M5	POS (A)	POS	nk	nk	nk	nk	NEG	NEG
36	12	46,XY[24]	nk	POS (A)	POS	nk	nk	nk	NEG	NEG	NEG

Table 1: Features of AML patients. FAB: French-American-British classification.

Zebrafish (*Danio rerio*) housing and maintenance

Zebrafish embryos were raised and maintained under standard conditions according to the national guidelines (Italian decree March 4, 2014, n. 26). Embryos from AB and *Tg(CD41:GFP)* strains (119) were obtained by natural spawning, staged according to the reference guidelines (120) and raised at 28° C in E3 medium fish water (instant ocean, 0.1% methylene blue in petri dishes). From the stage of 24 hours post-fertilization (hpf) 0.003% 1-phenyl-2-thiourea (PTU, Sigma-Aldrich, Saint Louis, MO) was added to the fish water in order to prevent pigmentation. Before manipulations, embryos were dechorionated and

anesthetized with 0.016% tricaine (ethyl 3-aminobenzoate methanesulfonate salt; Sigma-Aldrich).

Chemical treatments in zebrafish embryos

TubastatinA (TubA; Sigma), cyclopamine (cyclo; Sigma) and cytarabine (AraC, Sigma) were dissolved in the Dimethyl sulfoxide (DMSO) vehicle. For the pharmacological treatments the drugs were directly added to the E3 medium fish water in a 24 multi-well containing a maximum of 15 embryos/well from the stage of 1.5 days post fertilization (dpf). The multi-well was then incubated at 28°C until 2.5 dpf. Embryos were treated with different concentrations of the compounds alone or in combination in 1 ml final volume of E3 with PTU 1X. The doses used were 100 to 35 μM of TubA and 5 μM cyclo for single treatments or 50 μM TubA and 2.5 μM cyclo for combination therapies with 50 μM AraC.

Chemical treatments in AML cell lines

OCI-AML2, U937, THP-1, and NB4 cell lines were originally obtained from ATCC/DSMZ repositories and since stored at the internal cell line bank at the Department of Experimental Oncology, IEO. Cell lines undergo regular authentication and mycoplasma testing. Cells were seeded at 10^4 cells/well in 96-well plates in 100 µl of growth medium and allowed to grow for 72 h prior to treatment commencement. Cyclopamine (cyclo) and TubastatinA (TubA) were dissolved in DMSO, diluted in the appropriate culture medium and added into plates, as indicated. The concentration range of both compounds has been determined based on published data and ranged between 0.6 μM and 4.8 µM for cyclo (121) and 1.25 μM to 10 μM for Tuba (122). 72 hours later, CellTiter-Glo assay (Promega) was performed as indicated in the manufacturer's instructions and read on GloMax (Promega) plate reader. Cells treated with DMSO (0.2% in appropriate medium) were used as a control.

mRNA synthesis and microinjection

DH5a *E.coli* cells were transformed with T7TS-*shh* expression plasmid and processed through MIDIprep DNA extraction (Promega) according to the manufacture instructions. The T7TS-*shh* expression plasmid was linearized with NotI (Promega) and the *shh* mRNA was *in vitro* transcribed and purified with the mMESSAGE mMACHINE T7 transcription kit (Invitrogen) following the manufactures instructions. For the synthesis of the human *HDAC6* mRNA we purchased bacterial stab transformed with the pCDNA3.1-*HDAC6* plasmid (Addgene, Watertown, MA 02472; USA). After, inoculations, bacterial cells were processed

with MIDIprep DNA extraction (Promega) and the extracted pcDNA3.1-*HDAC6* plasmid was linearized with KasI (Promega). The human *HDAC6* mRNA was then *in vitro* transcribed and purified with the mMESSAGE mMACHINE T7 transcription kit (Invitrogen) following the manufactures instructions. Once synthesized, mRNAs were quantified through spectrophotometry (Nanodrop) and run on 1% agarose gel to assess the integrity of the material.

4 nl of solution containing nucleases free water, the *red phenol* tracer (Invitrogen), and 200 pg/embryo of the *shh* mRNA or 250 pg/embryo of the human *HDAC6* mRNA was added into borosilicate needles and injected into 1 cell stage embryos of the *Tg(CD41:GFP)* line through the use of micromanipulator (Femtojet; Eppendorf). As a control, embryos were injected with the same amount of the *red-fluorescent-protein* (*rfp*) mRNA except when double immunofluorescence with a secondary red antibody was performed.

Reverse transcription and real-time quantitative techniques (RT-qPCR)

Total RNA was isolated from zebrafish embryos and cell lines using TRIZOL reagents (Life Technologies, Carlsbad, CA, USA) following the manufacturer's instructions. After DNaseI RNase-free (Roche Diagnostics, Basel, Swizterland) treatment to avoid genomic contamination, 1 µg of total RNA was used as a template for the synthesis of cDNA using the "GoScript™" Reverse Transcription system (Promega, Madison, Wisconsin USA). Quantitative real-time polymerase reactions (RT-qPCR) were conducted in a total volume of 10 µl containing iQ SYBR Green Super Mix (Promega, Madison, WI, USA) using the 384-well QuantStudio™ 5 Real-Time PCR System (Applied Biosystem, Whaltam, MA, USA). Genes of interest were normalized to *rpl8* and *beta-actin* for zebrafish and to *GAPDH* and *GUS* for human cell lines and AML samples. In table 2, is reported the list of the primers used for the RT-qPCR.

Primer	Sequence (5' – 3')
GLI1 HS FF	AGT ACA TGC TGG TGG TTC AC
GLI1 HS RR	AGG TTT TCGA GGC GTGA GTA
PTCH1 HS FF	AGG TGC TAA TGT CCT GAC CA
PTCH1 HS RR	CCA CTG CCT GTT GTA CAT GT
HDAC6 HS FF	CTG GCT TGG TGT TGG ATG AG
HDAC6 HS RR	CTC CTG GAT CAG TTG CTC C
ABCC1 HS FF	ATG CAG AGG AGA ACG GGG T

ABCC1 HS RR	CCT GCA CTG TCC GTC ACC
ASXL1 HS FF	TCA CGC TCA AGA AGG ATG CC
ASXL1 HS RR	CCC ACA GCT CTC CAC ATC AG
GAPDH HS FF	CAA CGA CCA CTT TGT CAA GC
GAPDH HS RR	CTG TGA GGA GGG GAG ATT CA
GUS HS FF	CGC CCT GCC TAT CTG TAT TC
GUS HS RR	TCC CCA CAG GGA GTG TGT AG
gli1a zf FF	ACA CAC TGA AAT CTC AGC CG
gli1a zf RR	GTC ATT ATT ATT GGC GCT CC
ptch1 zf FF	GGA GAA ACT CTG GGT AGA AG
ptch1 zf RR	CCT GAC GAG GCG TCT GTA TC
asxl1 zf FF	GTC GCT CTT CAC AGT CAG GG
asxl1 zf RR	CGT GTT CAC CGT TGA CCT TG
abcc1 zf FF	CGT GAG GAG ACA CAA CTG AG
abcc1 zf RR	AGT TGC AGT ACA CAG CCC TG
hdac6 zf FF	GCA GAG ACA CCT AAC CGT TC
hdac6 zf RR	CCA GCA GCC TCC AGA ACT AA
cmyb zf FF	GAC ACA AAG CTG CCC AGT TC
cmyb zf RR	GCT CTT CCG TCT TCC CAC AA
rpl8 zf FF	CTC CGT CTT CAA AGC CAA TG
rpl8 zf RR	TCC TTC ACG ATC CCC TTG AT
β-actin zf FF	GCA CGA GAG ATC TTC ACT CC
β-actin zf RR	GCA GCG ATT TCC TCA TCC AT

Table 2: Primers used for RT-qPCR analyses. HS: *Homo sapiens*; zf: zebrafish

Fluorescence activated cell sorting (FACS) analyses

Embryo's dissociation was performed as described in Bresciani et al. (2018) (123). FACS analysis were conducted on *Tg(CD41:GFP)* zebrafish embryos at 2.5 dpf as previously described (44). Flow cytometry acquisitions were performed using Attune NxT (Thermofisher). Analyses were done with Kaluza software from Beckman Coulter. Embryos of the wild-type AB strain were used to set the gate and exclude auto-fluorescence of cells. The gate for $GFP^{low/high}$ cells was set on control *Tg(CD41:GFP)* DMSO-treated embryos to distinguish a GFP^{low} population representing around 0.2% of total cells, as previously

reported (44), and applied to all categories analyzed. Hematopoietic stem and progenitor cells (HSPC-GFP^{low}) sorting from *Tg(CD41:GFP)* 2.5 dpf zebrafish embryos was performed with FACSAriaIIU from BD and data analyzed with FACSDiva software.

Immunofluorescence staining and image processing

PTU-treated embryos belonging from the *Tg(CD41:GFP)* line were fixed overnight in 4% paraformaldehyde (Sigma-Aldrich) in Phosphate Buffer Saline (PBS) at 4 °C. After 2 hours in blocking solution at room temperature embryos were incubated with the primary antibodies mouse anti-GFP (1:1000, Sigma-Aldrich) and rabbit anti-3PH (1:200, Sigma-Aldrich). The secondary antibodies were Alexa Fluor 488-conjugated goat anti-mouse IgG 1:400 (A11008, Invitrogen Life Technologies, Carlsbad, CA, USA) and Alexa 546-conjugated goat anti-rabbit IgG 1:400 (A11001 and A11010, Invitrogen Life Technologies). Staining was evaluated detecting GFP and/or 3PH fluorescence through confocal analyses (A1 HD25/A1R HD25 instrument, Nikon FRET-FLIM) provided by the UniTech nolimits NOxsz<LIMITS service (UNIMI department). For the count of proliferating HSPCs, confocal images were analyzed by ImageJ software. We selected the caudal hematopoietic tissue as region of interest (ROI) and set a common threshold for all the experimental group.

Western blotting analysis

Total proteins from AML cell lines or zebrafish embryos were extracted with Ripa buffer. 40 µg of extracts were loaded in a 10% acrylamide/polyacrilammide gel and subjected to electrophoresis. Proteins were transferred onto polyvinylidene fluoride (PVDF) membranes that were incubated with blocking solution (BS) (5% skimmed powder milk in TBS containing 0.1% TWEEN-20) for 1h at room temperature before overnight incubation at 4°C with primary antibodies: ac-α-tubulin (anti mouse 1:1000; Sigma-Aldrich) and total α -tubulin (anti rabbit 1:1000; Sigma-Aldrich) for AML cell lines and ac-α-tubulin (anti mouse 1:1000; Sigma-Aldrich) and vinculin (anti mouse 1:6000; Sigma-Aldrich) for zebrafish samples. Membranes were then incubated over-night at 4°C with HRP-conjugated secondary antibodies in blocking solution. Protein bands were detected by using WESTAR ECL detection system (Cyanagen, Bologna, Italy). Images were acquired with the Alliance MINI HD9 AUTO Western Blot Imaging System (UVItec Limited, Cambridge, UK) and analyzed with the related software.

Statistical analyses

All the statistical analyses were performed using the GraphPad (Prism) software (Version 9.1.2). For RT-qPCR and FACS experiments, data were statistically analyzed applying One-way analysis of variance (ANOVA) with Tukey post-hoc correction or Unpaired T-tests with Welch correction, defining P≤0.05 (*), P≤0.01 (**), and P≤0.001 (***) as statistically significant values. Data were analyzed using the comparative ΔΔCt method (124). For the correlation analyses in AML samples, we choose the Spearman correlation defining P≤0.05 (*), P≤0.01 (**), and P≤0.001 (***) as statistically significant values. The count of the proliferation rate of HSPCs was obtained by the ratio HSPCs positive for the 3PH staining/total number of HSPCs and analyzed with One-way analysis of variance (ANOVA) with Tukey post-hoc correction considering P≤0.05 (*), P≤0.01 (**), and P≤0.001 (***) as statistically significant values.

RESULTS

1. The expression of *Hh* and *HDAC6* positively correlates in adult AML patients

The interplay between the *Hh* signaling and *HDAC6* has never been investigated in AML. Therefore, we evaluated the relation between the expression levels of *HDAC6* and *Hh* target genes *GLI1* and *PTCH1* in a cohort of 36 adult AML patients. We found that the expression levels of both *Hh* targets and *HDAC6* was significantly increased in AML samples in comparison to healthy-donors (HD) (Fig.8A-C). Moreover, though correlation analyses we demonstrated that the expression levels of *GLI1* and *PTCH1* positively correlated with that of *HDAC6* (Fig.8D-E). Interestingly, also the expression of the Multi-Drug-Resistance (MDR) genes *ABCC1* and *ASXL1*, which was upregulated in AML patients in comparison to HD, positively correlates with the expression of *GLI1*, *PTCH1* and *HDAC6* (Fig.8F-M).

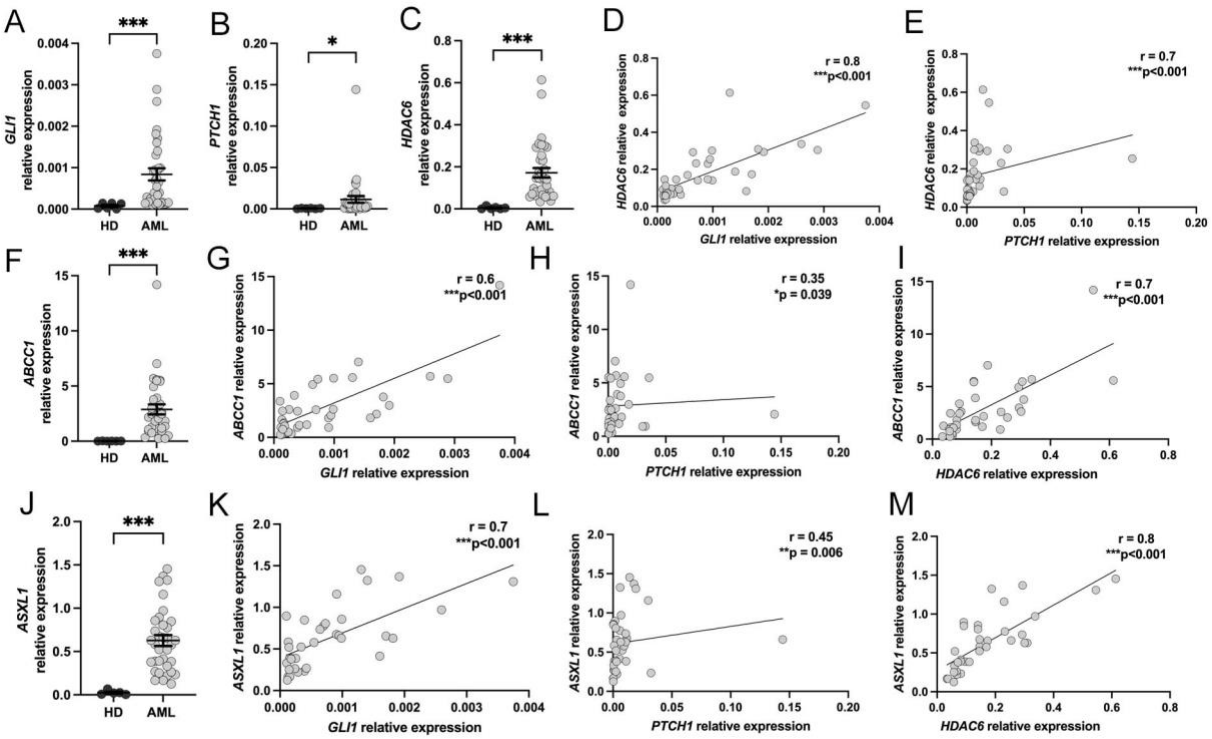

Fig. 8: *Hh*/*HDAC6*/*MDRs* correlation in AML patients in comparison to HD. A-C) Real-time qPCR analyses of *Hh* signaling target genes (**A**) *GLI1*, (**B**) *PTCH1* and (**C**) *HDAC6* in a cohort of adult AML patients. **D-E**) Correlation analyses between the expression levels of *HDAC6* and (**D**) *GLI1* and (**E**) *PTCH1.* **F-M**) Real-time qPCR and correlation analyses of the *Multi-Drug-Resistance* (MDR) genes (**F, G-I**) *ABCC1* and (**J, K-M)** *ASXL1*. **A-C**; **F; J**) Unpaired T-test with Welch correction. **D-E**; **G-I; K-M**) Spearman correlation. ***p<0.001; **p<0.01; *p<0.05. HD: healthy donor; AML: acute myeloid leukemia. Results are presented as mean ± SEM.

We confirmed these correlations in the TGCA LAML dataset by means of the GEPIA2 web-tool (Fig.9). These data indicates that *Hh* signaling, *HDAC6* and *MDR* genes are upregulated and positively correlated in AML patients and suggest that *Hh* and *HDAC6* might contribute to the generation of the leukemic condition and resistance to chemotherapy.

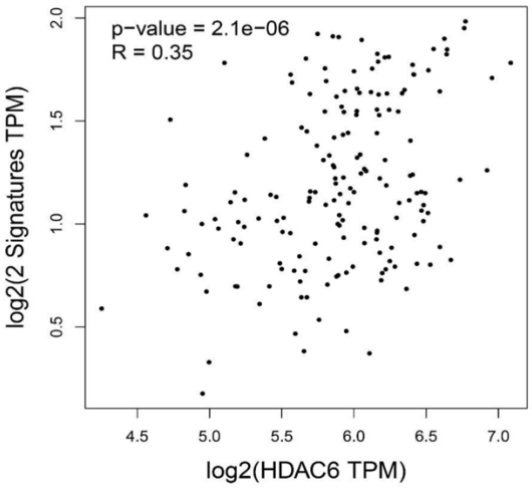

Fig. 9: GEPIA2 correlation analyses: *Hh*/*HDAC6*/*MDRs* in LALM dataset. Correlation analyses between the expression levels of HDAC6 (HDAC6 TPM) and GLI1 and PTCH1 (2 signature TPM). Spearman correlation. ***p<0.001. LAML: Acute Myeloid Leukemia; TPM: transcript per millions.

2. In zebrafish, *Hh* hyperactivation elicits the expansion of the HSPCs

To assess the functional role of the *Hh/HDAC6* signaling during hematopoiesis, we overexpressed the *shh* mRNA in zebrafish embryos in order to generate an *in vivo* model with *Hh* hyperactivation. At the stage of 2.5 dpf we firstly verified that *shh* mRNA injection determined an increase of the *Hh* signaling target genes *gli1a* and *ptch1* (Fig.10A-B). We also confirmed that this model recapitulates the genetic regulation found in our AML cohort as we detected enhanced expression of *hdac6, abcc1* and *asxl1* (Fig.10C-E). Through immunofluorescence (IF) analyses in the *Tg(CD41:GFP)* transgenic line expressing GFP protein in the hematopoietic stem and progenitor cells (HSPCs) we showed that *shh* mRNA injection elicited an expansion of this population in the caudal hematopoietic tissue (CHT) at the stage of 2.5 dpf when definitive hematopoiesis is well established, and enhances the expression of the HSPCs marker *cmyb* (Fig.10F-G).

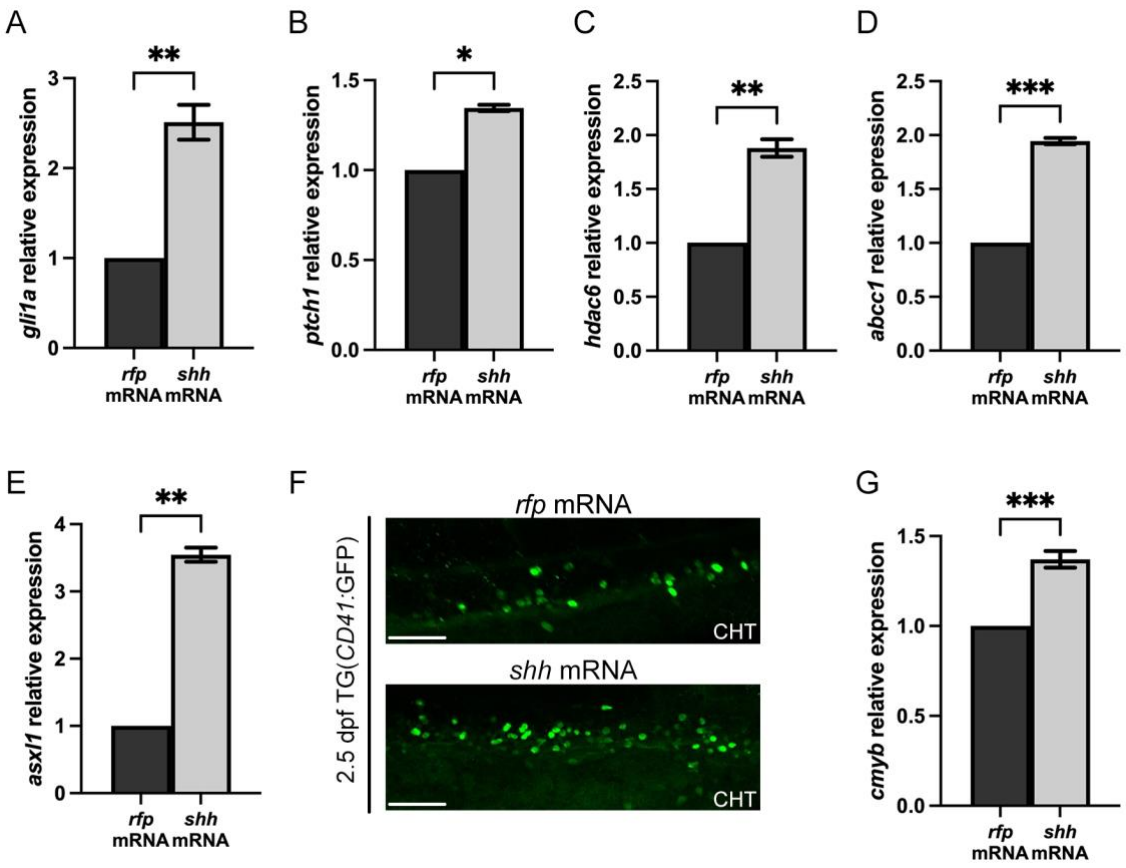

Fig. 10: *Hh*/*hdac6*/*MDRs* expression and HSPCs expansion in the zebrafish model with *Hh* hyperactivation. Real-time qPCR analyses of *Hh* signaling target genes (**A**) *gli1a*, (**B**) *ptch1*, (**C**) *hdac6* and the *Multi-Drug-Resistance* (MDR) genes (**D**) *abcc1*, and (**E**) *asxl1.* **F**) IF assays showing the HSPCs in the CHT (n=3) in *Tg(CD41:GFP)* control (*rfp* mRNA) and *shh* overexpressing embryos. **G**) Real-time qPCR analyses of *cmyb* expression. In all the analyses *shh* mRNA injected embryos were compared to *rfp*-mRNA control embryos. Unpaired T-test with Welch correction. ***p<0.001; **p<0.01; *p<0.05. Results are presented as mean ± SEM. Scale bar indicates 100 μm. n indicates the number of embryos analyzed. CHT: caudal hematopoietic tissue.

To investigate if the hematopoietic phenotype could be rescued by pharmacological inhibition of either *Hh* or Hdac6 we decided to treat *shh* mRNA overexpressed embryos with selective inhibitors, cyclopamine and TubastatinA respectively, addressing firstly their molecular validation.

3. TubastatinA efficiently blocks the zebrafish Hdac6

In order to select the proper dose of TubastatinA (TubA) to use for rescue experiments, a dose-response assay was performed. Embryos of the *Tg(CD41:GFP)* transgenic line were incubated with increasing concentration of the inhibitor from the stage of 1.5 *day post fertilization* (dpf). One day later, embryos were analyzed for the screening of morphologic defects. No significant differences in the axial body have been observed at all the doses

tested in comparison to embryos treated with the DMSO vehicle (Fig.11A). We also evaluated embryos survival at 1 day *post treatment* (dpt) and we did not detect an increase in embryos mortality even at the higher dose used (Fig.4B). From these experiments, and according to data reported in Leyk et al. we selected 100 μM as the working dose (125). Further we validated the HDAC6 inhibition by means of western blot assays. As expected, TubA treated embryos showed a significant increase in the level of the acetylated-α-tubulin in comparison to DMSO-treated control embryos (Fig.11C). We also performed a functional validation of the inhibitor analyzing the formation of the cilia in the pronephric duct, a region commonly used for the screening of defects in cilia formation (126). Accordingly, by means of immunofluorescence analyses with the acetylated-α–tubulin antibody, we found that TubA treatment increased the length of the cilia in this region (Fig.11D).

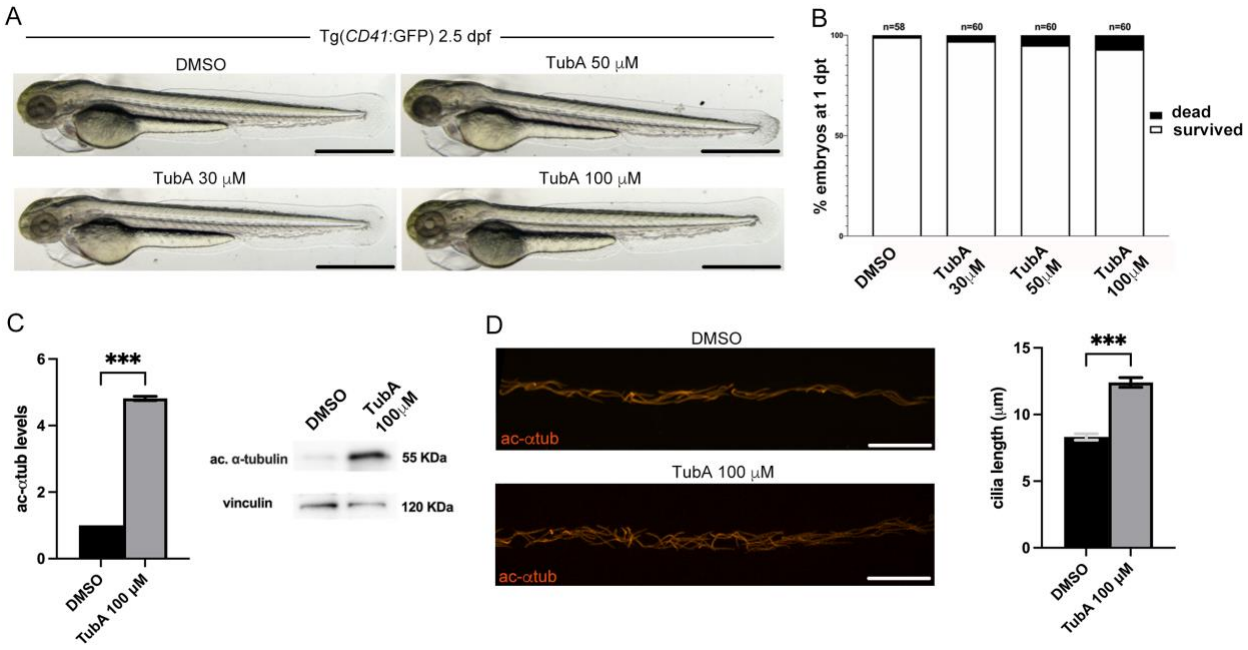

Fig. 11: Validation of HDAC6 inhibition in zebrafish. A) Morphological evaluation and **B**) survival of embryos treated with different doses of TubA. **C**) Western-blot analyses of the ac-α-tubulin levels and relative quantification. **D**) IF analyses of the cilia in the pronephric region and measurement of their length through the ImageJ software (n=3). Unpaired T-test with Welch correction. ***p<0.001. Results are presented as mean ± SEM. Scale bar indicates 5 mm in A and 100 μm in D. n indicates the number of embryos analyzed; dpt: days post treatment; TubA: TubastatinA.

All together, these data indicated that TubA has no toxic effect in our model system and efficiently blocks the deacetylase activity of the endogenous Hdac6 increasing the levels of the main Hdac6 target acetylated-α-tubulin. Moreover, TubA administration *in vivo*

modulated the ciliogenesis, a process in which HDAC6 has been described to play a pivotal role (127).

4. Cyclopamine administration rescues the *Hh* hyperactivation in the zebrafish model with *shh* mRNA overexpression.

According to a previous work of our group, we decided to use 5 μM of cyclopamine as working dose (128). However, this dose has been administrated with a different procedure and we investigated if 5 μM of cyclopamine was sufficient in blocking the *Hh* signaling transduction in our experimental setting and in the zebrafish model with *Hh* hyperactivation. Therefore, embryos of the *Tg(CD41:GFP)* transgenic line injected with the *shh* mRNA were incubated with 5 μM of cyclopamine from the stage of 1.5 to 2.5 dpf. By means of RT-qPCR we verified that in *shh* mRNA overexpressed embryos and treated with 5 mM of cyclopamine the expression levels of the *Hh* signaling target genes (*gli1a*, *ptch1*) were significantly reduced in comparison to *shh* mRNA embryos treated with the DMSO (Fig.12A-B). These data indicated that in *shh* mRNA overexpressed embryos, 5 μM cyclopamine efficiently rescued the *Hh* signaling hyperactivation.

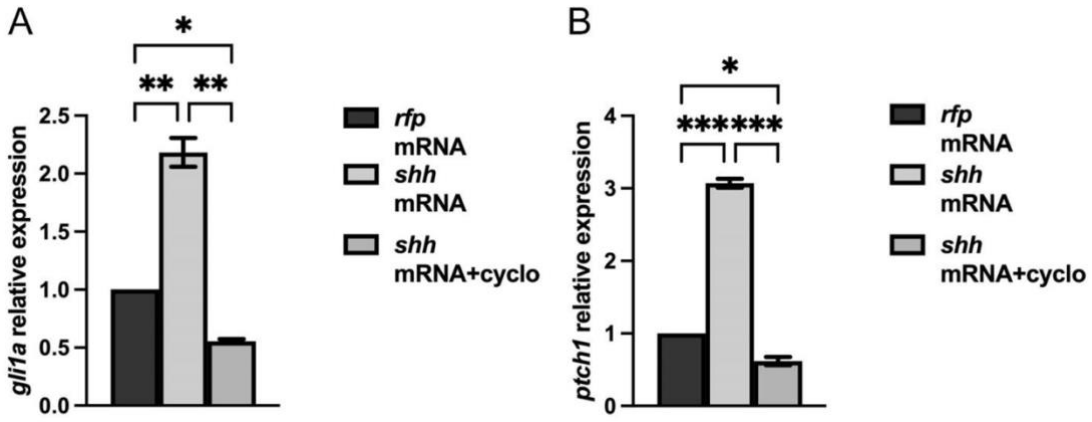

Fig. 12: Validation of the efficacy of *Hh* inhibition in the zebrafish model with *Hh* upregulation. Real-time qPCR analyses of the *Hh* target genes (A) *gli1a,* (B) *ptch1* in controls (*rfp*-mRNA), *Hh* overexpressed (*shh*-mRNA injected), and cyclopamine treated embryos. ONE-way ANOVA with Tukey post hoc correction. ***p<0.001; **p<0.01; *p<0.05. cyclo: cyclopamine.

5. HSPCs expansion is rescued by HDAC6 specific inhibition.

To evaluate the effects of drugs administration on HSPCs we treated *Tg(CD41:GFP) shh* mRNA injected embryos with 5 μM of cyclopamine or 100 μM of TubA from the stage of 1.5 dpf and performed IF analyses one day later. We confirmed that *shh* mRNA injection determines a significant expansion of the HSCPs in comparison to control embryos injected with *rfp* mRNA and treated with the solvent DMSO (Fig.13A-B). Surprisingly, the increased number of HSPCs in the CHT of *Hh* overexpressing embryos, was not rescued by cyclopamine treatment (Fig.13C). On the contrary, we achieved the reduction of the HSPCs to levels comparable to the controls when *shh* mRNA embryos were treated with the HDAC6 inhibitor (Fig.13D). The increase of the HSPCs in *Hh* overexpressing embryos and the effect of the pharmacological treatment were also quantified through FACS analyses on the GFP^{low}-CD41 cells (Fig.13E-F).

To further characterize the effects of cyclopamine and TubA administration in *Hh* overexpressing embryos, we performed RT-qPCR analyses. As expected, the HSPCs marker *cmyb* was increased in *shh* mRNA injected embryos and only TubA administration, restored *cmyb* expression to levels comparable to the controls (Fig.13G). Cyclopamine did not elicited such reduction even though its administration efficiently achieved the inhibition of the Hh signaling as the target genes *gli1a* and *ptch1* were significantly reduced (Fig.13H-I). Interestingly, we found that TubA administration elicited an inhibitory effect on *ptch1* expression, suggesting a feed-back loop activity among them (Fig.13I). The expression of the multi-drug-resistance genes *abcc1* and *asxl1*, increased in *Hh* overexpressing embryos, was instead reduced by both TubA and cyclopamine thus indicating that their expression is regulated by both *Hh* signaling and HDAC6 (Fig.13J-K).

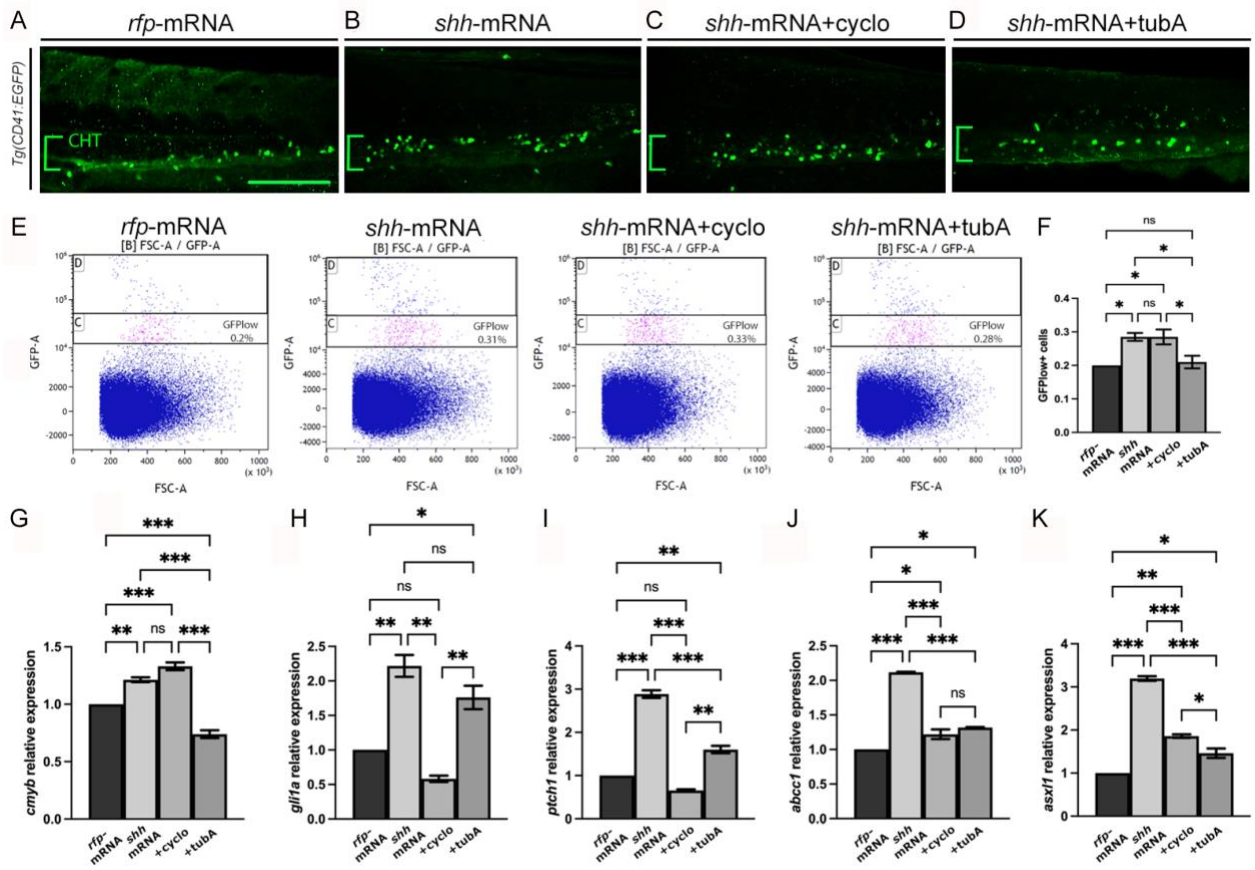

Fig. 13: Effects of *Hh* and HDAC6 inhibition. A-D) Confocal images of the caudal hematopoietic tissue (CHT) of 2.5 dpf embryos (n=6) of the *Tg(CD41:GFP)* transgenic line: **A**) control embryos injected with r*fp* mRNA or with (**B**) *shh* mRNA and treated with (**C**) cyclopamine or (**D**) TubastatinA. **E**) FACS analyses of the GFPl^{ow}-CD41 cells and (**F**) quantification. **G-K**) RT-qPCR analyses of (**G**) *cmyb,* (**H**) *gli1a*, (**I**) *ptch1* and the Multi-Drug-Resistance genes (**J**) *abcc1* and (**K**) *asxl1*. ONE-way ANOVA with Tukey post hoc correction. ***p<0.001; **p<0.01; *p<0.05; ns not significant. Results are presented as mean ± SEM. Scale bar indicates 100 µm. cyclo: cyclopamine; TubA: TubastatinA.

6. HSPCs expansion is due to their increased proliferation

To determine if HSPCs expansion depended on an increased proliferation we performed phospho-histone H3 immunofluorescence analyses evaluating the proliferation rate of the HSPCs, indicated as the percentage of double positive HSPCs/3PH on the total of HSPCs. We found that *Hh* overexpressing embryos showed more proliferating HSPCs in the CHT in comparison to the control embryos (Fig.14A-B; E). The proliferation rate was reduced only when embryos were treated with TubA and not with cyclopamine (Fig.14C-D; E). These data indicate that the HSPCs expansion is due to an increase proliferation and that this process in mainly mediated by HDAC6.

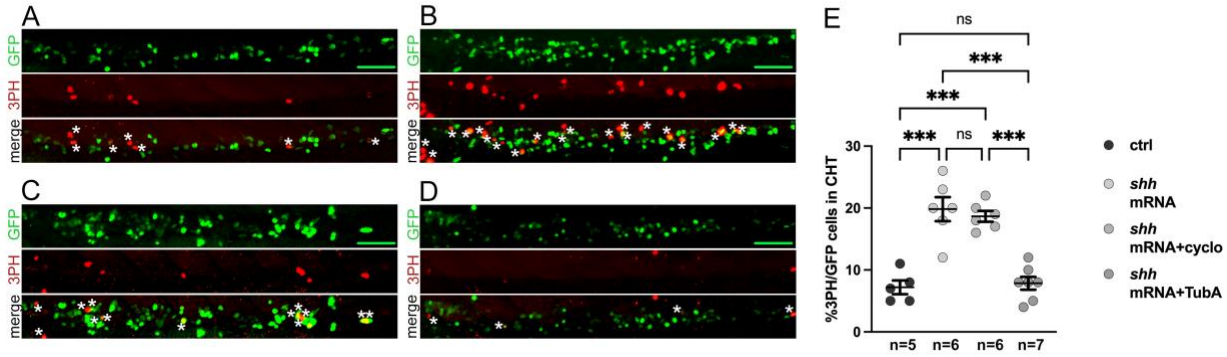

Fig. 14: *Hh* mediated hyperproliferation and pharmacological treatments. **A-D**) Confocal images of the caudal hematopoietic tissue (CHT) of the *Tg(CD41:GFP)* zebrafish embryos at 2.5 dpf; (A) control embryos (n=5), (B) *shh* mRNA, and *shh* mRNA (n=6) treated with (**C**) cyclopamine (n=6) or (**D**) TubastatinA (n=7). Asterisks indicate the double GFP/3PH cells. (**E**) quantification of HSPCs proliferative rate. ONE-way ANOVA with Tukey post hoc correction. ***p<0.001; ns not significant. Results are presented as mean ± SEM. Scale bar indicates 100 µm. cyclo: cyclopamine; TubA: TubastatinA; n:number of embryos analyzed.

7. HDAC6 drives HSPCs expansion in zebrafish

To assess the functional role of HDAC6 in the HSPCs population we generated a zebrafish model with the overexpression of the human *HDAC6* mRNA in *Tg(CD41:GFP)* embryos and evaluated the hematopoietic phenotype. We count the number of GFP^+ HSPCs cell in the CHT od 2.5 dpf embryos and confirmed the expansion of the cell population in *HDAC6* overexpressing embryos in comparison to *rfp* mRNA injected controls (Fig.15A). Moreover, TubA administration rescued the hematopoietic defect confirming the specificity of the phenotype (Fig.15A). By means of IF analyses with the phospho-histone H3 antibody we found that the proliferation rate of the HSPCs was increased in *HDAC6* overexpressing embryos, in comparison to uninjected controls embryos, and specifically reduced upon TubA administration (Fig.15B-E). These data identify HDAC6 as a player that controls the proliferation of the HSPCs in zebrafish.

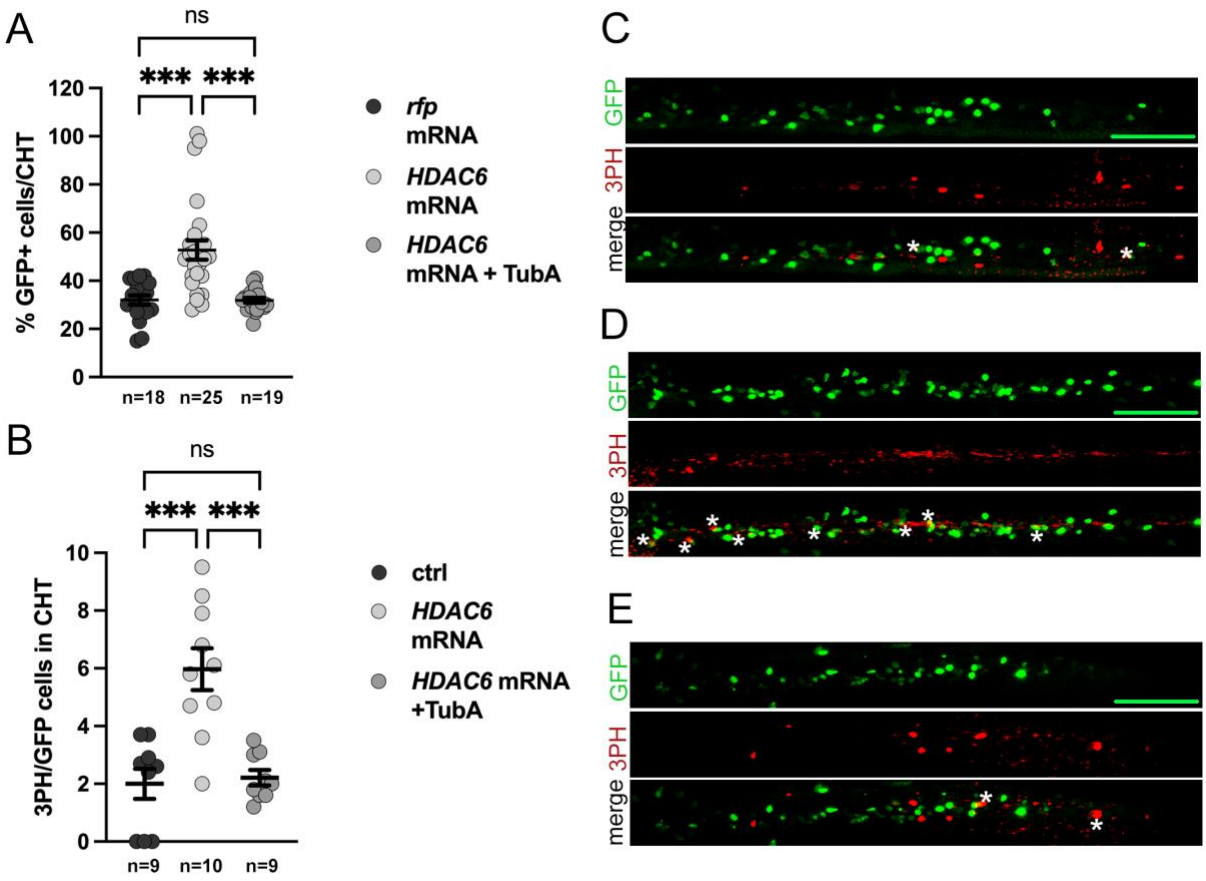

Fig. 15: *HDAC6* overexpression induces HSPCs hyperproliferation. **A**) Graph dot summarizing the number of HSPCs in the CHT of control *rfp* mRNA injected embryos, *HDAC6* mRNA injected embryos and *HDAC6* mRNA injected embryos treated with TubastatinA. **B**) Percentage of proliferating HSPCs in control embryos, *HDAC6* mRNA injected embryos and *HDAC6* mRNA injected embryos treated with TubastatinA. **C**-**E**) Confocal images of the caudal hematopoietic tissue (CHT) of the *Tg(CD41:GFP)* zebrafish embryos at 2.5 dpf; (**C**) control embryos (n=9), (**D**) *HDAC6* mRNA (n=10), and (**C**) *HDAC6* mRNA (n=9) treated with TubastatinA. Asterisks indicate the double GFP/3PH cells. ONE-way ANOVA with Tukey post hoc correction. ***p<0.001; ns not significant. Results are presented as mean ± SEM. Scale bar indicates 100 µm. TubA: TubastatinA; n: number of embryos analyzed.

8. Zebrafish HSPCs present the primary cilium

Cell proliferation is dependent on the presence/absence of the primary cilium on the cell membrane, and HDAC6 drives the disassembly of these structure through its α-tubulin deacetylase activity (69). Therefore, HDAC6 might regulates HSPCs proliferation controlling the stability of the primary cilium. Notably, in zebrafish the primary cilium has been detected in the hemogenic endothelium prior to the developmental stage of 28 hpf (129) but no data are described about the presence of the primary cilium in the HSPCs. By FACS-sorting HSPC-GFP^{low} cells from 2.5 dpf *Tg(CD41:GFP)* embryos ,we shoved the presence of the

primary cilium, labelled with the acetylated-α-tubulin antibody, in these cells (Fig.16). This data suggests that the rescue of the HSPCs expansion through TubA administration might depends on block of the cilium disassembly in these cell population.

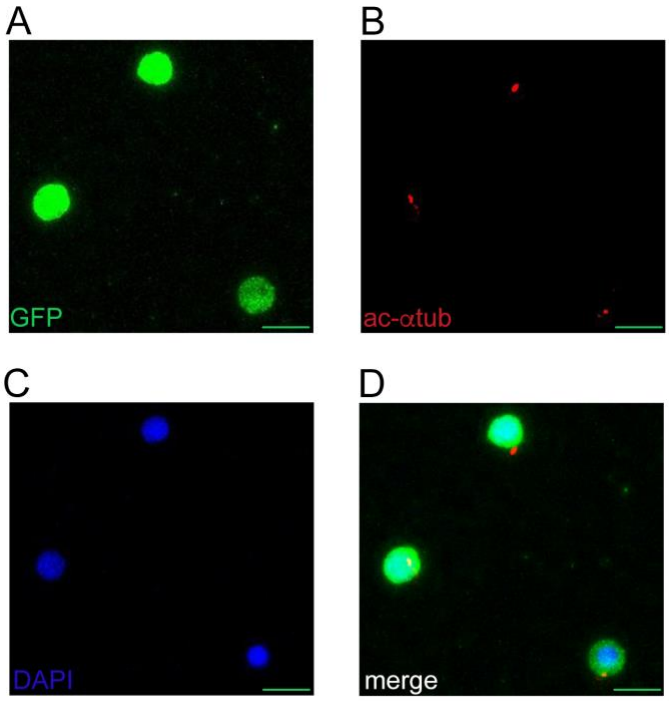

Fig.16: Primary cilium on zebrafish HSPCs.**A-D**) Immunofluorescence analyses of sorted HSPC-GFP^{low} cells: **A**) CD41 GFP; signal; **B**) acetylated α-tubulin labelling the PC; **C**) DAPI; **D**) merge of the channels. Scale bar indicates 10 µm.

9. HDAC6 inhibition reduces the viability of leukemic cell lines

To investigate the effects of *Hh*/HDAC6 inhibition to human model, we decided to perform the pharmacological treatments on human myeloid cell lines. We performed RT-qPCR analyses on a sub-set of AML cell lines and chose four lines with different *Hh* expression and *HDAC6* expression. In detailed, we selected the U937 and THP-1 cell lines which showed higher *Hh* and *HDAC6* expression in comparison to the OCI-AML2 and NB-4 cell lines (Fig.17A-C). We also verified that the *HDAC6* expression was inversely correlated to the levels of acetylated-α-tubulin, thus confirming that *HDAC6* expression reflects HDAC6 activity in these cells (Fig.17D). Moreover, we showed that also the expression of the *MDR* genes was higher in the U937 and THP-1 cell lines in comparison to the OCI-AML2 and NB-4 cell lines (Fig.17E-F). All together, these data confirm *in-vitro* the presence of the positive correlation between *Hh/HDAC6/MDRs*.

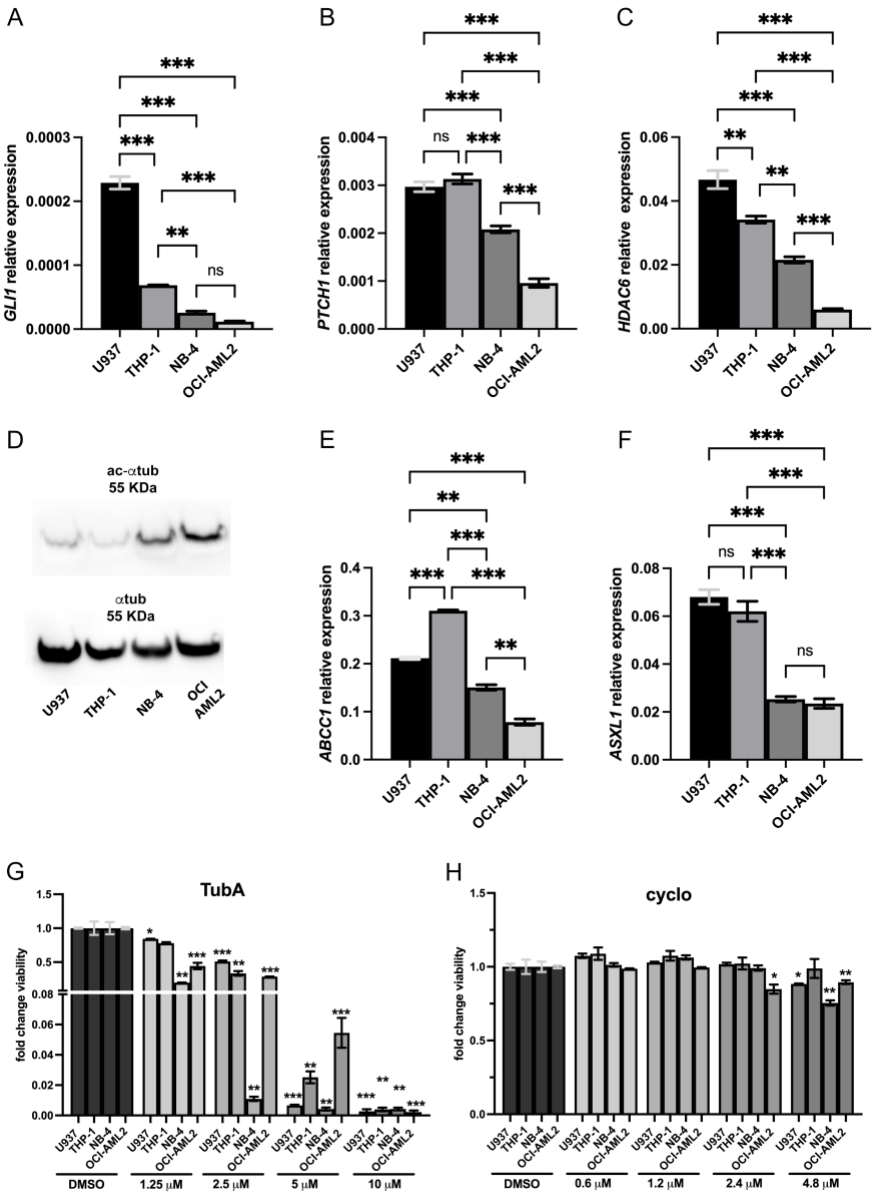

Fig. 17: *Hh/HDAC6/MDRs* expression and effects of cyclopamine and TubastinA tadministration in the U937, THP1, NB-4 AML and OCI-AML2 cell lines. A-C) Real-time qPCR analyses of (**A**) *GLI1*, (**B**) *PTCH1*, (**C**) *HDAC6*, (**D**) *ABCC1*, (**E**) *ASXL1*. (**D**) Western-blotting analyses of the ac-α-tubulin protein levels in comparison to the total α-tubulin protein levels. **E-F)** Real-time qPCR analyses of (**E**) *ABCC1* and (**F**) *ASXL1***G-H)** Analyses of cytostatic and cytotoxic effect of cyclo and TubA in AML cell lines. **G-H) C**ell lines were treated for 72 hours with different concentration of (**G**) TubastatinA or (**H)** cyclopamine; DMSO at the higher dose was used as a control. CTG assay was used to assess the effect of the treatment on the cell viability. For Real-time qPCR ONE-way ANOVA with Tukey post hoc correction was performed. Instead, unpaired T-test with Welch correction was used for (**G**-**H**); for simplicity only data with $p<0.05$ are shown. ***$p<0.001$; **$p<0.01$; *$p<0.05$; ns not significant. Results are presented as mean ± SEM.

To exploit the effects of HDAC6 and *Hh* inhibition, we treated these cells with increasing concentrations of TubA and cyclopamine and evaluated their viability through the CTG luminescence assay, an indicator of metabolically active cells. We found that TubA decreased cell viability (Fig.17G), with higher efficacy in NB-4 cell lines, considered good responders due to their low *Hh* and *HDAC6* expression. On the contrary, cyclopamine did not significantly impact on cell viability, apart with the higher dose we tested (Fig.17H). These data indicate that only HDAC6 inhibition significantly reduced leukemic cells viability, in line with what described in the zebrafish model.

10. *Hh* and *HDAC6* expression in *NPMc+* and *FLT3-ITD* leukemic cell lines

It has been described that AML patients carrying the *FLT3-ITD* mutation show the hyperactivation of the *Hh* signaling pathway in comparison to those carrying the wild-type *FLT3* form (130). We selected the MV4.11 AML line with FLT3-ITD mutation to address if the *Hh* signaling hyperactivation was correlated to an increased *HDAC6* expression and compare them to the OCI-AML3 cell line carrying the *NPMc+* mutation. Through RT-qPCR analyses we verified that both *Hh* signaling target genes and *HDAC6* were significantly increased in MV4.11 AML cell line in comparison to the OCI-AML cells (Fig.18A-C).

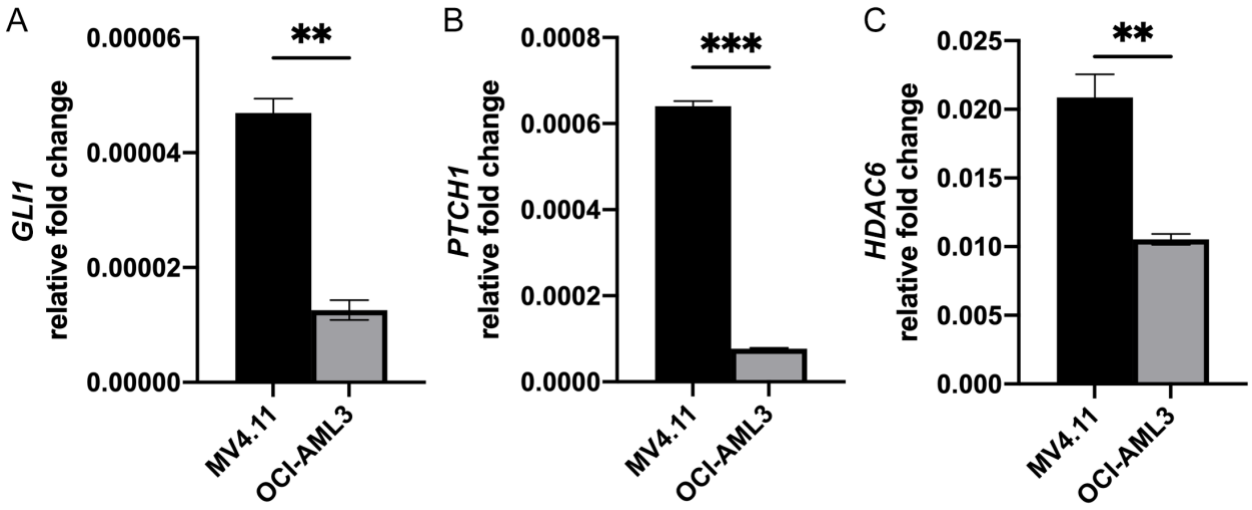

Fig. 18: *Hh/HDAC6* expression *FLT3-ITD* and *NPMc+* AML cell lines. A-C) Real-time qPCR analyses of (**A**) *GLI1*, (**B**) *PTCH1*, (**C**) *HDAC6*, (**D**) *ABCC1*, (**E**) *ASXL1*. Unpaired T-test with Welch correction ***p<0.001; **p<0.01. Results are presented as mean ± SEM.

Our results confirmed that the *Hh/HDAC6* genetic regulation is present also in specific AML condition and that both *Hh* signaling and *HDAC6* expressions are significantly increased in the presence of *FLT3-ITD* mutation.

11. HDAC6 inhibition rescues HSPCs expansion in two zebrafish AML models

We decided to test the effects of *Hh* or HDAC6 inhibition in two well-established zebrafish models of AML carrying the forced expression of the human *NPMC+* and *FLT3-ITD* mRNAs. We verified, in line with what descried in literature, that their overexpression elicited the expansion of HSPCs in the CHT of 2.5 dpf *Tg(CD41:GFP)* (Fig.19A-B).

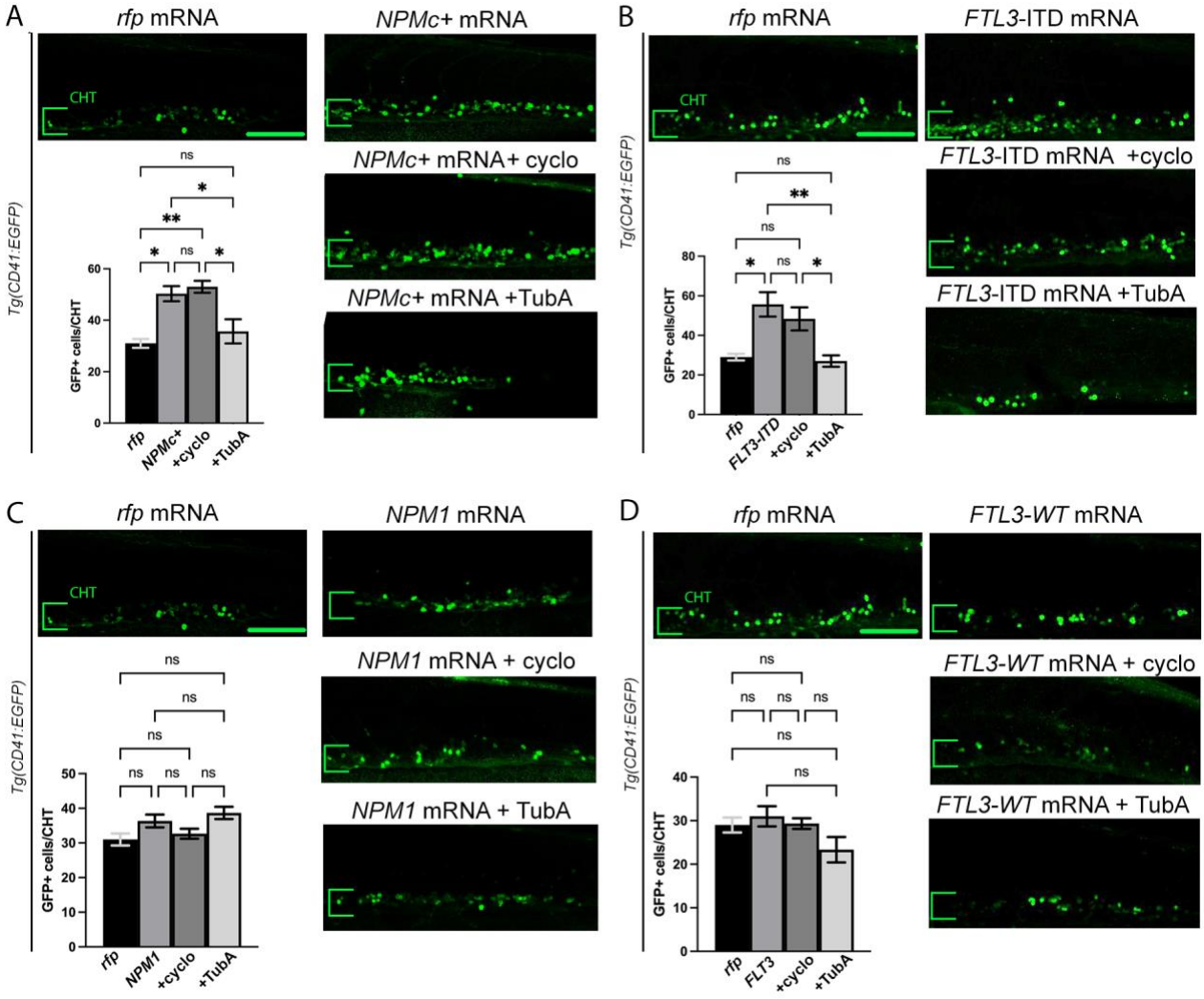

Fig. 19: HDAC6 and *Hh* inhibition in the *NPMc+* and *FLT3-ITD* zebrafish models of AML. A-E) Confocal images of the caudal hematopoietic tissue (CHT) of the *Tg(CD41:GFP)* zebrafish embryos at 2.5 dpf and quantification of the HSCs number (histograms). **A**) *NPMc+* model, **B**) *FLT3-ITD* model, **C**) *NPM1* model and **D**) *FLT3* model. Embryos injected with the mutant (*NPMc+* or *FLT3-ITD*) or the wild-type (*NPM1* or *FLT3*) mRNAs were treated with TubastatinA or cyclopamine and compared to controls embryos injected with the *rfp*-mRNA. In all models, 3 embryos were analyzed for each category. ONE-way ANOVA with Tukey post hoc correction. **p<0.01; **pz0.05; ns not significant. Results are presented as mean ± SEM. Scale bar indicates 100 µm. TubA: TubastatinA.

As expected, the overexpression of the wild-type forms (*NPM1a* and *FLT3*) did not induce HSPCs expansion in the CHT (Fig.19C-D). The administration of TubA reduced the number of HSPCs in both the *NPMC+* and *FLT3-ITD* overexpressing embryos, while cyclopamine did not rescue the hematopoietic phenotype (Fig.19A-B). However, HDAC6 inhibition did not reduced the number of HSPCs in the CHT of the embryos with the overexpression of the wild-type forms (Fig.19C-D).

These data confirmed the efficacy of TubA administration in the reduction of HSPCs and indicate that HDAC6 inhibition might be active only on proliferating HSPCs.

12. Synergistic effects of TubA and cytarabine combination therapy in the zebrafish models of AML.

The use of combination treatments is considered an attractive strategy for the treatment of several cancers, including AML. Therefore, we treated the AML zebrafish models with TubA and the chemotherapic agent cytarabine to assess if the combined administration might improve the HSPCs reduction. We performed the drugs administration in a combination setting selecting doses which did not rescue the HSPCs expansion: 50 μM TubA and 50 μM cytarabine. In both AML models, we found that TubA or cytarabine administration, which not diminished the number of HSPCs in the CHT when administrated singularly, significantly reduced HSPCs expansion in the combination setting (Fig.20A-B). Notably, we did not obtain any HSPCs reduction in the combination therapy based on cyclopamine (2.5 μM) and cytarabine administration (Fig.20A-B). These analyses indicate that the administration of HDAC inhibitors might improve the antiproliferative activity of the coμμon chemotherapic agents.

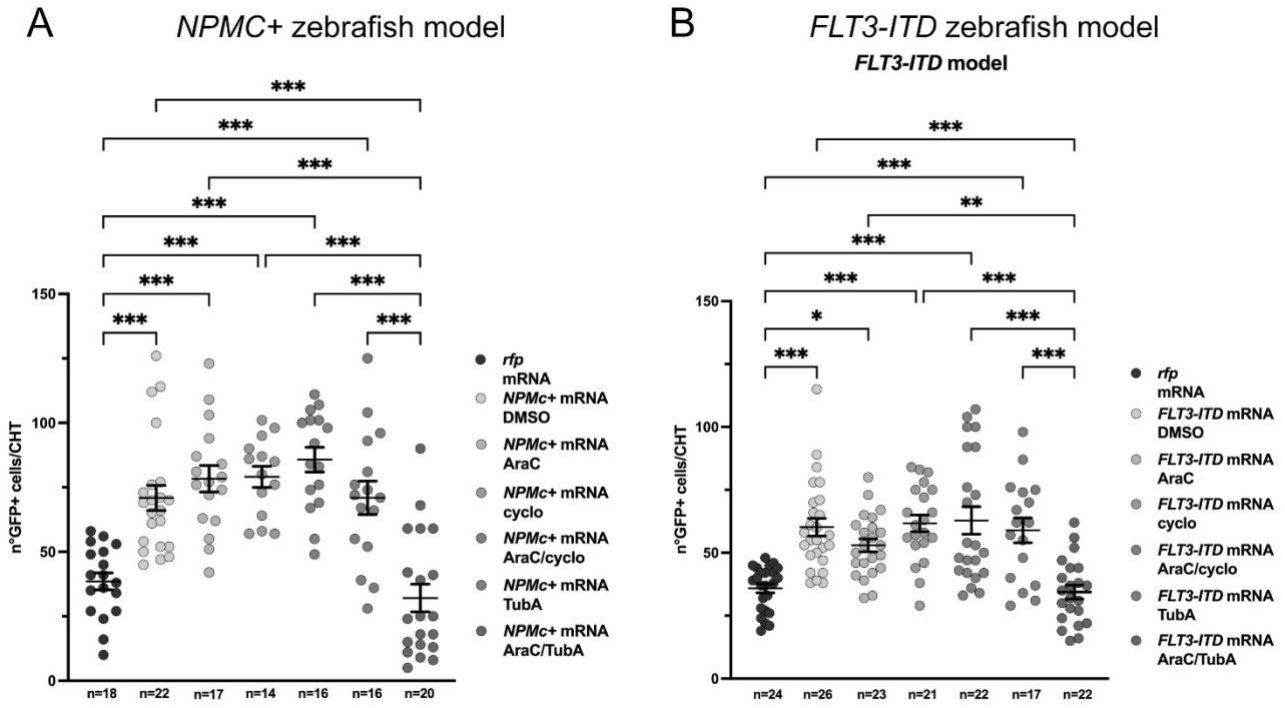

Fig. 20: Combination therapy in the *NPMc+* and *FLT3-ITD* zebrafish models of AML A-B) Count of the HSPCs in the caudal hematopoietic tissue (CHT) of the *Tg(CD41:GFP)* zebrafish embryos at 2.5. **A**) *NPMc+* model, **B**) *FLT3-ITD* model. Embryos injected with the mutant *NPMc+* or *FLT3-ITD* mRNAs were treated with 50 μM cytarabine, 50 μM TubastatinA, 2.5 μM cyclopamine alone or in combination setting. ONE-way ANOVA with Tukey post hoc correction. ***p<0.001; **p<0.01; **pz0.05. Results are presented as mean ± SEM. Scale bar indicates 100 μm. AraC: cytarabine; cyclo: cyclopamine; TubA: TubastatinA. n indicates the number of embryos analyzed.

DISCUSSION AND CONCLUSION

Acute myeloid leukemia (AML) identifies a group of hematological malignancies characterized by the uncontrolled proliferation of immature myeloid cells. AML is currently curable only in 35-40% of patients under 60 years of age and only in 5–15% of patients older than 60 years (131), and nearly 60% of elderly patients fail in inducing chemotherapy due to recurrence, and >85% of patients fail in treatment (56). Leukemic blasts carry genetic and epigenetic changes causative of alterations in cell proliferation, cell death and differentiation (132). Even though the pathogenetic role of specific genetic alterations has been recognized, in most cases, the mechanisms at the basis of AML development are unknown.

Among the pathways that are involved in AML insurgence there is the *Hh* signaling. Indeed, the hyperactivation of the *Hh* signaling supports the expansion of the leukemic blasts (57). Moreover, the activation of the *Hh* signaling pathway correlates with worst outcome in AML patients, conferring Multi-Drug-Resistance (MDR) to standard therapies (59) and decreasing event-free and overall survival (133). The mechanisms at the basis of MDR are only partially understood. To date, it has been demonstrated by *in vitro* studies using AML cell lines, that GLI1 upregulation confers resistance, reducing the efficacy of chemotherapy agents through UGT1A-mediated glucuronidation (134).

Different clinical trials are testing the repositioning of *Hh* inhibitors from solid tumors to AML patients, such as the SMO inhibitors vismodegib and sonidegib. However, despite promising results in pre-clinical analyses, they showed minimal clinical efficacy in patients without improvement in the overall or median survival (135). Only one *Hh* inhibitor (gladegib) has been approved by the Federal Drug Administration (FDA) for the treatment of AML patients. Clinical trials demonstrated that glasdegib administration in combination with low doses of cytarabine significantly increases the overall survival of AML patients (136). The dissection of the *Hh* signaling transduction roles in the development of the leukemic condition might lead to the identification of new therapeutic targets to improve the treatment of AML patients.

The hyperactivation of the *Hh* pathway leads to increased expression of target genes including those involved in the *Hh* signaling transduction such as *GLI1* and *PTCH1* (137). Therefore, to elucidate the *Hh/MDRs* interplay we analyzed their expression levels of *Hh* target genes and *MDR* genes in cohort of 36 adult AML individuals with AML. We excluded from the analyses patients' samples carrying deletion or lacking the chromosome X in which there is the *HDAC6* locus. In literature, expression analyses revealed that an increase in *Hh*

signaling leads to the increased expression of its downstream effectors *SMO* and *GLI*1 in AML cells, especially in radiation-resistance myeloid leukemia cells (59) (138). Accordingly, we described that in our cohort of AML patients, the expression levels of *GLI1* and *PTCH1* and of the *MDR* genes *ABCC1* and *ASXL1* were significantly increased and positively correlated in AML samples in comparison to healthy donors. We verified the conservation of this regulatory network in zebrafish, as the hyperactivation of *Hh* signaling determines the increased expression of the zebrafish *MDR* orthologues *abcc1* and *asxl1*. We confirmed the conservation of the *Hh/MDR* molecular circuit also in human AML cell lines, selecting those with high (U937, THP-1) or low (OCI-AML2, NB-4) *Hh* expression. Indeed, we detected higher *MDR* expression in the cell lines with higher *Hh* signaling in comparison to those with lower expression.

To assess the functional role of the *Hh* signaling during hematopoiesis, we took advantage of the zebrafish model system. Indeed, zebrafish represents a robust model for studying hematopoiesis in both physiological and pathological conditions, as the molecular mechanisms and the cell populations underlying this process are evolutionarily conserved (102). Different signaling pathways have been described as crucial mechanisms for the formation of HSPCs (139). For instance, the Notch signaling pathway seems to positively regulates HSPCs expansion. Indeed, the HSPCs markers *runx1* and *cmyb*, were significantly reduced in zebrafish embryos treated with the Notch inhibitor DAPT, or in the *mindbomb* mutants, while they are increased in the *hsp70:gal4;uas:NICD* overexpression system (102). Similarly, the overexpression of the Wnt inhibitor *dkk1b* results in the loss of *runx1* expression in zebrafish embryos (106). The *Hh* signaling has already been described to play a role during definitive zebrafish hematopoiesis, as embryos mutant in the *Hh* pathway or treated with the *Hh* inhibitor cyclopamine fail to form HSPCs (140) Notably, cells of the hemogenic endothelium undergoes to epithelial-to-mesenchymal transition to generate HSPCs (103). This process in vertebrates, is tightly regulated by the *Hh* signaling transduction as it drives the expression of genes involved in this conversion such as *FOXC2* and the *Snail family transcriptional repressor* (141). Here, we described for the first time that the forced hyperactivation of the *Hh* signaling in zebrafish activates the hematopoietic cascade by inducing the hyperproliferation and the consequent expansion of HSPCs, a situation that recapitulates the increase of blast progenitors in AML patients.

Different works indicated that *Hh* inhibition reduces viability of leukemic cells and sensitizes them to conventional chemotherapy (142); (143). We inhibited the *Hh* signaling through the use of cyclopamine which blocks the *Hh* signaling transduction targeting the

SMO receptor (61). The use of cyclopamine in the zebrafish model has been already tested and is efficient in reducing *Hh* signaling activation (144). In these works, cyclopamine is administrated from the early stages of development with doses ranging from 50 to 100 μM The *Hh* signaling was significantly reduced with consequent morphological defects. Our group has already tested that low doses of cyclopamine (5 μM) efficiently reduced *Hh* signaling transduction with minor effects on axial body formation (128). Therefore, we selected 5 μM cyclopamine as the working dose for our experiments. Here we confirmed that cyclopamine efficiently reduces the expression of the of *Hh* target genes *gli1a and ptch1* and of the *MDR* genes also in a zebrafish model with forced activation of the *Hh* signaling. However, the administration of cyclopamine did not rescue the HSPCs expansion, suggesting that *Hh* inhibition is insufficient to restore the downstream molecular mechanism activated by its overexpression. The HSPCs expansion might be explained (and rescued) by other molecular mechanisms.

Therefore, we hypothesized that the hematopoietic defect might depend on the activity of the histone deacetylase HDAC6. Indeed, the *Hh/HDAC6* signaling has been already described in different cancer forms, such as glioblastoma and multiple myeloma (82), but no data are reported about HDAC6 involvement in AML. We demonstrated that *HDAC6* expression is significantly increased and positively correlated with the *Hh* signaling and *MDR* genes in our AML cohort, in zebrafish embryos and in human AML cell lines. Thus, we proposed *HDAC6* as a direct or indirect target of the *Hh* signaling in AML condition and suggested that its dysregulation might contribute to the generation of the leukemic condition and the insurgence of resistance mechanisms to chemotherapy.

Different HDAC6 inhibitors are already used for the treatment of several cancer forms and most of them (i.e., TubastatinA) have been already tested in zebrafish (145). Here we described that HDAC6 is one player in HSPCs expansion, as the administration of the HDAC6 inhibitor TubastatinA counteracts the hyperproliferation of this cell population in the zebrafish model with *Hh* hyperactivation. In multiple myeloma and human pancreatic cancer cells it has been demonstrated that HDAC6 specific inhibition overcomes drug resistance mechanisms (146) (147). Similarly, we demonstrated that HDAC6 inhibition significantly reduces the expression of the *MDR* genes in the *Hh*-overexpressing zebrafish model. HDAC6 inhibition impacts also on the expression of the *Hh* components. Indeed, HDAC6 specific inhibition leads to the reduction of Ptch1 at both mRNA and protein levels in 51A and SU-2 glioblastoma cell lines (148). In line with this observation, we found that HDAC6 inhibition elicited an inhibitory effect on *ptch1* expression.

The role of HDAC6 during hematopoiesis is still under investigation. For instance, it is known that HDAC6 regulates the formation of T cell lymphocytes and red blood cells (149). It was also demonstrated that HDAC6 has a critical role in platelet formation. Indeed, human-derived megakaryocytes in which HDAC6 was pharmacologically inhibited or downregulated, failed in the production of platelets (150). We performed the analyses of the hematopoietic phenotype on *Hh* overexpressing embryos using the *Tg(CD41:GFP)* line in which the expression of the reporter GFP is under the control of the *CD41* promoter (119). In zebrafish, *CD41* is expressed in both the HSPCs and in thrombocytes, the platelet precursors, with different GFP fluorescence intensity, low and high respectively (119). Through FACS analyses, we demonstrated that *Hh* hyperactivation elicited the HDAC6 overexpression, the expansion of the HSPCs, and increased the thrombocytes population. Then, to test the specific effect of HDAC6 hyperactivation on hematopoiesis, we overexpressed the human *HDAC6* mRNA in zebrafish and demonstrated the hyperproliferation of HSPCs. The expansion of this cell population is specifically caused by *HDAC6* overexpression as we rescued the hematopoietic defect through HDAC6 specific inhibition. Interestingly, other members of the HDAC family are involved in hematopoiesis. Indeed, our group has already described the regulation of the HSPCs proliferation by HDAC8. Its overexpression in zebrafish embryos elicited the hyperproliferation and the expansion of the HSPCs, while its specific inhibition through the selective inhibitor PCI-3045 determines the reduction of proliferation and increases apoptosis in HSPCs (132).

In both *Hh* and *HDAC6* overexpressing embryos we detected increased proliferation of the HSPCs suggesting an implication of the primary cilium (PC), the microtubules-based organelle in which the *Hh* signaling is transduced (20). Indeed, the assembly of the PC formation requires the rearrangement of the mother centriole into a basal body, therefore blocking the formation of the mitotic spindle with the consequent reduction in cell proliferation (68). Several works identified HDAC6 as a direct player in cell proliferation, as through it's α-tubulin deacetylase activity drives the disassembly of the PC (69). Cancer cells, defined by uncontrolled proliferation, fail to present the PC (151). For instance, it was demonstrated that the PC is only present on almost 40% of leukemic cells (152). Also, the link between the *Hh* signaling and the PC has been already described in literature. The *wimple* and *flexo* mice mutants which bear mutations in the PC intra-flagellar transport genes I*FT88* and *IFT172* lack in the formation of ventral neural cell types similarly to what described in mice lacking the Gli transcription factors (153) (154). Furthermore, in zebrafish,

the loss of PC leads to defects in *Hh*-dependent patterning similar to what was observed in the mice models (155).

Taking advantage of the zebrafish *Tg(βact:Arl13b–GFP/kdrl:mCherry/runx1:en-GFP)* transgenic line, Zhibin Liu and colleagues described that cells of the hemogenic endothelium region of 28 hpf embryos present the PC (129). Here, by FACS-sorting analyses, we isolated the HSPCs from *Tg(CD41:GFP)* embryos and demonstrated that they presented the PC on their surface. It could be of interest to quantify the percentage of HSPCs that show the PC in *Hh* or HDAC6 overexpressing *Tg(CD41:GFP)* embryos and the effects of HDAC6 inhibition on this cell population. Although we were able to detect the PC in zebrafish HSPCs, in human HSPCs the PC is hard to identify, probably due to technical difficulties in labeling such a delicate structure (152). Therefore, we were not able to investigate the effects on PC of pharmacological treatments. However, to overcome this limitation, we demonstrated that HDAC6 inhibition impairs the process of ciliogenesis of another ciliated organ in zebrafish, the pronephric duct. Indeed, motile cilia of pronephros are longer than the PC and we can easy measure their length as well as their presence/absence. Zebrafish ciliated organs, such as the pronephric region or the optic vesicle, are used for the screening of defects in the process of ciliogenesis. For instance, Lars D. Maerz and colleagues, described the role of the origin recognition complex factors (ORC) in the process of ciliogenesis in zebrafish, analyzing the cilia of the optic vesicle (156).

The blockade of HSPCs proliferation might also be explained by other mechanisms: the expression and localization of the CYLD protein involved in the processes of cell growth and division. Indeed, it has been demonstrated that CYLD-mediated HDAC6 inhibition reduces the rate of cytokinesis, therefore, delaying the cell cycle (82).

To test the potentiality of HDAC6 inhibition in human models, we treated AML cell lines with high (U937, THP-1) or low (OCI-AML2, NB-4) *Hh*/HDAC6 expression and activity. In these cells, similarly to what was observed in the zebrafish models, we demonstrated the efficacy of HDAC6 inhibition in reducing cell viability, especially in AML cell lines characterized by low *Hh*/HDAC6 expression and activity, that, accordingly, represent good responders to HDAC6 inhibition. Our results strongly support the efficacy of HDAC6 inhibition to counteract leukemic cell viability and are in line with previous works in which selective HDAC6 inhibition reduced AML cell viability and proliferation (91). To further address the role of HDAC6 in the reduction of *MDR* genes expression and its interplay with the *Hh* signaling, it could be interesting to evaluate the expression levels of *HDAC6* and the effect of its inhibition in the myeloid HL-60 cell lines that acquired radio- and chemo-

resistance (HL-60/RX and HL-60/ADR, respectively). Indeed, they express higher levels of the *Hh* receptor SMO and the effector GLI1 compared to chemo-sensitive cells (157). To date, we have no data showing the effect of HDAC6 inhibition on PC stabilization in AML cell lines. However, it has been demonstrated that the selective HDAC6 inhibition reduced the proliferation of leukemic cells through the stabilization of the PC on their surface (158).

As HDAC6, also HDAC8 targeted the PC. Indeed, through acetylation profile analyses performed on *HDAC8* overexpressed embryos and those treated with the HDAC8 specific PCI-3045 inhibitor, our group demonstrated that α-tubulin, which is the main component of the axoneme of the PC, is also targeted by HDAC8 (159). Therefore, it could be interesting to assess if HDAC8 inhibition might stabilize the PC on the cell surface in the AML p53-null HL60 line. Indeed, in a recent work, Spreafico and colleagues (132) demonstrated that HDAC8 inhibition induces apoptosis in the THP-1 AML cell lines while HL60, which lacks a functional p53, remains blocked in G0/G1. This is the cell cycle phase in which the PC is formed (160). Interestingly, HDAC6 and HDAC8 present several overlaps such as the cytosolic localization, their overexpression and roles in leukemic conditions, the similarity in their active site structure (161), and their shared key substrate proteins (i.e. α-tubulin) (159). Therefore, it could be interesting to evaluate the effects of HDAC6/HDAC8 dual inhibition. The simultaneous inhibition of these HDACs isoform can be achieved with the co-administration of specific inhibitors or with small molecules able to target both isoforms. Indeed, we are currently testing the effects of new dual-acting small molecules, developed to specifically block the deacetylase activity of both HDAC6 and HDAC8. These compounds have been tested in *in vitro* AML cell lines and show high selectivity at low micromolar concentration. In zebrafish, we found that these compounds are well tolerated and do not induce neither morphological defects, nor increased embryos lethality when compared to the DMSO-treated control embryos. Moreover, we verified that these molecules, *in vivo*, efficiently enhance the levels of the acetylated-α–tubulin. In the future, we will address the efficacy of these dual inhibitors on the HSPCs expansion in the *Hh* and *HDAC6* overexpressed zebrafish embryos.

Recent reports, though the examination of gene expression data sets and primary AML specimens, indicated hyperactivation of *Hh* signaling through *GLI2* overexpression in a specific category of AML patients carrying the *FLT3-ITD* mutation compared to those carrying the wild-type FLT3 form (130). Interestingly, our *in silico* analyses in the TGCA LAML datasets indicated that patients carrying the *FLT3-ITD* mutation show also higher *HDAC6* expression than patients harboring another common mutation in AML: *NPMc+*

mutation. *FLT3* mutation represents the second-hit driver alteration that cooperates with other somatic mutations to ensure the AML progression and, therefore, is an attractive therapeutic target (162). Indeed, selective FLT3-ITD inhibitors are already available, and some of them have been approved by the Federal Drug Administration (163). Despite the potency and the specificity of FLT3 inhibitors, the insurgence of resistance mechanisms represents a significant challenge (164). The origin of these resistance mechanisms to these FLT3 inhibitors is under investigation, even though it has been demonstrated that also the wild-type form of FLT3 may contribute to resistance (165). To note, we have preliminary data indicating that human AML cells (MV4.11) carrying the *FLT3-ITD* mutation show higher expression and activity of HDAC6 in comparison to AML cells (OCI-AML3) with the *NPMc+* mutation. Thus, HDAC6 inhibition might represent an attractive therapeutic strategy to be exploited for these patients. We addressed this point taking advantage of two well-established zebrafish models of AML carrying the overexpression the human *NPMc+* and *FLT3-ITD* transcripts (110) (111). As for *Hh* overexpressing embryos, also in zebrafish AML models we were able to block HSPCs expansion only by administrating the HDAC6 inhibitor TubastatinA and not with the *Hh* selective inhibition through cyclopamine. As a control and according to published data, by injecting the wild-type form of the human transcripts *NPM1* and *FLT3* we did not detect the expansion of HSPC, nor the reduction of the HSPCs population upon TubastatinA administration. These results confirmed the specificity of the HDAC6 inhibitors to target cells that are specifically in active proliferation such as in AML models, without affecting the viability of normal cells (166). It is worth to note that in these zebrafish models of AML, we did not detect any significant differences in the expression of both *Hh* downstream genes and *hdac6,* thus describing for the first time that HDAC6 inhibition might represent a therapeutic strategy to reduce cell proliferation even in conditions in which it is not overexpressed.

Recently, HDAC inhibitors have been proposed alone or combination with other drugs that specifically target proteins that are aberrantly expressed or altered in AML patients. For instance, it has been demonstrated that HDAC8 inhibitors synergize with FLT3 inhibitors to reduce the proliferation of *FLT3-ITD*$^{+}$ AML cells (167). Moreover, it has been demonstrated that the administration of arsenic trioxide (ATO) blocks HDAC6 activity and increases the acetylation of its target HSP90, leading to the proteasome degradation of the FLT3-ITD protein (168). Proteasome inhibitors (i.e., bortezomib), as well, induce FLT3-ITD degradation via autophagy in AML cell lines (169). However, the treatment with bortezomib did not induce a response in murine models of AML (170). The inhibition of HDAC6 in this

combination setting might represent a valuable strategy to be exploited. Indeed, another role of HDAC6 is to bind polyubiquitinated proteins leading to their degradation by autophagy (171). In the contest of AML, pre-clinical studies indicate that the inhibition of ubiquitinated protein degradation by the proteasome system exerts promising effects in reducing the survival of leukemic blasts (172). We speculated that the co-administration of proteasome and HDAC6 inhibitors may induce cellular stress and enhance apoptosis in AML, but the effects of this combination treatment have never been investigated. The use of the zebrafish model will improve the comprehension of these mechanisms. Indeed, *Hh* or *HDAC6* overexpression or inhibition in the *Tg(CMV3:GFP)* zebrafish line (173), which easily enables to follow *in vivo* the progression of the autophagic process, could give new insights of these processes. To date, we have already tested the effects of HDAC6 inhibition on the autophagic process in another tumor system overexpressing HDAC6: the glioblastoma cell lines U87 (174). Our preliminary data indicated that HDAC6 inhibition leads to the block of the autophagic process in U87 cells, impairing the fusion of phagosomes to lysosomes.

Current AML therapy is mainly based on the administration of cytarabine (AraC) and anthracyclines (i.e., daunorubicin) in the induction phase, followed by consolidation therapy during remission (63). Different treatments are under investigation also in clinical trials and, among them, combination therapies are at the leading edge of research. Most of these therapies combine the standard chemotherapic agents with pan-HDACs inhibitors. Unfortunately, due to the lack of isoform specificity, pan-HDACs inhibitors show pleiotropic side effects and did not significantly improve patient outcomes. For instance, two large phase II trials combining the administration of the chemotherapic agent azacytidine with pan-HDAC inhibitors (entinostat or vorinostat) failed to provide any survival benefit compared with azacytidine monotherapy (175). The future challenge for cancer treatment might be the administration of standard chemotherapic agents with HDAC inhibitors that are able to target specific HDAC isoforms. For instance, it was recently described that the co-administration of the chemotherapic agent cytarabine and the HDAC8 selective inhibitor PCI-3045 synergistically reduces AML cell lines viability (132). Several reports (176) also pinpoint that the HDAC6 inhibitors show high potency in reducing cancer cell viability also at low micromolar concentration, and therefore are particularly suitable for combination therapies. For instance, the HDAC6 inhibitor ST80 significantly reduced AML cell viability at low concentration (1 μM) (177). Moreover, HDAC6 specific inhibitors are already in use to treat solid cancers and result in sensitizing cells to chemotherapy (178). The rescue of the hematopoietic phenotype we obtained upon TubastatinA administration in zebrafish AML

and human AML cell lines, indicates that the repositioning of the already available HDAC6 inhibitor in combination therapies might represent a therapeutic strategy for the treatment of AML patients. Indeed, we demonstrated the efficacy of the combination therapy based on the use of TubastatinA and the chemotherapic agents cytarabine in the *NPMc+* and *FLT3-ITD* AML zebrafish models. Through these experiments we demonstrated that in both models the co-administration of subcritical doses of the chemotherapic agents cytarabine together with the HDAC6 inhibitor, led to a significant reduction of the HSPCs population. In contrast, the combination therapy with the selective *Hh* inhibitor cyclopamine does not elicit such effect.

In conclusion, in this work, we demonstrated that also in AML patients both *Hh*, *HDAC6* and *MDR* genes are positively, correlated. Moreover, we confirmed that the *Hh/HDAC6* genetic regulation is evolutionarily conserved and generates a pre-leukemic phenotype in zebrafish, as both *Hh* or *HDAC6* overexpression induces the hyperproliferation and the expansion of the HSPCs population. This aberrant proliferation rate might depend on alteration on the PC that we describe to be present on HSPCs. In addition, as described for *Hh* inhibition, we demonstrated that also HDAC6 inhibition significantly reduces the expression of *MDR* genes allowing us to hypothesize the use of HDAC6 inhibitors to counteract resistance mechanisms in AML patients. We also described the potency of HDAC6 inhibition also in a condition in which it is not overexpressed such as in rescuing the HSPCs increase in zebrafish AML models *NPMc+* or *FLT3-ITD*. Interestingly, HDAC6 inhibition is efficient also in combination therapies with chemotherapic agents.

Zebrafish represent a suitable model for the studying the effects of genetic alterations or pharmacological treatments on HSPCs. In fact, several transgenic lines are available and allow to follow *in vivo* the development of this cell population such as the *Tg(cmyb:GFP), Tg(runx1:GFP)* and the *Tg(CD41:GFP)* transgenic lines (102). This one, that we use for our work, is a well-established tool for to the detection of the HSPCs. An example of the potentiality of this transgenic for screening the effects of pharmacological treatments is described in the work of Mazzola et al (44). An example of the potentiality of this transgenic for screening the effects of pharmacological treatments is described in the work of Mazzola et al (44). In this work, the authors identified the molecular interplay between the mutated NPMc+ and the cohesin regulator Nipbl, but also their synergistic role in driving the hyper-activation of the canonical Wnt/β-catenin signaling pathway specifically in HSPCs. Indeed,

they rescued the HSPCs expansion through the administration of the Wnt inhibitor indomethacin that is currently in trial for human therapy.

The small size and the abundance of embryos make zebrafish suitable for high-throughput screenings (179). Here, we demonstrated that different signaling pathways can be easily modulated simply adding the pharmacological compound directly into the embryo medium. Moreover, the use of transgenic lines enables the rapid analyses of drug effects. Our work suggests that the combined use of zebrafish with human AML cell lines easily allows to carry out pharmacological treatments cutting the time and the cost of pre-clinical analyses. The generation of a zebrafish model of xenotransplantation could be a future step to study *in vivo* the effects of HDAC6 inhibition on cancer progression. Indeed, different studies demonstrated the potentiality of these models to comprehend the effects of pharmacological treatments on the major biological processes involved in cancer progression, such as tumor growth and cell migration (180).

AKNOLEDGMENTS

First, I would like to thank the University of Milan and the PhD course in Experimental Medicine (DMEM) that support my PhD studies. A special thanks to Prof. Nicoletta Landsberger, Prof. Cristina Battaglia and all the secretariat members, for having accompanied these three years with integrative training courses essential for personal scientific growth.

In this PhD, I had the opportunity to undertake several collaborations, which allowed me to implement my knowledge and technical skills. Therefore, I sincerely thank Prof. Paola Viani and Dr. Loredana Brioschi and the group of Prof. Francesco Bifari, members of the BIOMETRA department, with whom I had the pleasure of actively collaborate. Great gratitude also goes to the group of Prof. Franco Taroni, Istituto Neurologico Carlo Besta and to the group of Prof. Claudia Ghigna, CNR Pavia. Thanks to all these collaborations, I have learned how to face a biological problem using different experimental approaches.

A special thank also to Dr. Alberto Rissone (NIH institute) that contributes to improve the quality of my PhD project and submitted paper, underlining the potential critical issues and the strategies to overcome them.

A special thank, which I am aware will never be enough, goes to my tutor Prof Anna Pistocchi. Thanks, Anna, for teaching me that we are still human beings, even in scientific research. In a laboratory, you are never alone. I was lucky enough to meet beautiful people with whom a relationship was born beyond simple working collaboration. I would like to thank all the Pistocchi's team members Mr. Marco Cafora, Mrs. Alessia Brix, Dr. Marco Spreafico, Mrs. Ilaria Gentile, without whom nothing of what I have achieved would have been possible.

A special thank also to Prof Anna Marozzi, trustworthy tutor that directs the practical and theoretical aspects of experimentation and lives all the successes and failures with us.

REFERENCES

1. Echelard Y, Epstein DJ, St-Jacques B, Shen L, Mohler J, McMahon JA, et al. Sonic hedgehog, a member of a family of putative signaling molecules, is implicated in the regulation of CNS polarity. Cell. 1993;
2. Armas-López L, Zúñiga J, Arrieta O, Ávila-Moreno F. The Hedgehog-GLI pathway in embryonic development and cancer: Implications for pulmonary oncology therapy. Vol. 8, Oncotarget. 2017.
3. di Magliano MP, Hebrok M. Hedgehog signalling in cancer formation and maintenance. Vol. 3, Nature Reviews Cancer. 2003.
4. Braun S, Oppermann H, Mueller A, Renner C, Hovhannisyan A, Baran-Schmidt R, et al. Hedgehog signaling in glioblastoma multiforme. Cancer Biology and Therapy. 2012;13(7).
5. Sari IN, Phi LTH, Jun N, Wijaya YT, Lee S, Kwon HY. Hedgehog signaling in cancer: A prospective therapeutic target for eradicating cancer stem cells. Vol. 7, Cells. 2018.
6. Dellovade T, Romer JT, Curran T, Rubin LL. The hedgehog pathway and neurological disorders. Vol. 29, Annual Review of Neuroscience. 2006.
7. Bak M, Hansen C, Tommerup N, Larsen LA. The Hedgehog signaling pathway - Implications for drug targets in cancer and neurodegenerative disorders. Pharmacogenomics. 2003.
8. Lee RTH, Zhao Z, Ingham PW. Hedgehog signalling. Development [Internet]. 2016 Feb 1;143(3):367–72. Available from: https://doi.org/10.1242/dev.120154
9. Briscoe J, Thérond PP. The mechanisms of Hedgehog signalling and its roles in development and disease. Nature Reviews Molecular Cell Biology. 2013.
10. Nozawa YI, Lin C, Chuang PT. Hedgehog signaling from the primary cilium to the nucleus: An emerging picture of ciliary localization, trafficking and transduction. Current Opinion in Genetics and Development. 2013.
11. Sasai N, Toriyama M, Kondo T. Hedgehog Signal and Genetic Disorders. Vol. 10, Frontiers in Genetics. 2019.
12. Varjosalo M, Taipale J. Hedgehog: Functions and mechanisms. Vol. 22, Genes and Development. 2008.
13. Kong JH, Siebold C, Rohatgi R. Biochemical mechanisms of vertebrate hedgehog signaling. Development (Cambridge). 2019.
14. Buglino JA, Resh MD. Hhat is a palmitoylacyltransferase with specificity for N-palmitoylation of Sonic Hedgehog. Journal of Biological Chemistry. 2008;

15. Manikowski D, Kastl P, Grobe K. Taking the Occam's Razor approach to Hedgehog lipidation and its role in development. Vol. 6, Journal of Developmental Biology. 2018.
16. Venugopal N, Ghosh A, Gala H, Aloysius A, Vyas N, Dhawan J. The primary cilium dampens proliferative signaling and represses a G2/M transcriptional network in quiescent myoblasts. BMC Molecular and Cell Biology. 2020;21(1).
17. Nigg EA, Stearns T. The centrosome cycle: Centriole biogenesis, duplication and inherent asymmetries. Vol. 13, Nature Cell Biology. 2011.
18. Basten SG, Giles RH. Functional aspects of primary cilia in signaling, cell cycle and tumorigenesis. Vol. 2, Cilia. 2013.
19. Ke YN, Yang WX. Primary cilium: An elaborate structure that blocks cell division? Vol. 547, Gene. 2014.
20. Bangs F, Anderson K v. Primary cilia and Mammalian Hedgehog signaling. Cold Spring Harbor Perspectives in Biology. 2017;
21. Davies JP, Ioannou YA. Topological analysis of Niemann-Pick C1 protein reveals that the membrane orientation of the putative sterol-sensing domain is identical to those of 3-hydroxy-3-methylglutaryl-CoA reductase and sterol regulatory element binding protein cleavage-activating protein. Journal of Biological Chemistry. 2000;275(32).
22. Gong X, Qian H, Cao P, Zhao X, Zhou Q, Lei J, et al. Structural basis for the recognition of Sonic Hedgehog by human Patched1. Science. 2018;
23. Li J, Wang C, Wu C, Cao T, Xu G, Meng Q, et al. PKA-mediated Gli2 and Gli3 phosphorylation is inhibited by Hedgehog signaling in cilia and reduced in Talpid3 mutant. Developmental Biology. 2017;429(1).
24. Bhatia N, Thiyagarajan S, Elcheva I, Saleem M, Dlugosz A, Mukhtar H, et al. Gli2 is targeted for ubiquitination and degradation by β-TrCP ubiquitin ligase. Journal of Biological Chemistry. 2006;281(28).
25. Yao HHC, Capel B. Disruption of testis cords by cyclopamine or forskolin reveals independent cellular pathways in testis organogenesis. Developmental Biology. 2002;246(2).
26. Mukhopadhyay S, Wen X, Ratti N, Loktev A, Rangell L, Scales SJ, et al. The ciliary G-protein-coupled receptor Gpr161 negatively regulates the sonic hedgehog pathway via cAMP signaling. Cell. 2013;152(1–2).
27. Humke EW, Dorn K v., Milenkovic L, Scott MP, Rohatgi R. The output of Hedgehog signaling is controlled by the dynamic association between Suppressor of Fused and the Gli proteins. Genes and Development. 2010;

28. Szczepny A, Wagstaff KM, Dias M, Gajewska K, Wang C, Davies RG, et al. Overlapping binding sites for importin β1 and suppressor of fused (SuFu) on glioma-associated oncogene homologue 1 (Gli1) regulate its nuclear localization. Biochemical Journal. 2014;461(3).
29. Sigafoos AN, Paradise BD, Fernandez-Zapico ME. Hedgehog/gli signaling pathway: Transduction, regulation, and implications for disease. Cancers. 2021;13(14).
30. Incardona JP, Gruenberg J, Roelink H. Sonic hedgehog induces the segregation of patched and smoothened in endosomes. Current Biology. 2002;12(12).
31. Tukachinsky H, Petrov K, Watanabe M, Salic A. Mechanism of inhibition of the tumor suppressor Patched by Sonic Hedgehog. Proceedings of the National Academy of Sciences of the United States of America. 2016;113(40).
32. Kavran JM, Ward MD, Oladosu OO, Mulepati S, Leahy DJ. All mammalian hedgehog proteins interact with cell adhesion molecule, down-regulated by oncogenes (CDO) and brother of CDO (BOC) in a conserved manner. Journal of Biological Chemistry. 2010;285(32).
33. Hwang SH, White KA, Somatilaka BN, Shelton JM, Richardson JA, Mukhopadhyay S. The G protein-coupled receptor Gpr161 regulates forelimb formation, limb patterning and skeletal morphogenesis in a primary cilium-dependent manner. Development (Cambridge). 2018;145(1).
34. Yue S, Chen Y, Cheng SY. Hedgehog signaling promotes the degradation of tumor suppressor Sufu through the ubiquitin-proteasome pathway. Oncogene. 2009;28(4).
35. Hui CC, Slusarski D, Platt KA, Holmgren R, Joyner AL. Expression of three mouse homologs of the drosophila segment polarity gene cubitus interruptus, Gli, Gli-2, and Gli-3, in ectoderm-and mesoderm-derived tissues suggests multiple roles during postimplantation development. Developmental Biology. 1994;162(2).
36. Peterson KA, Nishi Y, Ma W, Vedenko A, Shokri L, Zhang X, et al. Neural-specific Sox2 input and differential Gli-binding affinity provide context and positional information in Shh-directed neural patterning. Genes and Development. 2012;26(24).
37. Stecca B, Mas C, Clement V, Zbinden M, Correa R, Piguet V, et al. Melanomas require HEDGEHOG-GLI signaling regulated by interactions between GLI1 and the RAS-MEK/AKT pathways. Proceedings of the National Academy of Sciences of the United States of America. 2007;104(14).

38. Riobó NA, Lu K, Ai X, Haines GM, Emerson CP. Phosphoinositide 3-kinase and Akt are essential for Sonic Hedgehog signaling. Proceedings of the National Academy of Sciences of the United States of America. 2006;103(12).
39. Whisenant TC, Ho DT, Benz RW, Rogers JS, Kaake RM, Gordon EA, et al. Computational prediction and experimental verification of new MAP kinase docking sites and substrates including Gli transcription factors. PLoS Computational Biology. 2010;6(8).
40. Wang Y, Hsu JM, Kang Y, Wei Y, Lee PC, Chang SJ, et al. Oncogenic functions of Gli1 in pancreatic adenocarcinoma are supported by its PRMT1-mediated methylation. Cancer Research. 2016;76(23).
41. Mazumdar T, DeVecchio J, Agyeman A, Shi T, Houghton JA. The GLI genes as the molecular switch in disrupting Hedgehog signaling in colon cancer. Oncotarget. 2011;2(8).
42. Singh RR, Cho-Vega JH, Davuluri Y, Shuguang M, Kasbidi F, Milito C, et al. Sonic hedgehog signaling pathway is activated in ALK-positive anaplastic large cell lymphoma. Cancer Research. 2009;69(6).
43. Saultz J, Garzon R. Acute Myeloid Leukemia: A Concise Review. Journal of Clinical Medicine. 2016;
44. Mazzola M, Deflorian G, Pezzotta A, Ferrari L, Fazio G, Bresciani E, et al. NIPBL: A new player in myeloid cell differentiation. Haematologica. 2019;
45. Döhner H, Weisdorf DJ, Bloomfield CD. Acute myeloid leukemia. New England Journal of Medicine. 2015.
46. Bruneau J, Molina TJ. WHO Classification of Tumors of Hematopoietic and Lymphoid Tissues. In 2020.
47. Estey EH. Acute myeloid leukemia: 2019 update on risk-stratification and management. American Journal of Hematology. 2018;93(10).
48. Yu J, Li Y, Li T, Li Y, Xing H, Sun H, et al. Gene mutational analysis by NGS and its clinical significance in patients with myelodysplastic syndrome and acute myeloid leukemia. Experimental Hematology and Oncology. 2020;9(1).
49. di Nardo CD, Cortes JE. Mutations in AML: Prognostic and therapeutic implications. Hematology. 2016;2016(1).
50. Borer RA, Lehner CF, Eppenberger HM, Nigg EA. Major nucleolar proteins shuttle between nucleus and cytoplasm. Cell. 1989;56(3).

51. Federici L, Falini B. Nucleophosmin mutations in acute myeloid leukemia: A tale of protein unfolding and mislocalization. Vol. 22, Protein Science. 2013.
52. Gary Gilliland D, Griffin JD. The roles of FLT3 in hematopoiesis and leukemia. Vol. 100, Blood. 2002.
53. Grafone T, Palmisano M, Nicci C, Storti S. An overview on the role of FLT3-tyrosine kinase receptor in acute myeloid leukemia: Biology and treatment. Vol. 6, Oncology Reviews. 2012.
54. Tao S, Wang C, Chen Y, Deng Y, Song L, Shi Y, et al. Prognosis and outcome of patients with acute myeloid leukemia based on FLT3-ITD mutation with or without additional abnormal cytogenetics. Oncology Letters. 2019;18(6).
55. Ministero della salute. I numeri del cancro in Italia 2019, il rapporto Aiom-Airtum. http://www.salute.gov.it/portale/news/p3_2_1_1_1.jsp?lingua=italiano&menu=notizie&p=dalministero&id=3897. 2019;
56. Zhang J, Gu Y, Chen B. Mechanisms of drug resistance in acute myeloid leukemia. Vol. 12, OncoTargets and Therapy. 2019.
57. Khan AA, Harrison CN, McLornan DP. Targeting of the Hedgehog pathway in myeloid malignancies: still a worthy chase? Vol. 170, British Journal of Haematology. 2015.
58. Döhner H, Estey E, Grimwade D, Amadori S, Appelbaum FR, Büchner T, et al. Diagnosis and management of AML in adults: 2017 ELN recommendations from an international expert panel. Vol. 129, Blood. 2017.
59. Wellbrock J, Latuske E, Kohler J, Wagner K, Stamm H, Vettorazzi E, et al. Expression of hedgehog pathway mediator GLI represents a negative prognostic marker in human acute myeloid leukemia and its inhibition exerts Antileukemic effects. Clinical Cancer Research. 2015;21(10).
60. Kobune M, Takimoto R, Murase K, Iyama S, Sato T, Kikuchi S, et al. Drug resistance is dramatically restored by hedgehog inhibitors in CD34+ leukemic cells. Cancer Science. 2009;
61. Chen JK. I only have eye for ewe: The discovery of cyclopamine and development of Hedgehog pathway-targeting drugs. Vol. 33, Natural Product Reports. 2016.
62. Lauth M, Bergström Å, Shimokawa T, Toftgård R. Inhibition of GLI-mediated transcription and tumor cell growth by small-molecule antagonists. Proceedings of the National Academy of Sciences of the United States of America. 2007;104(20).

63. Aberger F, Hutterer E, Sternberg C, del Burgo PJ, Hartmann TN. Acute myeloid leukemia - Strategies and challenges for targeting oncogenic Hedgehog/GLI signaling. Cell Communication and Signaling. 2017.
64. Terao T, Minami Y. Targeting Hedgehog (Hh) Pathway for the Acute Myeloid Leukemia Treatment. Cells. 2019;
65. Jamieson C, Martinelli G, Papayannidis C, Cortes JE. Hedgehog Pathway Inhibitors: A New Therapeutic Class for the Treatment of Acute Myeloid Leukemia. Blood Cancer Discovery. 2020;1(2).
66. Zhao X, Ponomaryov T, Ornell KJ, Zhou P, Dabral SK, Pak E, et al. RAS/MAPK activation drives resistance to Smo inhibition, metastasis, and tumor evolution in Shh pathway-dependent tumors. Cancer Research. 2015;75(17).
67. Pricl S, Cortelazzi B, Dal Col V, Marson D, Laurini E, Fermeglia M, et al. Smoothened (SMO) receptor mutations dictate resistance tovismodegib in basal cell carcinoma. Molecular Oncology. 2015;9(2).
68. Goto H, Inoko A, Inagaki M. Cell cycle progression by the repression of primary cilia formation in proliferating cells. Cellular and Molecular Life Sciences. 2013.
69. Ran J, Yang Y, Li D, Liu M, Zhou J. Deacetylation of α-tubulin and cortactin is required for HDAC6 to trigger ciliary disassembly. Scientific Reports. 2015;
70. Dhanyamraju PK, Holz PS, Finkernagel F, Fendrich V, Lauth M. Histone deacetylase 6 represents a novel drug target in the oncogenic Hedgehog signaling pathway. Molecular Cancer Therapeutics. 2015;
71. Wu YW, Hsu KC, Lee HY, Huang TC, Lin TE, Chen YL, et al. A novel dual HDAC6 and tubulin inhibitor, MPT0B451, displays anti-tumor ability in human cancer cells in vitro and in vivo. Frontiers in Pharmacology. 2018;
72. Seto E, Yoshida M. Erasers of histone acetylation: The histone deacetylase enzymes. Cold Spring Harbor Perspectives in Biology. 2014;
73. RUIJTER AJM de, GENNIP AH van, CARON HN, KEMP S, KUILENBURG ABP van. Histone deacetylases (HDACs): characterization of the classical HDAC family. Biochemical Journal [Internet]. 2003;370(3):737–49. Available from: http://www.biochemj.org/cgi/doi/10.1042/bj20021321
74. Park SY, Kim JS. A short guide to histone deacetylases including recent progress on class II enzymes. Vol. 52, Experimental and Molecular Medicine. 2020.
75. Eckschlager T, Plch J, Stiborova M, Hrabeta J. Histone deacetylase inhibitors as anticancer drugs. International Journal of Molecular Sciences. 2017.

76. Marks PA, Rifkind RA, Richon VM, Breslow R, Miller T, Kelly WK. Histone deacetylases and cancer: Causes and therapies. Nature Reviews Cancer. 2001;1(3).
77. Hai Y, Christianson DW. Histone deacetylase 6 structure and molecular basis of catalysis and inhibition. Nature Chemical Biology. 2016;12(9).
78. Li T, Zhang C, Hassan S, Liu X, Song F, Chen K, et al. Histone deacetylase 6 in cancer. Journal of Hematology and Oncology. 2018;11(1):1–10.
79. Seidel C, Schnekenburger M, Dicato M, Diederich M. Histone deacetylase 6 in health and disease. Epigenomics. 2015.
80. Skultetyova L, Ustinova K, Kutil Z, Novakova Z, Pavlicek J, Mikesova J, et al. Human histone deacetylase 6 shows strong preference for tubulin dimers over assembled microtubules. Scientific Reports. 2017;
81. Tran ADA, Marmo TP, Salam AA, Che S, Finkelstein E, Kabarriti R, et al. HDAC6 deacetylation of tubulin modulates dynamics of cellular adhesions. Journal of Cell Science. 2007;
82. Sakamoto KM, Aldana-Masangkay GI. The role of HDAC6 in cancer. Journal of Biomedicine and Biotechnology. 2011;2011.
83. Wickström SA, Masoumi KC, Khochbin S, Fässler R, Massoumi R. CYLD negatively regulates cell-cycle progression by inactivating HDAC6 and increasing the levels of acetylated tubulin. EMBO Journal. 2010;
84. Xiang W, Guo F, Cheng W, Zhang J, Huang J, Wang R, et al. HDAC6 inhibition suppresses chondrosarcoma by restoring the expression of primary cilia. Oncology Reports. 2017;38(1).
85. Kovacs JJ, Murphy PJM, Gaillard S, Zhao X, Wu JT, Nicchitta C v., et al. HDAC6 regulates Hsp90 acetylation and chaperone-dependent activation of glucocorticoid receptor. Molecular Cell. 2005;
86. Pandey UB, Nie Z, Batlevi Y, McCray BA, Ritson GP, Nedelsky NB, et al. HDAC6 rescues neurodegeneration and provides an essential link between autophagy and the UPS. Nature. 2007;
87. Boyault C, Gilquin B, Zhang Y, Rybin V, Garman E, Meyer-Klaucke W, et al. HDAC6-p97/VCP controlled polyubiquitin chain turnover. EMBO Journal. 2006;
88. Wang R, Tan J, Chen T, Han H, Tian R, Tan Y, et al. ATP13A2 facilitates HDAC6 recruitment to lysosome to promote autophagosome–lysosome fusion. Journal of Cell Biology. 2019;218(1).

89. Carew JS, Giles FJ, Nawrocki ST. Histone deacetylase inhibitors: Mechanisms of cell death and promise in combination cancer therapy. Cancer Letters. 2008.
90. Bradbury CA, Khanim FL, Hayden R, Bunce CM, White DA, Drayson MT, et al. Histone deacetylases in acute myeloid leukaemia show a distinctive pattern of expression that changes selectively in response to deacetylase inhibitors. Leukemia. 2005 Oct 25;19(10):1751–9.
91. Hackanson B, Rimmele L, Benkißer M, Abdelkarim M, Fliegauf M, Jung M, et al. HDAC6 as a target for antileukemic drugs in acute myeloid leukemia. Leukemia Research. 2012 Aug;36(8):1055–62.
92. Tu H-J, Lin Y-J, Chao M-W, Sung T-Y, Wu Y-W, Chen Y-Y, et al. The anticancer effects of MPT0G211, a novel HDAC6 inhibitor, combined with chemotherapeutic agents in human acute leukemia cells. Clinical Epigenetics. 2018 Dec 29;10(1):162.
93. Robertson AL, Avagyan S, Gansner JM, Zon LI. Understanding the regulation of vertebrate hematopoiesis and blood disorders - big lessons from a small fish. FEBS Letters. 2016 Nov;590(22):4016–33.
94. Lux CT, Yoshimoto M, McGrath K, Conway SJ, Palis J, Yoder MC. All primitive and definitive hematopoietic progenitor cells emerging before E10 in the mouse embryo are products of the yolk sac. Blood. 2008 Apr 1;111(7):3435–8.
95. Zizioli D, Mione M, Varinelli M, Malagola M, Bernardi S, Alghisi E, et al. Zebrafish disease models in hematology: Highlights on biological and translational impact. Biochimica et Biophysica Acta (BBA) - Molecular Basis of Disease. 2019 Mar;1865(3):620–33.
96. Gering M, Rodaway ARF, Göttgens B, Patient RK, Green AR. The SCL gene specifies haemangioblast development from early mesoderm. The EMBO Journal. 1998 Jul 15;17(14):4029–45.
97. de Jong JLO, Zon LI. Use of the Zebrafish System to Study Primitive and Definitive Hematopoiesis. Annual Review of Genetics. 2005 Dec 1;39(1):481–501.
98. Bennett CM, Kanki JP, Rhodes J, Liu TX, Paw BH, Kieran MW, et al. Myelopoiesis in the zebrafish, Danio rerio. Blood. 2001 Aug 1;98(3):643–51.
99. Herbomel P, Thisse B, Thisse C. Zebrafish Early Macrophages Colonize Cephalic Mesenchyme and Developing Brain, Retina, and Epidermis through a M-CSF Receptor-Dependent Invasive Process. Developmental Biology. 2001 Oct;238(2):274–88.

100. Mommaerts H, Esguerra C v., Hartmann U, Luyten FP, Tylzanowski P. Smoc2 modulates embryonic myelopoiesis during zebrafish development. Developmental Dynamics. 2014 Nov;243(11):1375–90.
101. Jin H, Li L, Xu J, Zhen F, Zhu L, Liu PP, et al. Runx1 regulates embryonic myeloid fate choice in zebrafish through a negative feedback loop inhibiting Pu.1 expression. Blood. 2012 May 31;119(22):5239–49.
102. Gore A v., Pillay LM, Venero Galanternik M, Weinstein BM. The zebrafish: A fintastic model for hematopoietic development and disease. WIREs Developmental Biology. 2018 May 13;7(3).
103. Kissa K, Herbomel P. Blood stem cells emerge from aortic endothelium by a novel type of cell transition. Nature. 2010 Mar 14;464(7285):112–5.
104. Zhang Y, Jin H, Li L, Qin FX-F, Wen Z. cMyb regulates hematopoietic stem/progenitor cell mobilization during zebrafish hematopoiesis. Blood. 2011 Oct 13;118(15):4093–101.
105. Bertrand JY, Cisson JL, Stachura DL, Traver D. Notch signaling distinguishes 2 waves of definitive hematopoiesis in the zebrafish embryo. Blood. 2010 Apr 8;115(14):2777–83.
106. Burns CE, Traver D, Mayhall E, Shepard JL, Zon LI. Hematopoietic stem cell fate is established by the Notch–Runx pathway. Genes & Development. 2005 Oct 1;19(19):2331–42.
107. Zhen F, Lan Y, Yan B, Zhang W, Wen Z. Hemogenic endothelium specification and hematopoietic stem cell maintenance employ distinct Scl isoforms. Development. 2013 Oct 1;140(19):3977–85.
108. Yeh J-RJ, Munson KM, Chao YL, Peterson QP, MacRae CA, Peterson RT. AML1-ETO reprograms hematopoietic cell fate by downregulating *scl* expression. Development. 2008 Jan 15;135(2):401–10.
109. Forrester AM, Grabher C, McBride ER, Boyd ER, Vigerstad MH, Edgar A, et al. NUP98-HOXA9-transgenic zebrafish develop a myeloproliferative neoplasm and provide new insight into mechanisms of myeloid leukaemogenesis. British Journal of Haematology. 2011 Oct;155(2):167–81.
110. Bolli N, Payne EM, Grabher C, Lee J-S, Johnston AB, Falini B, et al. Expression of the cytoplasmic NPM1 mutant (NPMc+) causes the expansion of hematopoietic cells in zebrafish. Blood. 2010 Apr 22;115(16):3329–40.

111. He B-L, Shi X, Man CH, Ma ACH, Ekker SC, Chow HCH, et al. Functions of flt3 in zebrafish hematopoiesis and its relevance to human acute myeloid leukemia. Blood [Internet]. 2014 Apr 17;123(16):2518–29. Available from: https://ashpublications.org/blood/article/123/16/2518/32662/Functions-of-flt3-in-zebrafish-hematopoiesis-and
112. Gross S, Cairns RA, Minden MD, Driggers EM, Bittinger MA, Jang HG, et al. Cancer-associated metabolite 2-hydroxyglutarate accumulates in acute myelogenous leukemia with isocitrate dehydrogenase 1 and 2 mutations. The Journal of experimental medicine. 2010 Feb 15;207(2):339–44.
113. Shi X, He B-L, Ma ACH, Guo Y, Chi Y, Man CH, et al. Functions of idh1 and its mutation in the regulation of developmental hematopoiesis in zebrafish. Blood. 2015 May 7;125(19):2974–84.
114. Papaemmanuil E, Gerstung M, Bullinger L, Gaidzik VI, Paschka P, Roberts ND, et al. Genomic Classification and Prognosis in Acute Myeloid Leukemia. New England Journal of Medicine. 2016 Jun 9;374(23):2209–21.
115. Sood R, English MA, Belele CL, Jin H, Bishop K, Haskins R, et al. Development of multilineage adult hematopoiesis in the zebrafish with a runx1 truncation mutation. Blood. 2010 Apr 8;115(14):2806–9.
116. Sun J, Liu W, Li L, Chen J, Wu M, Zhang Y, et al. Suppression of Pu.1 function results in expanded myelopoiesis in zebrafish. Leukemia. 2013 Sep 4;27(9):1913–7.
117. Zhuravleva J, Paggetti J, Martin L, Hammann A, Solary E, Bastie J-N, et al. MOZ/TIF2-induced acute myeloid leukaemia in transgenic fish. British Journal of Haematology. 2008 Nov;143(3):378–82.
118. Walter RB, Othus M, Burnett AK, Löwenberg B, Kantarjian HM, Ossenkoppele GJ, et al. Significance of FAB subclassification of “acute myeloid leukemia, NOS” in the 2008 WHO classification: analysis of 5848 newly diagnosed patients. Blood. 2013 Mar 28;121(13):2424–31.
119. Lin H-F, Traver D, Zhu H, Dooley K, Paw BH, Zon LI, et al. Analysis of thrombocyte development in CD41-GFP transgenic zebrafish. Blood. 2005 Dec 1;106(12):3803–10.
120. Kimmel CB, Ballard WW, Kimmel SR, Ullmann B, Schilling TF. Stages of embryonic development of the zebrafish. Developmental Dynamics. 1995 Jul;203(3):253–310.

121. Kobune M, Murase K, Iyama S, Sato T, Takimoto R, Kawano Y, et al. Cyclopamine Induced Apoptosis in Primary CD34+ Acute Leukemic Cells. Blood. 2009 Nov 20;114(22):3768–3768.
122. Shi L, Huang Y, Huang X, Zhou W, Wei J, Deng D, et al. Analyzing the key gene expression and prognostics values for acute myeloid leukemia. Translational Cancer Research. 2020;9(11).
123. Bresciani E, Broadbridge E, Liu PP. An efficient dissociation protocol for generation of single cell suspension from zebrafish embryos and larvae. MethodsX. 2018;5:1287–90.
124. Livak KJ, Schmittgen TD. Analysis of relative gene expression data using real-time quantitative PCR and the 2-ΔΔCT method. Methods. 2001;
125. Leyk J, Daly C, Janssen-Bienhold U, Kennedy BN, Richter-Landsberg C. HDAC6 inhibition by tubastatin A is protective against oxidative stress in a photoreceptor cell line and restores visual function in a zebrafish model of inherited blindness. Cell death & disease. 2017;
126. He L, Xu W, Jing Y, Wu M, Song S, Cao Y, et al. Yes-Associated Protein (Yap) Is Necessary for Ciliogenesis and Morphogenesis during Pronephros Development in Zebrafish (*Danio Rerio*). International Journal of Biological Sciences. 2015;11(8):935–47.
127. Łysyganicz PK, Pooranachandran N, Liu X, Adamson KI, Zielonka K, Elworthy S, et al. Loss of Deacetylation Enzymes Hdac6 and Sirt2 Promotes Acetylation of Cytoplasmic Tubulin, but Suppresses Axonemal Acetylation in Zebrafish Cilia. Frontiers in Cell and Developmental Biology. 2021;9.
128. Brusegan C, Pistocchi A, Frassine A, della Noce I, Schepis F, Cotelli F. ccdc80-l1 Is Involved in Axon Pathfinding of Zebrafish Motoneurons. PLoS ONE. 2012 Feb 22;7(2):e31851.
129. Liu Z, Tu H, Kang Y, Xue Y, Ma D, Zhao C, et al. Primary cilia regulate hematopoietic stem and progenitor cell specification through Notch signaling in zebrafish. Nature Communications. 2019;
130. Lim Y, Gondek L, Li L, Wang Q, Ma H, Chang E, et al. Integration of Hedgehog and mutant FLT3 signaling in myeloid leukemia. Science Translational Medicine. 2015 Jun 10;7(291).

131. Durst KL, Lutterbach B, Kummalue T, Friedman AD, Hiebert SW. The inv(16) Fusion Protein Associates with Corepressors via a Smooth Muscle Myosin Heavy-Chain Domain. Molecular and Cellular Biology. 2003;23(2).
132. Spreafico M, Gruszka AM, Valli D, Mazzola M, Deflorian G, Quintè A, et al. HDAC8: A Promising Therapeutic Target for Acute Myeloid Leukemia. Frontiers in Cell and Developmental Biology. 2020 Sep 4;8.
133. Bai LY, Chiu CF, Lin CW, Hsu NY, Lin CL, Lo WJ, et al. Differential expression of Sonic hedgehog and Gli1 in hematological malignancies [16]. Vol. 22, Leukemia. 2008.
134. Zahreddine HA, Culjkovic-Kraljacic B, Assouline S, Gendron P, Romeo AA, Morris SJ, et al. The sonic hedgehog factor GLI1 imparts drug resistance through inducible glucuronidation. Nature. 2014;
135. Bixby D, Noppeney R, Lin TL, Cortes J, Krauter J, Yee K, et al. Safety and efficacy of vismodegib in relapsed/refractory acute myeloid leukaemia: results of a phase Ib trial. British Journal of Haematology. 2019 May 11;185(3):595–8.
136. Cortes JE, Heidel FH, Hellmann A, Fiedler W, Smith BD, Robak T, et al. Randomized comparison of low dose cytarabine with or without glasdegib in patients with newly diagnosed acute myeloid leukemia or high-risk myelodysplastic syndrome. Leukemia. 2019 Feb 16;33(2):379–89.
137. Ingham PW. Hedgehog signalling. Vol. 18, Current Biology. 2008.
138. Li X, Chen F, Zhu Q, Ding B, Zhong Q, Huang K, et al. Gli-1/PI3K/AKT/NF-kB pathway mediates resistance to radiation and is a target for reversion of responses in refractory acute myeloid leukemia cells. Oncotarget. 2016 May 31;7(22):33004–15.
139. Zhang C, Patient R, Liu F. Hematopoietic stem cell development and regulatory signaling in zebrafish. Biochimica et Biophysica Acta (BBA) - General Subjects. 2013 Feb;1830(2):2370–4.
140. Gering M, Patient R. Hedgehog Signaling Is Required for Adult Blood Stem Cell Formation in Zebrafish Embryos. Developmental Cell. 2005 Mar;8(3):389–400.
141. Omenetti A, Porrello A, Jung Y, Yang L, Popov Y, Choi SS, et al. Hedgehog signaling regulates epithelial-mesenchymal transition during biliary fibrosis in rodents and humans. Journal of Clinical Investigation. 2008 Sep 18;
142. Fukushima N, Minami Y, Kakiuchi S, Kuwatsuka Y, Hayakawa F, Jamieson C, et al. Small-molecule Hedgehog inhibitor attenuates the leukemia-initiation potential of acute myeloid leukemia cells. Cancer Science. 2016 Oct 2;107(10):1422–9.

143. Sadarangani A, Pineda G, Lennon KM, Chun H-J, Shih A, Schairer AE, et al. GLI2 inhibition abrogates human leukemia stem cell dormancy. Journal of Translational Medicine. 2015 Dec 21;13(1):98.
144. Mich JK, Blaser H, Thomas NA, Firestone AJ, Yelon D, Raz E, et al. Germ cell migration in zebrafish is cyclopamine-sensitive but Smoothened-independent. Developmental Biology. 2009 Apr;328(2):342–54.
145. Leyk J, Daly C, Janssen-Bienhold U, Kennedy BN, Richter-Landsberg C. HDAC6 inhibition by tubastatin A is protective against oxidative stress in a photoreceptor cell line and restores visual function in a zebrafish model of inherited blindness. Cell death & disease. 2017;
146. Sun X, Xie Y, Sun X, Yao Y, Li H, Li Z, et al. The selective HDAC6 inhibitor Nexturastat A induces apoptosis, overcomes drug resistance and inhibits tumor growth in multiple myeloma. Bioscience Reports. 2019 Mar 29;39(3).
147. Park S-J, Joo SH, Lee N, Jang W-J, Seo JH, Jeong C-H. ACY-241, an HDAC6 inhibitor, overcomes erlotinib resistance in human pancreatic cancer cells by inducing autophagy. Archives of Pharmacal Research. 2021 Dec 10;44(12):1062–75.
148. Yang W, Liu Y, Gao R, Yu H, Sun T. HDAC6 inhibition induces glioma stem cells differentiation and enhances cellular radiation sensitivity through the SHH/Gli1 signaling pathway. Cancer Letters. 2018 Feb;415:164–76.
149. Wang P, Wang Z, Liu J. Role of HDACs in normal and malignant hematopoiesis. Molecular Cancer. 2020 Dec 7;19(1):5.
150. Messaoudi K, Ali A, Ishaq R, Palazzo A, Sliwa D, Bluteau O, et al. Critical role of the HDAC6–cortactin axis in human megakaryocyte maturation leading to a proplatelet-formation defect. Nature Communications. 2017 Dec 27;8(1):1786.
151. Higgins M, Obaidi I, McMorrow T. Primary cilia and their role in cancer (Review). Oncology Letters. 2019 Jan 17;
152. Singh M, Chaudhry P, Merchant AA. Primary cilia are present on human blood and bone marrow cells and mediate Hedgehog signaling. Experimental Hematology. 2016;
153. Huangfu D, Liu A, Rakeman AS, Murcia NS, Niswander L, Anderson K v. Hedgehog signalling in the mouse requires intraflagellar transport proteins. Nature. 2003 Nov 6;426(6962):83–7.
154. Motoyama J, Milenkovic L, Iwama M, Shikata Y, Scott MP, Hui C. Differential requirement for Gli2 and Gli3 in ventral neural cell fate specification. Developmental Biology. 2003 Jul;259(1):150–61.

155. Guerra J, Chiodelli P, Tobia C, Gerri C, Presta M. Long-Pentraxin 3 Affects Primary Cilium in Zebrafish Embryo and Cancer Cells via the FGF System. Cancers. 2020 Jul 1;12(7):1756.
156. Maerz LD, Casar Tena T, Gerhards J, Donow C, Jeggo PA, Philipp M. Analysis of cilia dysfunction phenotypes in zebrafish embryos depleted of Origin recognition complex factors. European Journal of Human Genetics. 2019 May 29;27(5):772–82.
157. Queiroz KCS, Ruela-de-Sousa RR, Fuhler GM, Aberson HL, Ferreira C v, Peppelenbosch MP, et al. Hedgehog signaling maintains chemoresistance in myeloid leukemic cells. Oncogene. 2010 Dec 30;29(48):6314–22.
158. Hackanson B, Rimmele L, Benkißer M, Abdelkarim M, Fliegauf M, Jung M, et al. HDAC6 as a target for antileukemic drugs in acute myeloid leukemia. Leukemia Research [Internet]. 2012;36(8):1055–62. Available from: http://dx.doi.org/10.1016/j.leukres.2012.02.026
159. Spreafico M, Cafora M, Bragato C, Capitanio D, Marasca F, Bodega B, et al. Targeting HDAC8 to ameliorate skeletal muscle differentiation in Duchenne muscular dystrophy. Pharmacological Research. 2021 Aug;170:105750.
160. Plotnikova O v., Pugacheva EN, Golemis EA. Primary Cilia and the Cell Cycle. In 2009. p. 137–60.
161. Ho TCS, Chan AHY, Ganesan A. Thirty Years of HDAC Inhibitors: 2020 Insight and Hindsight. Journal of Medicinal Chemistry. 2020 Nov 12;63(21):12460–84.
162. Welch JS, Ley TJ, Link DC, Miller CA, Larson DE, Koboldt DC, et al. The Origin and Evolution of Mutations in Acute Myeloid Leukemia. Cell. 2012 Jul;150(2):264–78.
163. Antar AI, Otrock ZK, Jabbour E, Mohty M, Bazarbachi A. FLT3 inhibitors in acute myeloid leukemia: ten frequently asked questions. Leukemia. 2020 Mar 9;34(3):682–96.
164. Daver N, Cortes J, Ravandi F, Patel KP, Burger JA, Konopleva M, et al. Secondary mutations as mediators of resistance to targeted therapy in leukemia. Blood. 2015 May 21;125(21):3236–45.
165. Daver N, Schlenk RF, Russell NH, Levis MJ. Targeting FLT3 mutations in AML: review of current knowledge and evidence. Leukemia. 2019 Feb 16;33(2):299–312.
166. Lee J-H, Yao Y, Mahendran A, Ngo L, Venta-Perez G, Choy ML, et al. Creation of a histone deacetylase 6 inhibitor and its biological effects. Proceedings of the National Academy of Sciences. 2015 Sep 29;112(39):12005–10.

167. Long J, Jia M-Y, Fang W-Y, Chen X-J, Mu L-L, Wang Z-Y, et al. FLT3 inhibition upregulates HDAC8 via FOXO to inactivate p53 and promote maintenance of FLT3-ITD+ acute myeloid leukemia. Blood. 2020 Apr 23;135(17):1472–83.
168. Wang R, Li Y, Gong P, Gabrilove J, Waxman S, Jing Y. Arsenic Trioxide and Sorafenib Induce Synthetic Lethality of FLT3-ITD Acute Myeloid Leukemia Cells. Molecular Cancer Therapeutics. 2018 Sep;17(9):1871–80.
169. Colado E, Alvarez-Fernandez S, Maiso P, Martin-Sanchez J, Vidriales MB, Garayoa M, et al. The effect of the proteasome inhibitor bortezomib on acute myeloid leukemia cells and drug resistance associated with the CD34+ immature phenotype. Haematologica. 2008 Jan 1;93(1):57–66.
170. Bernot KM, Nemer JS, Santhanam R, Liu S, Zorko NA, Whitman SP, et al. Eradicating acute myeloid leukemia in a MllPTD/wt:Flt3ITD/wt murine model: a path to novel therapeutic approaches for human disease. Blood. 2013 Nov 28;122(23):3778–83.
171. Liang T, Fang H. Structure, Functions and Selective Inhibitors of HDAC6. Current Topics in Medicinal Chemistry. 2019 Feb 12;18(28):2429–47.
172. Csizmar CM, Kim D-H, Sachs Z. The role of the proteasome in AML. Blood Cancer Journal. 2016 Dec 2;6(12):e503–e503.
173. Varga M, Fodor E, Vellai T. Autophagy in zebrafish. Methods. 2015 Mar;75:172–80.
174. Oh S-J, Yang J-I, Kim O, Ahn E-J, Kang WD, Lee J-H, et al. Human U87 glioblastoma cells with stemness features display enhanced sensitivity to natural killer cell cytotoxicity through altered expression of NKG2D ligand. Cancer Cell International. 2017 Dec 10;17(1):22.
175. Bewersdorf JP, Shallis R, Stahl M, Zeidan AM. Epigenetic therapy combinations in acute myeloid leukemia: what are the options? Therapeutic Advances in Hematology. 2019 Jan 11;10:204062071881669.
176. Hackanson B, Rimmele L, Benkißer M, Abdelkarim M, Fliegauf M, Jung M, et al. HDAC6 as a target for antileukemic drugs in acute myeloid leukemia. Leukemia Research. 2012;
177. Hackanson BW, Rimmele L, Jung M, Lübbert M. Selective HDAC6 Inhibition and Antileukemic Activity of the Novel HDAC Inhibitor ST80 in Myeloid Leukemia Cell Lines. Blood. 2009 Nov 20;114(22):4808–4808.
178. Alothaim T, Charbonneau M, Tang X. HDAC6 inhibitors sensitize non-mesenchymal triple-negative breast cancer cells to cysteine deprivation. Scientific Reports. 2021 Dec 26;11(1):10956.

179. Murphey RD, Zon LI. Small molecule screening in the zebrafish. Methods. 2006 Jul;39(3):255–61.
180. Gamble JT, Elson DJ, Greenwood JA, Tanguay RL, Kolluri SK. The Zebrafish Xenograft Models for Investigating Cancer and Cancer Therapeutics. Biology. 2021 Mar 24;10(4):252.

LIST OF FIGURES AND TABLES

APPENDIX

Haematologica
HAEMATOL/2022/280682
Version 1

Targeting <I>Hedgehog</I> and HDAC6 in acute myeloid leukemia using in <I>vitro</I> and zebrafish models

Alex Pezzotta, Ilaria Gentile, Donatella Genovese, Maria Grazia Totaro, Cristina Battaglia, Anskar Leung, Monica Fumagalli, Matteo Parma, Gianni Cazzaniga, Grazia Fazio, Myriam Alcalay, Anna Marozzi, and Anna Pistocchi

Disclosures: All authors declare that they have no conflict of interest. Declaration of interest: none.

Contributions: Alex Pezzotta (AP1), AM, and Anna Pistocchi (AP2) conceived and designed the experiments. AP1 and IG performed the experiments on zebrafish. AP1 and DG performed experiments on AML cells. MGT performed the FACS analyses on zebrafish. MP and MF provided AML patients' samples. GC and GF setup patient material and data for molecular profiling (including karyotype data and RNA). ALYH provided FLT3 and FLT3-ITD plasmids. AP1and CB performed in silico analyses. AP1, IG, AM, and AP2 analyzed the data on zebrafish. DG and MA analyzed the data on AML cells. AP1 and AP2 wrote the manuscript. AP2 supervised the manuscript drafting and the research project. All authors contributed to the article and approved the submitted version.

TITLE: Targeting *Hedgehog* and *HDAC6* in acute myeloid leukemia using *in vitro* and zebrafish models

RUNNING TITLE: Hedgehog and HDAC6 inhibition in AML

AUTHORS: Alex Pezzotta[1], Ilaria Gentile[1], Donatella Genovese[2], Maria Grazia Totaro[3], Cristina Battaglia[1], Anskar Leung Yu Hung[4], Monica Fumagalli[5], Matteo Parma[5], Gianni Cazzaniga[6], Grazia Fazio[6], Myriam Alcalay[2,7], Anna Marozzi[1], Anna Pistocchi[1]

AFFILIATIONS:

1 Dipartimento di Biotecnologie Mediche e Medicina Traslazionale, Università degli Studi di Milano, Milano, Italy

2 Dipartimento di Oncologia Sperimentale, Istituto Europeo di Oncologia IRCCS, Milano, Italy

3 IFOM (FIRC institute of molecular oncology), Milano, Italy.

4 Department of Medicine, LSK Faculty of Medicine, Hong Kong, China

5 Hospital San Gerardo, Clinica Ematologica e Centro Trapianti di Midollo Osseo, Monza, Italy

6 Centro Ricerca Tettamanti, Clinica Pediatrica Università di Milano-Bicocca, Centro Maria Letizia Verga, Monza, Italy.

7 Dipartimento di Oncologia ed Emato-Oncologia, Università degli Studi di Milano, Milano, Italy

CORRESPONDING AUTHOR:

Anna Pistocchi, Department of Medical Biotechnology and Translational Medicine
University of Milan, LITA - Via Fratelli Cervi, 93 - 20090 Segrate (MI) Italy
phone: +39 0250330442
Email: anna.pistocchi@unimi.it

ABSTRACT

In Acute Myeloid Leukemia (AML), dysregulation of *Hedgehog* (*Hh*) signalling, one of the key regulators of cell differentiation, is involved in the development and expansion of leukemic cancer cells. Despite the achievement of response to chemotherapy, the majority of AML patients relapse and new therapeutic approaches are needed. We describe a positive correlation between *Hh*, *HDAC6*, and multidrug resistance genes in a cohort of adult AML patients and in a zebrafish model of *Hh* overexpression. Of note, *Hh* transduces through the membrane of the primary cilium, a structure presented by non-proliferating mammalian cells whose stabilization depends on the activity of HDAC6. In zebrafish *Hh* hyperactivation drives the increased proliferation of the hematopoietic stem and progenitor cells. Interestingly, this phenotype was rescued by the specific inhibition of HDAC6, but not of *Hh*, suggesting an involvement of the primary cilium in hematopoietic stem and progenitor cells. A reduction in vitality was obtained through HDAC6, and not *Hh* inhibition, in leukemic cell lines. Furthermore, using AML zebrafish models, we demonstrated the efficacy of combination therapy with the chemotherapeutic agent cytarabine and HDAC6 inhibition. Our findings open the possibility to reduce the proliferation of leukemic blasts through the inhibition of HDAC6 and cilium stabilization.

ABSTRACT WORD COUNT: 200

INTRODUCTION

The *Hedgehog* (*Hh*) pathway, one of the key regulators of vertebrate development, plays pivotal roles in different processes by controlling the expression of genes involved in cell proliferation, cell cycle, apoptosis and stem cell self-renewal [1,2]. Differently from other molecular mechanisms, this pathway is composed of a series of inhibitory events: in the absence of the *Hh* ligand/s, the transmembrane receptor patched (Ptch) inhibits the activity of smoothened (Smo) [3]. In this condition, suppressor of fused (Sufu) and protein kinase A (PkA) block the processing of the full-length glioma associated oncogenes Gli2/3 into their active forms. The binding of the *Hh* ligand/s to the receptor abrogates these inhibitory reactions, promoting the formation of the Gli1 proteins that enter into the nucleus and drive the transcription of target genes [4].

Hh signaling is also involved in the regulation of adult stem cell-maintenance and its aberrant activation is responsible for the pathogenesis of numerous cancers [5]. In Acute Myeloid Leukemia (AML), the dysregulation of the *Hh* signaling is involved in the development and expansion of leukemic cells and in the response to therapeutic agents [6]. Small molecule inhibitors targeting this pathway (i.e. cyclopamine) have been developed, and promising preliminary results were obtained in cancers that bear mutations in the *Hh* pathway [7]. However, approximately half of the patients with *Hh*-dependent tumors show primary drug resistance or develop secondary drug resistance and, subsequently, tumor relapse [8]. Notably, only one *Hh* inhibitor (glasdegib) has been approved by the FDA as AML therapeutic strategy, in combination with cytarabine [9]. The discovery of new therapeutic targets that modulate the *Hh* signaling might improve the treatment and the survival chances of AML patients.

One characteristic of the *Hh* pathway is its localization on the membrane of primary cilium (PC), a microtubule-based organelle expressed by almost all mammalian cells. There is an inverse association between the presence of the PC and cell proliferation: in dividing cells the PC is absent since the centrosomes participate in the formation of the mitotic spindle [10]. In recent years, there has been more focus on the association between PC and cancer. For instance, AML cell lines failed to

express the PC on their surface and present a high rate of proliferation [11]. Novel therapeutic approaches to restore PC on the surface of cancer cells, the so-called “ciliotherapy”, are now emerging [12]. One of the key players in PC destabilization is HDAC6, a class IIb member of the histone deacetylase (HDAC) family of proteins. HDAC6-mediated deacetylation of alpha tubulin triggers primary cilium disassembly by destabilizing axonemal stability and increasing the polymerization of actin filaments [13]. Interestingly, *HDAC6* is overexpressed in several tumors such as glioblastoma, multiple myeloma, melanoma and colon cancer [14], and drugs that selectively prevent HDAC6 activity (i.e. TubastatinA) are currently in use [15]. However, *HDAC6* expression and its relationship with *Hh* signaling in AML has never been investigated so far. Here we provide evidence that in adult AML patients and leukemic cell lines, the expression of *Hh* positively correlates with that of *HDAC6* and *MDR* resistance genes. Moreover, in a zebrafish model with *Hh* overexpression *hdac6* expression was increased, with consequent expansion of the hematopoietic stem and progenitor cell (HSPCs) population. We demonstrated that the treatment of *Hh* overexpressing zebrafish embryos with the *Hh* inhibitor cyclopamine did not elicit a rescue in the HSPCs, while the use of the HDAC6 inhibitor TubastatinA efficiently restored the hematopoietic phenotype. Indeed, HDAC6 inhibition might stabilize the PC, which we found present on the cell membrane of HSPCs, leading to a reduction in proliferation rate. Moreover, we generated AML zebrafish models for two of the most frequent human mutations: *Nucleophosmin1* (*NPMc+*) and *FLT3-ITD* [16–18]. These AML models responded to HDAC6 inhibition alone or in combination with the common chemotherapeutic agent cytarabine. Our results demonstrate a positive correlation between *Hh* signaling and *HDAC6* expression in blasts from AML patients, cell lines and in a zebrafish model, opening the possibility for strategies to modulate this pathway in combination with the agents currently in use in AML therapy.

MATERIALS AND METHODS

Patients

Diagnostic bone marrow samples from healthy subjects and 36 adult patients affected by AML were collected and characterized as described in Supplementary Materials. Patients' material was collected after obtaining informed consent (protocol ASGMA-052A approved on May 8th, 2012 by Azienda San Gerardo). The clinical features of the participants are reported in **Supplementary Table S1**. Human material and derived data were used in accordance with the Declaration of Helsinki.

Animals

Zebrafish embryos were raised and maintained according to international (European Union Directive 2010/63/EU) and national (Italian decree n. 26 of March 4th, 2014) guidelines on the protection of animals used for scientific purposes, as described in the Supplementary Materials.

Reverse transcription and real-time quantitative techniques (RT-qPCR) in human samples, cell lines and zebrafish

Total RNA was extracted from human samples and whole zebrafish embryos using TRIZOL reagents (Life Technologies, Carlsbad, CA, USA), following the manufacturer's protocol. Quantitative reverse transcriptase polymerase chain reaction (RT-PCR) experiments on human and zebrafish samples were performed using the 384-well QuantStudio™ 5 Real-Time PCR System (Applied Biosystem, Whaltam, MA, USA). Primers are listed in the **Supplementary Table S2**.

Immunofluorescence staining and image processing

Immunostaining was performed as described in the Supplementary Materials. Primary antibodies were mouse anti-GFP (1:1000, Sigma-Aldrich) and rabbit anti-3PH (1:200, Sigma-Aldrich) and secondary antibody was Alexa Fluor 488-conjugated goat anti-mouse IgG 1:400 (A11008, Invitrogen Life Technologies, Carlsbad, CA, USA) and Alexa 546-conjugated goat anti-rabbit IgG 1:400 (A11001 and A11010, InvitrogenLife Technologies). Staining was evaluated detecting GFP and/or 3PH fluorescence through confocal analyses (A1 HD25/A1R HD25 instrument, Nikon FRET-FLIM) provided by the UniTech nolimits NOxsz<LIMITS service (University of Milan).

Fluorescence activated cell sorting (FACS) analyses

Embryo dissociation was obtained as described [19]. FACS analyses were performed as described in the Supplementary Materials. Flow cytometry acquisitions were performed using Attune NxT (Thermofisher). Analyses were done with Kaluza software from Beckman Coulter.

mRNA synthesis and embryo microinjection

Zebrafish *shh* mRNA was *in-vitro* transcribed from the T7TS-*shh* plasmid using the mMESSAGE mMACHINE T7 transcription kit (Invitrogen), after linearization with NotI (Promega). Human *HDAC6* mRNA was *in-vitro* transcribed from the pCDNA3.1-*HDAC6* plasmid (Addgene), using the mMESSAGE mMACHINE T7 transcription kit (Invitrogen) after linearization with KasI (Invitrogen). 200 pg/embryo of the *shh* mRNA or 250 pg/embryo of the human *HDAC6* mRNA were injected into 1 cell stage embryos. As a control, embryos were injected with the same amount of *rfp*-mRNA except when double immunofluorescence with a secondary red antibody were performed.

Chemical treatments in zebrafish embryos

TubastatinA (TubA; Sigma), cyclopamine (cyclo; Sigma) and cytarabine (AraC, Sigma) were dissolved in Dimethyl sulfoxide (DMSO). Pharmacological treatments were done in a 24 multi-well placing a maximum of 15 embryos/well from the stage of 1.5 days post fertilization (dpf) to 2.5 dpf. Embryos were treated with different concentration of the compounds alone or in combination in 1 ml final volume of E3 with PTU 1X. The doses used were 100 to 25 μM of TubA and 5 μM cyclo for single treatments or 50 μM TubA and 2.5 μM cyclo for combination therapies with 50 μM AraC [20].

Chemical treatments in AML cell lines

OCI-AML2, U937, THP-1, and NB4 cell lines were originally obtained from ATCC/DSMZ repositories and since stored at the internal cell line bank at the Department of Experimental Oncology, IEO, seeded and treated with cyclopamine and TubastatinA dissolved in DMSO as described in the Supplementary Materials.

Western blotting analysis in AML cell lines

Protein extracts were prepared, loaded and quantified as described in the Supplementary Materials. Primary antibodies were ac-α-tubulin (anti mouse 1:1000; Sigma-Aldrich) and total α-tubulin (anti rabbit 1:5000; Sigma-Aldrich), HRP-conjugated secondary antibodies. Protein bands were detected by using WESTAR ECL detection system (Cyanagen, Bologna, Italy). Images were acquired with the Alliance MINI HD9 AUTO Western Blotting Imaging System (UVItec Limited, Cambridge, UK) and analyzed with the related software.

Statistical analyses

For RT-qPCR experiments, data were statistically analyzed applying One-way analysis of variance (ANOVA) with Tukey post-hoc correction or Unpaired T-tests with Welch correction, defining $P \leq 0.05$ (*), $P \leq 0.01$ (**), and $P \leq 0.001$ (***) as statistically significant values. Data were analyzed using the comparative $\Delta\Delta$Ct method. Both t- test and standard deviation (SD) values refer to data from triplicate samples. In zebrafish at least three different experiments were done for each analysis. The count of the proliferation rate of HSPCs was analyzed with One-way analysis of variance (ANOVA) with Tukey post-hoc correction considering $P \leq 0.05$ (*), $P \leq 0.01$ (**), and $P \leq 0.001$ (***) as statistically significant values.

Data Sharing Statement

The original contributions presented in the study are included in the article/Supplementary Materials. Other data that support the findings of this study are available from the corresponding author upon request.

RESULTS

Expression of *Hh* and *HDAC6* positively correlates in adult AML patients

Since the interplay between *Hh* and *HDAC6* has never been characterized so far, we investigated the relation between the expression of *HDAC6* and *Hh* target genes *GLI1* and *PTCH1* in a cohort of 36 adult patients with AML. The expression of both *Hh* downstream targets and *HDAC6* was significantly higher in AML patients compared with healthy donors (HD) (**Fig. 1A-C**). To gain insight into the association between *Hh* and *HDAC6*, correlation analyses were performed. In our patient cohort, the expression of *GLI1* and *PTCH1* positively correlated with *HDAC6* (**Fig. 1D-E**). Also, the expression of the *Multi-Drug-Resistance* (*MDR*) genes *ABCC1* and *ASXL1* was upregulated in AML patients and their expression positively correlates with that of *GLI1*, *PTCH1*

and *HDAC6,* respectively (**Fig. 1F-M**). This correlation was confirmed in the TCGA LAML dataset using the GEPIA2 (Gene Expression Profiling Interactive Analyses) web-tool (http://gepia2.cancer-pku.cn/) (**Supplementary Fig. 1**). Our data indicated that *Hh* and *HDAC6* upregulation positively correlates with the leukemic condition and resistance to chemotherapy.

***Hh/HDAC6* overexpression in zebrafish embryos elicits HSPCs expansion that is rescued by HDAC6 specific inhibition.**

To assess the functional role of *Hh*/HDAC6 signaling on hematopoiesis, we generated a zebrafish model with *Hh* upregulation by the injection of the *shh*-mRNA. We confirmed that, as in human AML patients, the expression of *Hh* positively correlates with HDAC6 expression. Indeed, embryos injected with *shh* mRNA showed an increased expression of the *Hh* targets *gli1a* and *ptch1* (**Fig. 2A-B**), but of *hdac6* and the MDR genes *abcc1* and *asxl1* as well (**Fig. 2C-E**). Next, we showed that *shh*-mRNA injection in the *Tg(CD41:GFP)* transgenic line expressing GFP protein in hematopoietic stem and progenitor cells (HSPCs; GFP^{low}) and thrombocytes (GFP^{high}) [21], elicited an expansion of HSPCs in the caudal hematopoietic tissue (CHT) (**Fig. 2F-G**). To assess if the hematopoietic phenotype could be rescued by pharmacological inhibition of either *Hh* or HDAC6, embryos were treated with specific inhibitors: 5 μM cyclo for *Hh* and 100 μM TubA for HDAC6. We validated the efficacy of *Hh* inhibition by analyzing the expression of its target genes *gli1a* and *ptch1*, which was almost completely abolished following cyclo administration (**Supplementary Fig. 2A-B**). Moreover, we verified by western blot analyses that the HDAC6 target α-tubulin [22] was increased in the acetylated form following TubA treatment (**Supplementary Fig. 2C-D**). Accordingly, since acetylated α-tubulin stabilized cilia, we also showed that TubA treatment increased the length and stabilization of cilia in the pronephric duct, one of the ciliated organs of zebrafish embryo (**Supplementary Fig. 2E-G**) [23].

Interestingly, the increased number of HSPCs in the CHT of *Hh* overexpressing embryos, was not rescued by cyclo treatment (**Fig. 2H**). On the contrary, TubA treatment restored HSPCs expansion to levels comparable to the control (**Fig. 2I**). The increase of HSPCs in *shh*-mRNA injected embryos and the effects of drug treatments were also quantified by FACS analyses of the GFP^{low}-CD41 cells (**Fig. 2J**).

To further evaluate the effects of pharmacological treatments in *Hh* overexpressing embryos, we performed RT-qPCR on 2.5 dpf treated embryos. As expected, the expression of the HSPCs marker *cmyb* [24] increased following *shh*-mRNA injection (**Fig 2K**). *Hh* inhibition was efficiently achieved as the expression of *Hh* target genes *gli1a* and *ptch1* was strongly reduced by cyclo administration (**Fig. 2L-M**). However, only TubA, but not cyclo, rescued the expression of *cmyb* (**Fig 2K**). On the contrary, the expression of MDR genes *abcc1* and *aslx1* was regulated by both *Hh* and HDAC6, as their increased expression in *Hh*-overexpressing embryos was reduced following both cyclo and TubA treatments (**Fig. 2N-O**). Interestingly, TubA treatment elicited an inhibitory effect on *ptch1* expression suggesting a feed-back loop activity among them (**Fig. 2M**).

Zebrafish HSPCs expansion is elicited through HDAC6 activity

To verify if the expansion of HSPCs was caused by an increased proliferation we performed phospho-histone H3 immunofluorescence analyses (P3H IF). *Hh* overexpressing embryos showed more proliferating cells in the CHT in comparison to the control (**Fig. 3A-B**). The proliferation rate (indicated as the percentage of double positive HSPCs/3PH on the total of HSPCs) was reduced only upon TubA treatment but not cyclo (**Fig. 3C-E**), suggesting that HDAC6 is involved in the self-renewal ability of HSPCs. To verify this hypothesis, we generated a zebrafish model overexpressing *HDAC6* by injecting human *HDAC6* mRNA, and we observed the expansion of HSPCs in the CHT of *Tg(CD41:GFP)* embryos at 2.5 dpf. As expected, the proliferation rate of HSPCs was also increased in *HDAC6* overexpressing embryos in comparison to the controls and

the effects were rescued by the administration of TubA, confirming the specificity of the phenotype (**Fig. 3F-I**).

Since cell proliferation is regulated by the presence/absence of primary cilium on the cell membrane, HDAC6 might regulate HSPCs proliferation through its stabilization. In zebrafish the presence of the primary cilium has been described in hemogenic endothelium prior to the developmental stage of 28 hpf [25]. Here, by FACS-sorting the HSPC-GFP^{low} positive cells from the *Tg(CD41:GFP)* embryos at 2.5 dpf, we showed the presence of a primary cilium, labelled with acetylated α-tubulin antibody, in these cells (**Fig. 3J-N**).

Inhibition of HDAC6 efficiently reduces proliferation of leukemic cell lines and HSPCs expansion in two AML zebrafish models

To evaluate the effects of *Hh* and HDAC6 inhibition also in human myeloid cells, we selected four adult AML cell lines expressing different levels of *Hh* and HDAC6: the U937 and THP-1 cells lines showed higher *Hh* and HDAC6 expression and activity compared with the OCI-AML2 and NB4 cell lines (**Fig. 4A-C, F**). We confirmed *in-vitro* the presence of a positive correlation between *Hh*/HDAC6/MDR resistant genes, previously observed in blasts from AML patients and zebrafish embryos (**Fig. 4D-E**). We treated these four AML cell lines for 72 hours with increasing concentrations of cyclo or TubA and evaluated their viability using CTG luminescence assay, an indicator of metabolically active cells. TubA decreased the viability of all cell lines (**Fig. 4G**), with higher efficacy in the OCI-AML2 and NB4, considered good-responders due to their lower *Hh* and HDAC6 expression in comparison with U937 and THP-1 cell lines (**Fig. 4G**). On the contrary, cyclo did not elicit significant effects on cell viability, apart with the higher dose we used, in line with what we observed in the rescue of the HSPCs phenotype in zebrafish (**Fig. 4H**).

We next generated well-established AML zebrafish models by introducing two of the most frequent mutations found in AML patients: *NPMc+* and *FLT3-ITD* [26]. Indeed, it has been previously reported that human *NPMC+* and *FLT3-ITD* mRNA injection determines an increase of HSPCs in zebrafish embryos [16–18]. On the contrary, the overexpression of the wild-type *NPM1* and *FLT3* mRNAs did not elicit such HSPCs expansion (**Supplementary Fig. 3A-B**). The inhibition of HDAC6 activity by TubA treatment reduced the number of HSPCs also in the *NPMc+* and *FLT3-ITD* embryos. In accordance with the results obtained in *Hh* overexpressing embryos, the inhibition of *Hh* by cyclo treatment of AML zebrafish models did not rescue the hematopoietic phenotype (**Fig. 5A-B**).

HDAC6 and cytarabine combination therapy shows synergistic effects in reducing HSPCs proliferation rate in zebrafish AML models

We treated the AML zebrafish models with TubA and cytarabine (AraC) to assess if the combined administration of an HDAC6 inhibitor might improve the antiproliferative activity of a chemotherapeutic agent that is commonly used for the treatment of AML. Each compound was used at a dose that did rescue the AML phenotype. While subcritical doses of each compound did not diminish the number of HSPCs in both *NPMc+* and *FLT3-ITD*-mRNAs injected embryos, combination therapy induced a significant reduction (**Fig. 6A-B**). Notably, similar results were not obtained with the combined inhibition of *Hh* and AraC, confirming that only the block of HDAC6 activity recovers the HSPCs expansion (**Fig. 6A-B**).

DISCUSSION

Activation of the *Hh* pathway has been reported to promote cell proliferation in cancers, including leukemia. For instance, the expression levels of the *Hh* downstream targets were increased [27] in acute myeloid and acute promyelocytic leukemia patients compared to healthy donors [28]. Notably, activation of *Hh* signaling in the granulocyte/monocyte compartment might induce AML

insurgence when combined to the *FLT3-ITD* mutation [29]. *In vitro*, myeloid HL-60 cell lines that acquired radio- and chemo-resistance (HL-60/RX and HL-60/ADR, respectively), expressed higher levels of the *Hh* receptor *SMO* and the effector *GLI1* in comparison to chemo-sensitive cells [30].

We found that the expression levels of *Hh* downstream targets *PTCH1* and *GLI1* are increased in a cohort of 36 AML adult patients in comparison with healthy donors.

Previous studies reported that the overexpression of *HDAC6* also caused proliferation of malignant cells and induced resistance to chemotherapy in acute leukemia patients [31]. In line with these observations, we found an increased expression of *HDAC6* in AML patients that positively correlates to *Hh* signaling and the multidrug resistant genes *ABCC1* and *ASXL1*. Previous studies reported that also the overexpression of *HDAC6* causes proliferation of malignant cells and induced resistance to chemotherapy in AML and ALL patients [31]. In line with these observations, we found an increased expression of *HDAC6* in our AML patients' cohort that is positively correlated to *Hh* signaling and the multidrug resistant genes *ABCC1* and *ASXL1*.

The role of *Hh* signaling in definitive hematopoiesis in zebrafish [32] has already been described, as embryos with mutations in the *Hh* pathway or treated with the *Hh* inhibitor cyclopamine lack HSPCs and *rag1* positive cells in the thymus [32]. Here, we described for the first time that the forced expression of *Hh* pathway in zebrafish activates the hematopoietic cascade by increasing the number of HSPCs, a situation that recapitulates the increase of blast progenitors in AML patients. Moreover, *Hh* over-activation determines an increased expression of *hdac6*, confirming in zebrafish the positive correlation of the two genes observed in AML patients and suggesting that HDAC6 is a direct or indirect target of *Hh*. Coherently, the overexpression of *HDAC6* in zebrafish also induced the expansion of HSPCs through their hyper-proliferation. Although it has been previously demonstrated that the reduced expression of *hdac6* resulted in the loss of HSPCs markers *runx1* and *cmyb* [33], to our knowledge this is the first time that the overexpression of *HDAC6* is linked to the hematopoietic phenotype in zebrafish.

Both *Hh* signaling and HDAC6 are inhibited with specific compounds that have been used in clinic. For instance, the inhibition of HDAC6 with drugs such as the pan-histone deacetylase inhibitors or the more specific HDAC6 inhibitors Tubacin and TubastatinA results in sensitization to chemotherapy both *in-vitro* and in patients [31,34]. In our zebrafish models with *Hh* overexpression, pharmacological inhibition of HDAC6 reduces the number of HSPCs, while we did not obtain this rescue by inhibiting *Hh*, suggesting that its reduction is not sufficient to restore the downstream molecular mechanisms activated by its overexpression.

Since we observed that expansion of HSPCs was provoked by an increase in their proliferation rate, we hypothesized an implication of the PC. It is known that HDAC6 inhibition prevents α-tubulin deacetylation and PC disassembly [15]. This condition blocks cell cycle progression as the mother centriole is used to form the basal bodies of the PC and cannot be used for the assembly of the mitotic spindle [10]. Therefore, an increase in HDAC6 activity contributes to PC destabilization and cell proliferation, while HDAC6 inhibition exerts opposite effects rescuing the over-proliferation of HSPCs observed in zebrafish embryos. We demonstrated that zebrafish HSPCs present a PC. While it has been already described that human blood and bone marrow cells present a PC that participates in *Hh* signaling, so far in zebrafish the PC had been identified only in hemogenic endothelium [25]. This could be due to differences in the developmental stages analyzed or in the time-point of cell growth. PC in HSPCs has been identified only very recently, probably due to technical difficulties in the labelling of such a delicate and temporary structure. For instance, in human hematopoietic cell cultures, PC was identified only when cells grew to confluence and were serum starved [11].

We demonstrated that selective HDAC6 inhibition is efficient both in zebrafish embryos and in established AML cell lines. We selected four AML cell lines with higher (U937, THP-1) or lower (OCI-AML2, NB4) *Hh*/HDAC6 expression and activity that, accordingly, represented poor or good-responders to HDAC6 inhibition. Then, we generated *in-vivo* AML zebrafish models overexpressing the *NPMc+* and *FLT3-ITD* human transcripts. Only the inhibition of HDAC6 by TubA administration was effective in rescuing the cell viability and the expansion observed in AML

cell lines and HSPCs of AML zebrafish models respectively, while blockade of the *Hh* pathway was ineffective. The expansion of HSPCs in the AML models was not caused by the upregulation of *Hh* or HDAC6 as we did not find differences in their expression in *NPMc+* and *FLT3-ITD* or wild-type *NPM1* and *FLT3* injected embryos. Although further analyses are necessary to better clarify this mechanism, we described for the first time that inhibition of HDAC6, also in a condition where it is not overexpressed, is efficient in blocking cell proliferation.

New therapeutic approaches are needed for AML patients, especially for those insensitive to chemotherapy and with negative prognosis. Numerous treatments are under development or in clinical trials and, among them, combination therapy or drugs against novel identified targets are at the leading edge of research. Current AML therapy is based on cytarabine (AraC) and anthracyclines (i.e. daunorubicin) in the induction phase, followed consolidation therapy during remission [28]. The inhibition of the *Hh* receptor *SMO* through glasdegib alone or in combination with low dose AraC, is under investigation in several clinical trials for AML [28] and improves overall survival when compared to chemotherapy alone. A novel dual HDAC/SMO inhibitor, named NL-103 [35], represents an attractive option for future therapeutic strategies [28]. Concerning HDAC6, the specific inhibitor ST80 can be used at a low concentration (1 μM) and is advantageous in avoiding additive toxicity when used in combination with standard chemotherapeutic agents [34]. We tested the possibility to inhibit HDAC6 in the *NPMc+* and *FLT3-ITD* AML zebrafish models and found that the combined treatment with TubA/AraC is more efficient in reducing HSPCs expansion. The use of zebrafish as a powerful model for drug treatments and the quantification of HSPCs in the *Tg(CD41:GFP)* line would allow high-throughput screenings, cutting the cost and time of preclinical analyses.

Our results highlight the relevance of the *Hh*/HDAC6 pathway in HSPCs expansion and propose a new pharmacological target for AML treatment.

MAIN TEXT WORD COUNT: 3823

363

ACKNOWLEDGMENTS

We thank Dr. Alberto Rissone from the Cell and Developmental Biology Center, NHLBI, NIH, Bethesda, MD, USA (National Institute of Health/NIH, USA) for fruitful comments and editing and Marco Spreafico, Marco Cafora, Gaia Galassi and Alessia Brix (University of Milan) for their priceless support in experimental procedures.

AUTHOR CONTRIBUTIONS

Alex Pezzotta (AP^1), AM, and Anna Pistocchi (AP^2) conceived and designed the experiments. AP^1 and IG performed the experiments on zebrafish. AP^1 and DG performed experiments on AML cells. MT performed the FACS analyses on zebrafish. MP and MF provided AML patients' samples. GC and GF setup patient material and data for molecular profiling (including karyotype data and RNA). ALYH provided *FLT3* and *FLT3-ITD* plasmids. AP^1 and CB performed *in silico* analyses. AP^1, IG, AM, and AP^2 analyzed the data on zebrafish. DG and MA analyzed the data on AML cells. AP^1 and AP^2 wrote the manuscript. AP^2 supervised the manuscript drafting. AP^2 supervised the research project. All authors contributed to the article and approved the submitted version.

FUNDING

This work was supported by the funds of DMEM, PhD school in Experimental Medicine (Dr. Alex Pezzotta). The funder had no role in the study design, data collection and interpretation, or the decision to submit the work for publication.

CONFLICT OF INTEREST STATEMENT

All authors declare that they have no conflict of interest. Declaration of interest: none.

DATA SHARING STATEMENT

All data presented in the manuscript will be available upon request to the corresponding author.

REFERENCES

1. Skoda AM, Simovic D, Karin V, Kardum V, Vranic S, Serman L. The role of the Hedgehog signaling pathway in cancer: A comprehensive review. Bosn J basic Med Sci 2018;18(1):8–20.
2. Gonnissen A, Isebaert S, Haustermans K. Targeting the Hedgehog signaling pathway in cancer: beyond Smoothened. Oncotarget 2015;6(16):13899–913.
3. Briscoe J, Thérond PP. The mechanisms of Hedgehog signalling and its roles in development and disease. Nat Rev Mol Cell Biol 2013;14(7):416–29.
4. Kong JH, Siebold C, Rohatgi R. Biochemical mechanisms of vertebrate hedgehog signaling. Development;146(10):.
5. Amakye D, Jagani Z, Dorsch M. Unraveling the therapeutic potential of the Hedgehog pathway in cancer. Nat Med 2013;19(11):1410–1422.
6. Kuo YH, Qi J, Cook GJ. Regain control of p53: Targeting leukemia stem cells by isoform-specific HDAC inhibition. Exp Hematol 2016;44(5):315–321.
7. Evangelista M, Tian H, de Sauvage FJ. The Hedgehog Signaling Pathway in Cancer. Clin Cancer Res 2006;12(20):5924–5928.
8. Peer E, Tesanovic S, Aberger F. Next-Generation Hedgehog/GLI Pathway Inhibitors for Cancer Therapy. Cancers (Basel) 2019;11(4):538.
9. Cortes JE, Douglas Smith B, Wang ES, et al. Glasdegib in combination with cytarabine and

daunorubicin in patients with AML or high-risk MDS: Phase 2 study results. Am J Hematol 2018;93(11):1301–1310.

10. Goto H, Inoko A, Inagaki M. Cell cycle progression by the repression of primary cilia formation in proliferating cells. Cell Mol Life Sci 2013;70(20):3893–3905.

11. Singh M, Chaudhry P, Merchant AA. Primary cilia are present on human blood and bone marrow cells and mediate Hedgehog signaling. Exp Hematol 2016;44(12):1181-1187.e2.

12. Tschaikner P, Enzler F, Torres-Quesada O, Aanstad P, Stefan E. Hedgehog and Gpr161: Regulating cAMP Signaling in the Primary Cilium. Cells 2020;9(1):118.

13. Ran J, Yang Y, Li D, Liu M, Zhou J. Deacetylation of α-tubulin and cortactin is required for HDAC6 to trigger ciliary disassembly. Sci Rep 2015;5(1):12917.

14. Li T, Zhang C, Hassan S, et al. Histone deacetylase 6 in cancer. J Hematol Oncol 2018;11(1):111.

15. Gradilone SA, Radtke BN, Bogert PS, Huang BQ, Gajdos GB, LaRusso NF. HDAC6 Inhibition Restores Ciliary Expression and Decreases Tumor Growth. Cancer Res 2013;73(7):2259–2270.

16. He B-L, Shi X, Man CH, et al. Functions of flt3 in zebrafish hematopoiesis and its relevance to human acute myeloid leukemia. Blood 2014;123(16):2518–2529.

17. Bolli N, Payne EM, Grabher C, et al. Expression of the cytoplasmic NPM1 mutant (NPMc+) causes the expansion of hematopoietic cells in zebrafish. Blood 2010;115(16):3329–3340.

18. Mazzola M, Deflorian G, Pezzotta A, et al. NIPBL□: a new player in myeloid cell differentiation. Haematologica 2019;104(7):1332–1341.

19. Bresciani E, Broadbridge E LP. An efficient dissociation protocol for generation of single cell suspension from zebrafish embryos and larvae. MethodsX 2018;10(5):1287–1290.

20. Vinothkumar Rajan, Nicole Melong, Wing Hing Wong, et al. Humanized zebrafish enhance human hematopoietic stem cell survival and promote acute myeloid leukemia clonal diversity. Haematologica 2019;105(10):2391–2399.

21. Lin HF, Traver D, Zhu H, et al. Analysis of thrombocyte development in CD41-GFP transgenic zebrafish. Blood 2005;106(12):3803–3810.

22. Valenzuela-Fernández A, Cabrero JR, Serrador JM, Sánchez-Madrid F. HDAC6: a key regulator of cytoskeleton, cell migration and cell–cell interactions. Trends Cell Biol 2008;18(6):291–297.

23. He L, Xu W, Jing Y, et al. Yes-Associated Protein (Yap) Is Necessary for Ciliogenesis and Morphogenesis during Pronephros Development in Zebrafish (Danio Rerio). Int J Biol Sci 2015;11(8):935–947.

24. Zhang Y, Jin H, Li L, Qin FX-F, Wen Z. cMyb regulates hematopoietic stem/progenitor cell mobilization during zebrafish hematopoiesis. Blood 2011;118(15):4093–4101.

25. Liu Z, Tu H, Kang Y, et al. Primary cilia regulate hematopoietic stem and progenitor cell specification through Notch signaling in zebrafish. Nat Commun 2019;10(1):1839.

26. Papaemmanuil E, Gerstung M, Bullinger L, et al. Genomic Classification and Prognosis in Acute Myeloid Leukemia. N Engl J Med 2016;374(23):2209–2221.

27. Cortes JE, Gutzmer R, Kieran MW, Solomon JA. Hedgehog signaling inhibitors in solid and hematological cancers. *Cancer Treatment Reviews.*

28. Aberger F, Hutterer E, Sternberg C, del Burgo PJ, Hartmann TN. Acute myeloid leukemia – strategies and challenges for targeting oncogenic Hedgehog/GLI signaling. Cell Commun Signal 2017;15(1):8.

29. Cochrane C, Szczepny A, Watkins D, Cain J. Hedgehog Signaling in the Maintenance of

Cancer Stem Cells. Cancers (Basel) 2015;7(3):1554–1585.

30. Queiroz KCS, Ruela-de-Sousa RR, Fuhler GM, et al. Hedgehog signaling maintains chemoresistance in myeloid leukemic cells. Oncogene 2010;29(48):6314–6322.

31. Ahmadzadeh A, Khodadi E, Shahjahani M, Bertacchini J, Vosoughi T, Saki N. The Role of HDACs as Leukemia Therapy Targets using HDI. Int J Hematol stem cell Res 2015;9(4):203–14.

32. Gering M, Patient R. Hedgehog Signaling Is Required for Adult Blood Stem Cell Formation in Zebrafish Embryos. Dev Cell 2005;8(3):389–400.

33. Huang HT, Kathrein KL, Barton A, et al. A Network of Epigenetic Regulators Guides Developmental Haematopoiesis in Vivo. Nat Cell Biol [Epub ahead of print].

34. Hackanson B, Rimmele L, Benkißer M, et al. HDAC6 as a target for antileukemic drugs in acute myeloid leukemia. Leuk Res 2012;36(8):1055–1062.

35. Zhao J, Quan H, Xie C, Lou L. NL-103, a novel dual-targeted inhibitor of histone deacetylases and hedgehog pathway, effectively overcomes vismodegib resistance conferred by Smo mutations. Pharmacol Res Perspect [Epub ahead of print].

FIGURE LEGENDS

Fig. 1: *Hh*/HDAC6/MDRs correlation in AML patients in comparison to HD. A-C) Real-time qPCR analyses of *Hh* signaling target genes (**A**) *GLI1*, (**B**) *PTCH1* and (**C**) *HDAC6* in a cohort of adult AML patients. **D-E**) Correlation analyses between the expression levels of *HDAC6* and (**D**) *GLI1* and (**E**) *PTCH1*. **F-M**) Real-time qPCR and correlation analyses of the *Multi-Drug-Resistance* (MDR) genes (**F, G-I**) *ABCC1* and (**J, K-M)** *ASXL1*. **A-C**; **F; J**) Unpaired T-test with

Welch correction. **D-E**; **G-I; K-M**) Spearman correlation. ***p<0.001; **p<0.01; *p<0.05. HD: healthy donor's samples; AML: acute myeloid leukemia samples. Results are presented as mean ± SEM.

Fig. 2: *Hh* signaling overexpression in zebrafish, HSPCs expansion and cyclopamine and TubastatinA treatments. A-E) Real-time qPCR analyses of the *Hh* target genes (**A**) *gli1*a, (**B**) *ptch1*, (**C**) *hdac6* and of the *Multi-Drug-Resistance* genes (**D**) *abcc1* and (**E**) *asxl1*. **F-I**) Confocal images of the caudal hematopoietic tissue (CHT) of 2.5 dpf embryos (N=6) of the *Tg(CD41:GFP)*transgenic line: control embryos injected with *rfp* mRNA (**F**) or with s*hh* mRNA (**G**) and treated with cyclopamine (**H**) or TubastatinA (**I**). **J**) Quantification of the HSPCs population by FACS analyses of the GFP^{low}-CD41 cells. **K-O**) RT-qPCR analyses of (**K**) *cmyb*; (**L**) *gli1a*, (**M**) *ptch1* and the *Multi-Drug-Resistance* (**N**) *abcc1* and (**O**) *asxl1*. **A-E**) Unpaired T-test with Welch correction. **F-O**) ONE-way ANOVA with Tukey post hoc correction. ***p<0.001; **p<0.01; *p<0.05; ns not significant. Results are presented as mean ± SEM. Scale bar indicates 100 µm. cyclo: cyclopamine; TubA: TubastatinA.

Fig. 3: *Hh/HDAC6* mediated hyperproliferation, pharmacological treatments and presence of primary cilium in zebrafish HSPCs. A-D, F-H) Confocal images of the caudal hematopoietic tissue (CHT) of the *Tg(CD41:GFP)* zebrafish embryos at 2.5 dpf; asterisks indicate the double GFP/3PH cells. GFP^{low} were HSPCs, GFP^{high} were trombocytes: (**A**) control embryos (N=5), (**B**) s*hh* mRNA, *shh* mRNA (N=6) treated with (**C**) cyclopamine (N=6) or (**D**) TubastatinA (N=7); (**E**) quantification of HSPCs proliferative rate. (**F**) control embryos (N=9) (**G**) *HDAC6* mRNA (N=10) (**H**) *HDAC6* mRNA and TubastatinA (N=9); (**I**) quantification of HSPCs proliferative rate. **J-N**) Immunofluorescence analyses of sorted HSPC-GFP^{low} cells: **J**) CD41 GFP; signal; **K**) acetylated α-tubulin; **L**) DAPI; **M**) merge of the channels; **N**) higher magnification of a HSPC and primary

cilium. **E**, **I**) cyclo: cyclopamine; TubA: TubastatinA. ONE-way ANOVA with Tukey post hoc correction. ***p<0.001; **p<0.01; ns not significant. Results are presented as mean ± SEM. Scale bar indicates 100 µm (CHT) and 10 µm (sorted cells).

Fig. 4: *Hh/HDAC6/MDRs* expression and cyclopamine and TubastinA treatments in the U937, THP1, NB-4 AML and OCI-AML2 cell lines. A-E) Real-time qPCR analyses of (**A**) *GLI1*, (**B**) *PTCH1*, (**C**) *HDAC6*, (**D**) *ABCC1*, (**E**) *ASXL1*. (**F**) Western-blotting analyses of the ac-α-tubulin protein levels in comparison to the total α-tubulin protein levels. **G-H)** Analyses of cytostatic and cytotoxic effect of cyclo and TubA in AML cell lines. **G-H) C**ell lines were treated for 72 hours with different concentration of (**G**) TubA or (**H)** cyclo; DMSO at the higher dose was used as a control. CTG assay was used to assess the effect of the treatment on the cell viability. ONE-way ANOVA with Tukey post hoc correction (**A**-**E**). Unpaired T-test with Welch correction (**G**-**H**); for simplicity only data with p<0.05 are shown. ***p<0.001; **p<0.01; *p<0.05; ns not significant. Results are presented as mean ± SEM.

Fig. 5: *Hh* and HDAC6 inhibition in the *NPMc+* and *FLT3-ITD* zebrafish models of AML. A-B) Confocal images of the caudal hematopoietic tissue (CHT) of the *Tg(CD41:GFP)* zebrafish (N=3) with the forced expression of the human (**A**) *NPMc+* or (**B**) *FLT3-ITD* mRNA treated with cyclo or TubA. Histograms represents the number of HSPC-GFP positive cells. cyclo: cyclopamine; TubA: TubastatinA. ONE-way ANOVA with Tukey post hoc correction. ***p<0.001; **p<0.01; *p<0.05; ns not significant. Results are presented as mean ± SEM. Scale bar indicates 100 µm.

Fig. 6: Combination therapy in the *NPMc+* and *FLT3-ITD* zebrafish models of AML. A-B) Quantification of HSPC-GFP positive cells in the region of the caudal hematopoietic tissue (CHT)

of *Tg(CD41:GFP)* transgenic embryos with forced expression of the human (**A**) *NPMc+* or (**B**) *FLT3-ITD* mRNA, treated with subcritical doses of cyclo or TubA alone or in combination with AraC. cyclo: cyclopamine; TubA: TubastatinA; AraC: cytarabine. ONE-way ANOVA with Tukey post hoc correction. ***p<0.001; **p<0.01; *p<0.05; ns not significant. Results are presented as mean ± SEM.

Figure 1

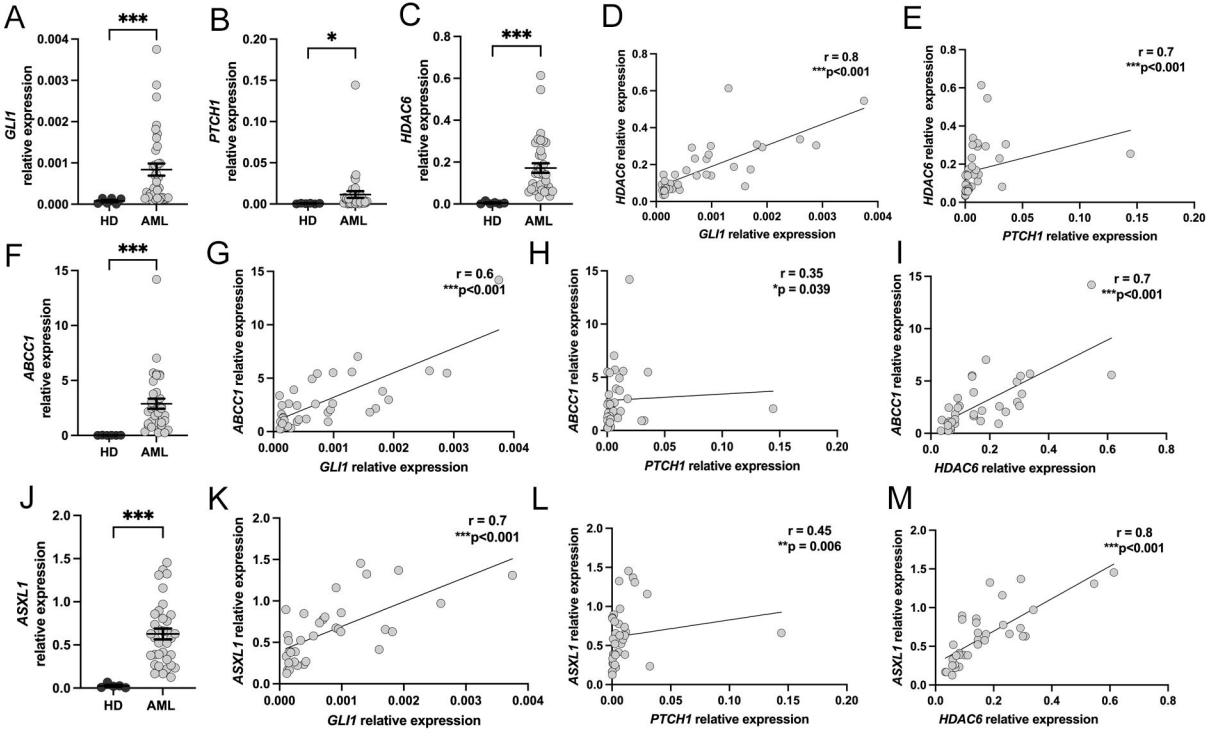
A
***
GLI1 relative expression
0.004
0.003
0.002
0.001
0.000
HD
AML
B
*
PTCH1 relative expression
0.20
0.15
0.10
0.05
0.00
HD
AML
C
***
HDAC6 relative expression
0.8
0.6
0.4
0.2
0.0
HD
AML
D
r = 0.8
***p<0.001
HDAC6 relative expression
GLI1 relative expression
0.000
0.001
0.002
0.003
0.004
E
r = 0.7
***p<0.001
HDAC6 relative expression
PTCH1 relative expression
0.00
0.05
0.10
0.15
0.20
F
***
ABCC1 relative expression
15
10
5
0
HD
AML
G
r = 0.6
***p<0.001
ABCC1 relative expression
GLI1 relative expression
H
r = 0.35
*p = 0.039
ABCC1 relative expression
PTCH1 relative expression
I
r = 0.7
***p<0.001
ABCC1 relative expression
HDAC6 relative expression
J
***
ASXL1 relative expression
2.0
1.5
1.0
0.5
0.0
HD
AML
K
r = 0.7
***p<0.001
ASXL1 relative expression
GLI1 relative expression
L
r = 0.45
**p = 0.006
ASXL1 relative expression
PTCH1 relative expression
M
r = 0.8
***p<0.001
ASXL1 relative expression
HDAC6 relative expression

Figure 2

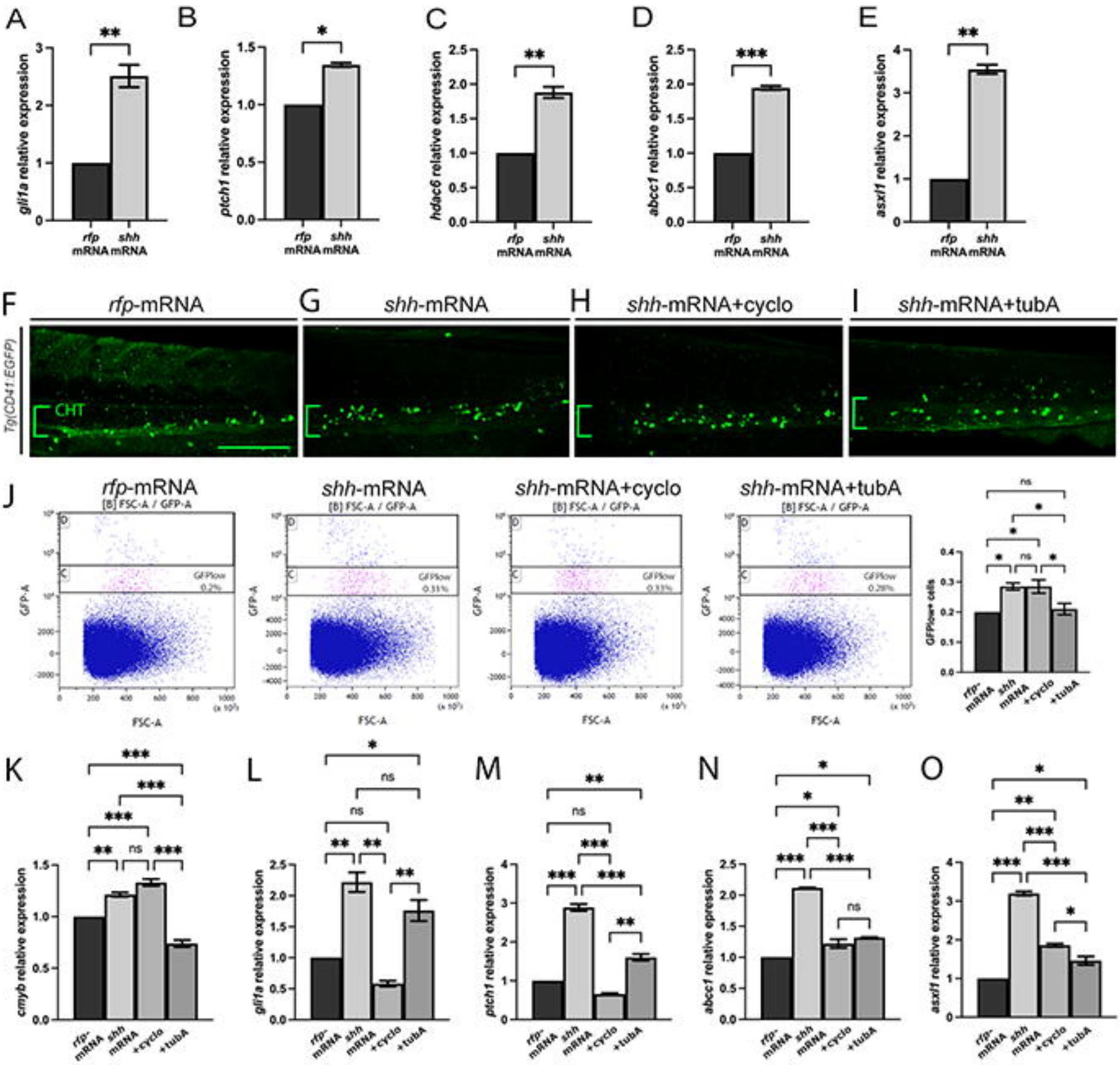
A
B
C
D
E
gli1a relative expression
ptch1 relative expression
hdac6 relative expression
abcc1 relative epression
asxl1 relative expression
rfp mRNA
shh mRNA
F
rfp-mRNA
G
shh-mRNA
H
shh-mRNA+cyclo
I
shh-mRNA+tubA
Tg(CD41:EGFP)
CHT
J
[B] FSC-A / GFP-A
GFPlow
GFP-A
FSC-A
GFPlow+ cells
rfp-mRNA
shh mRNA
+cyclo
+tubA
K
L
M
N
O
cmyb relative expression
gli1a relative expression
ptch1 relative expression
abcc1 relative epression
asxl1 relative expression
ns

Figure 3

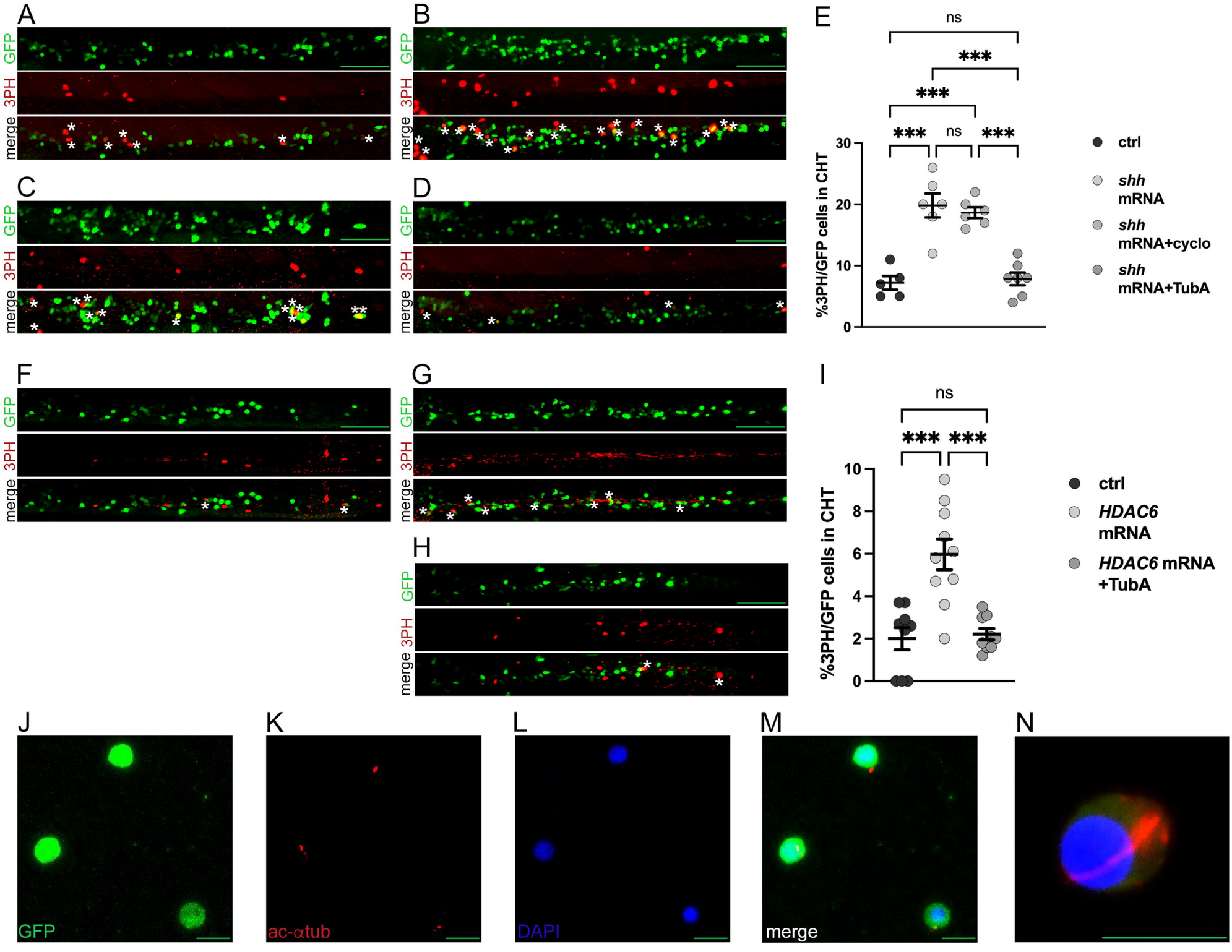
A
B
C
D
E
F
G
H
I
J
K
L
M
N
GFP
3PH
merge
ns
***
***
***
ns
***
%3PH/GFP cells in CHT
30
20
10
0
ctrl
shh mRNA
shh mRNA+cyclo
shh mRNA+TubA
***
***
ns
%3PH/GFP cells in CHT
10
8
6
4
2
0
ctrl
HDAC6 mRNA
HDAC6 mRNA +TubA
GFP
ac-αtub
DAPI
merge

Figure 4

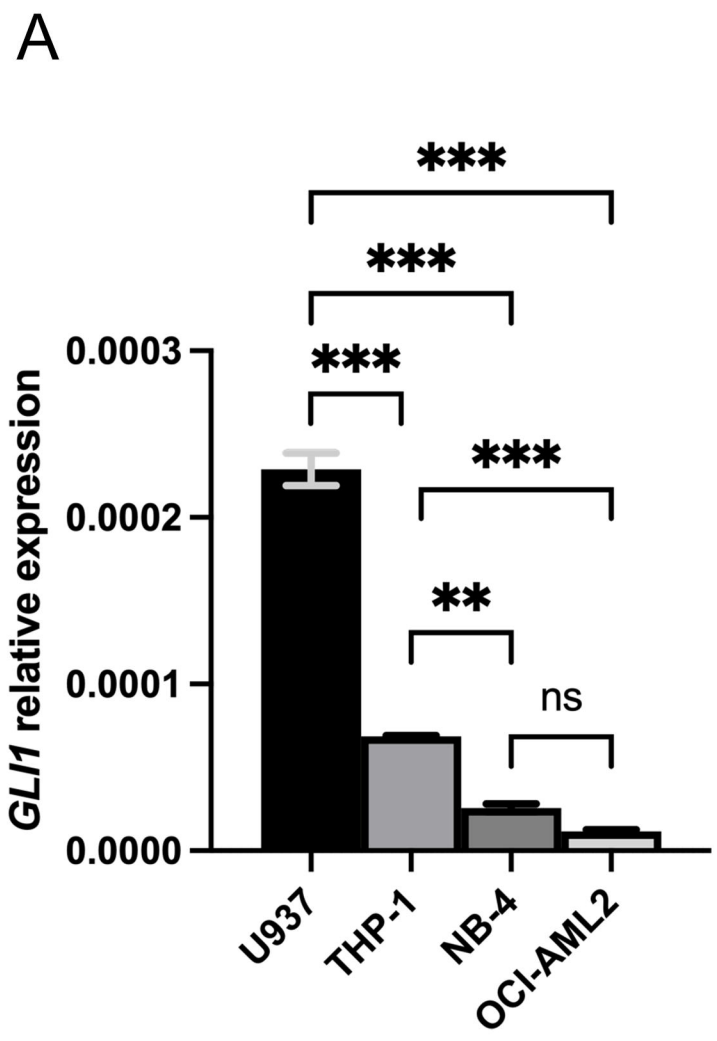

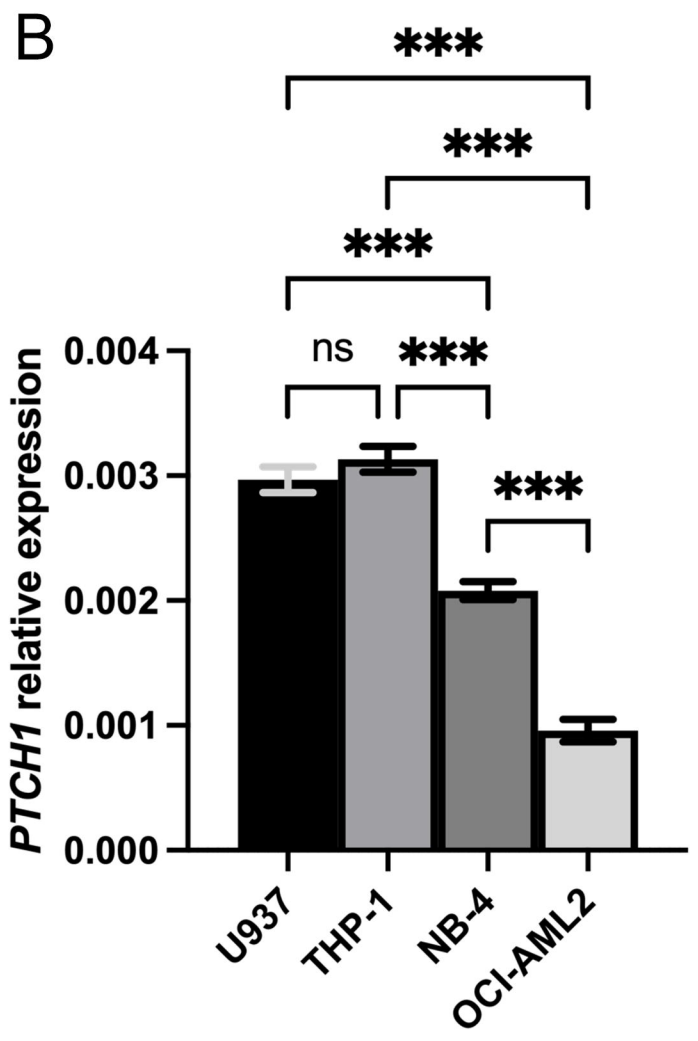

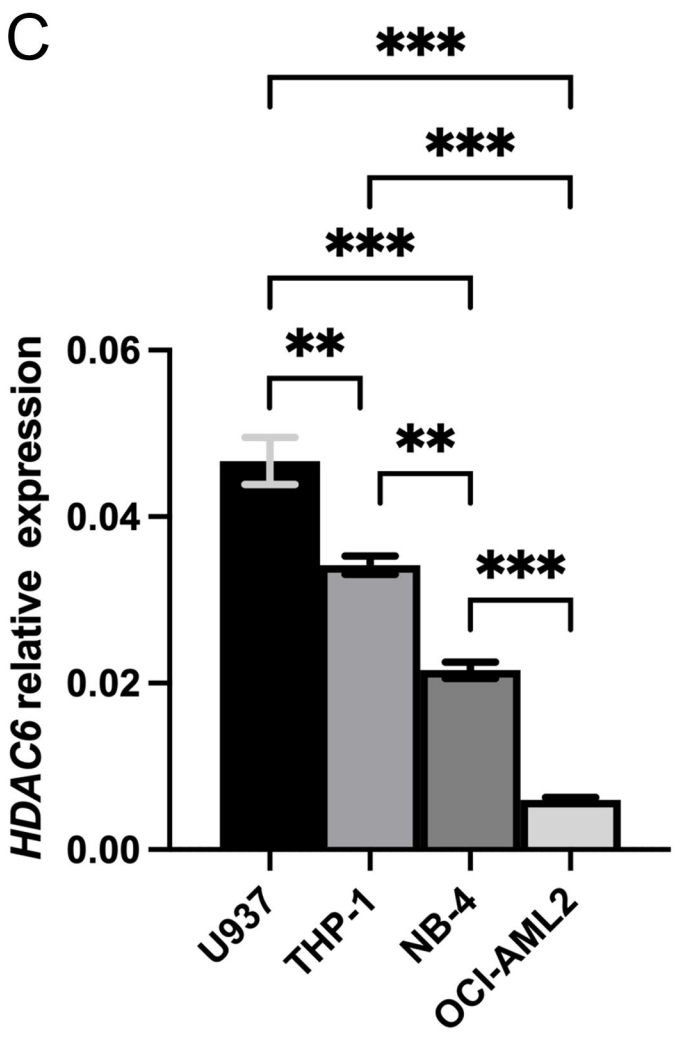

Haematologica HAEMATOL/2022/280682 Version 1

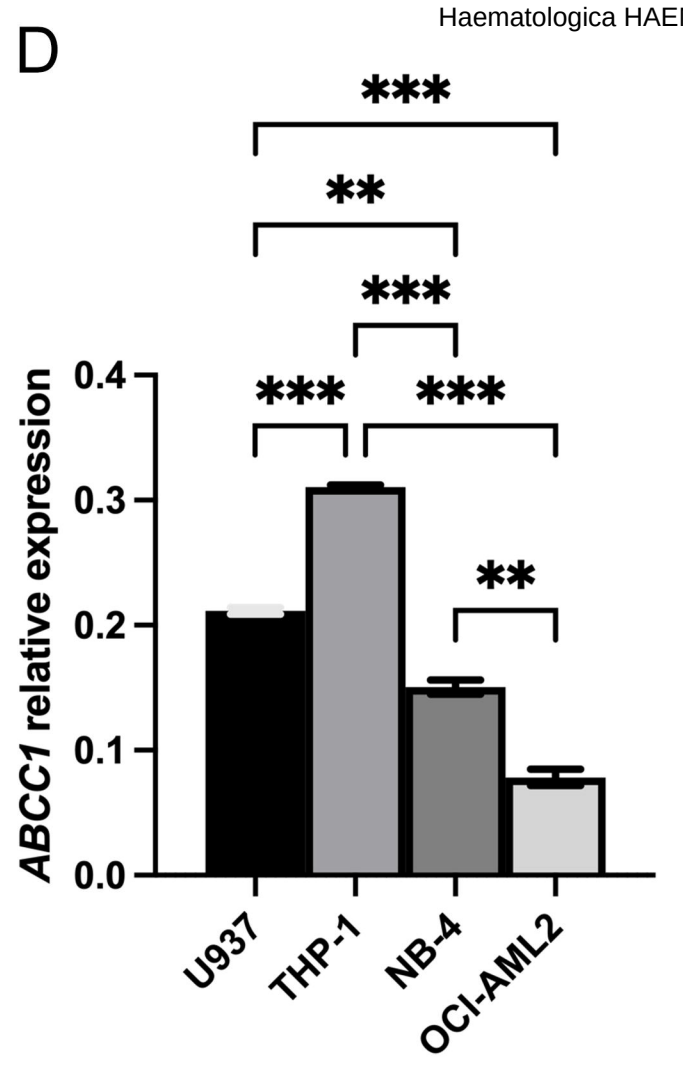

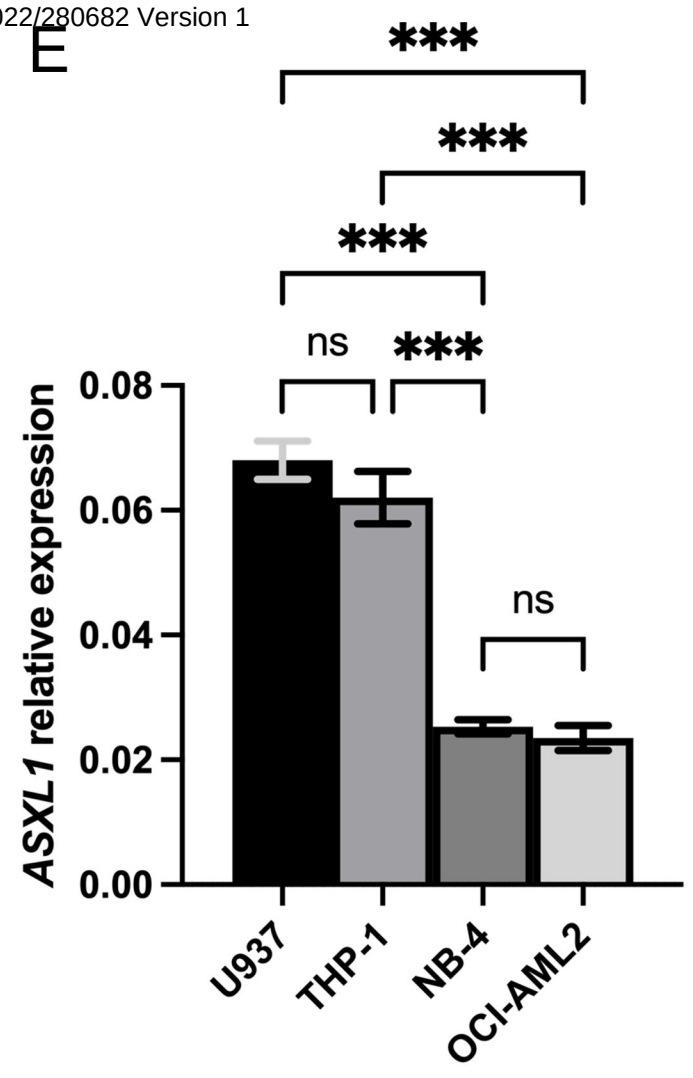

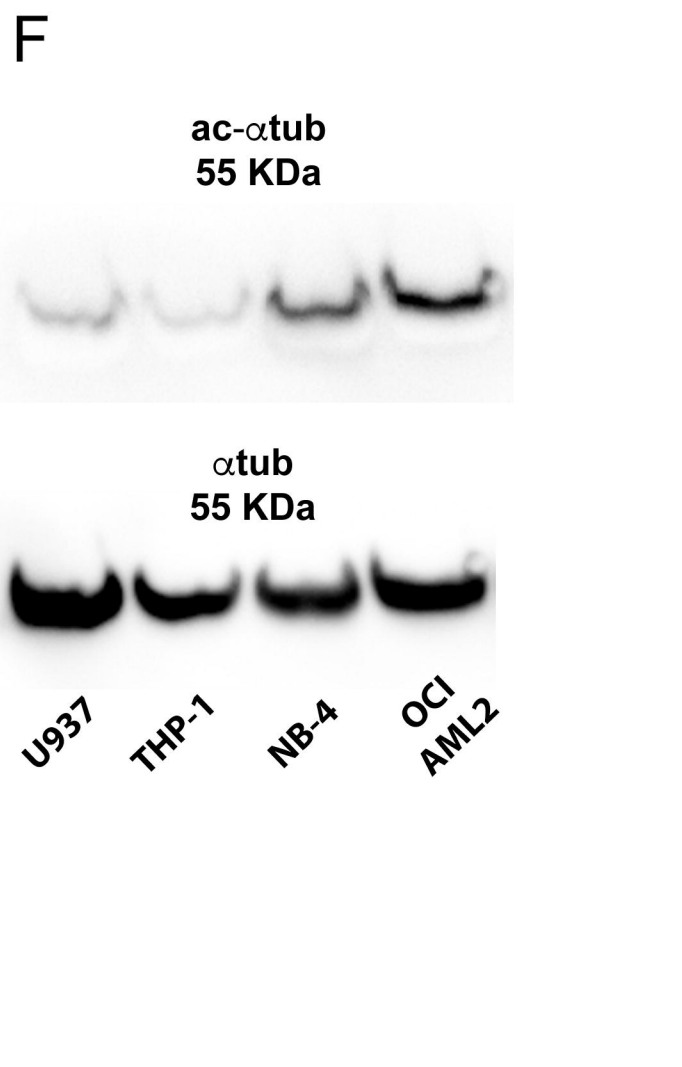

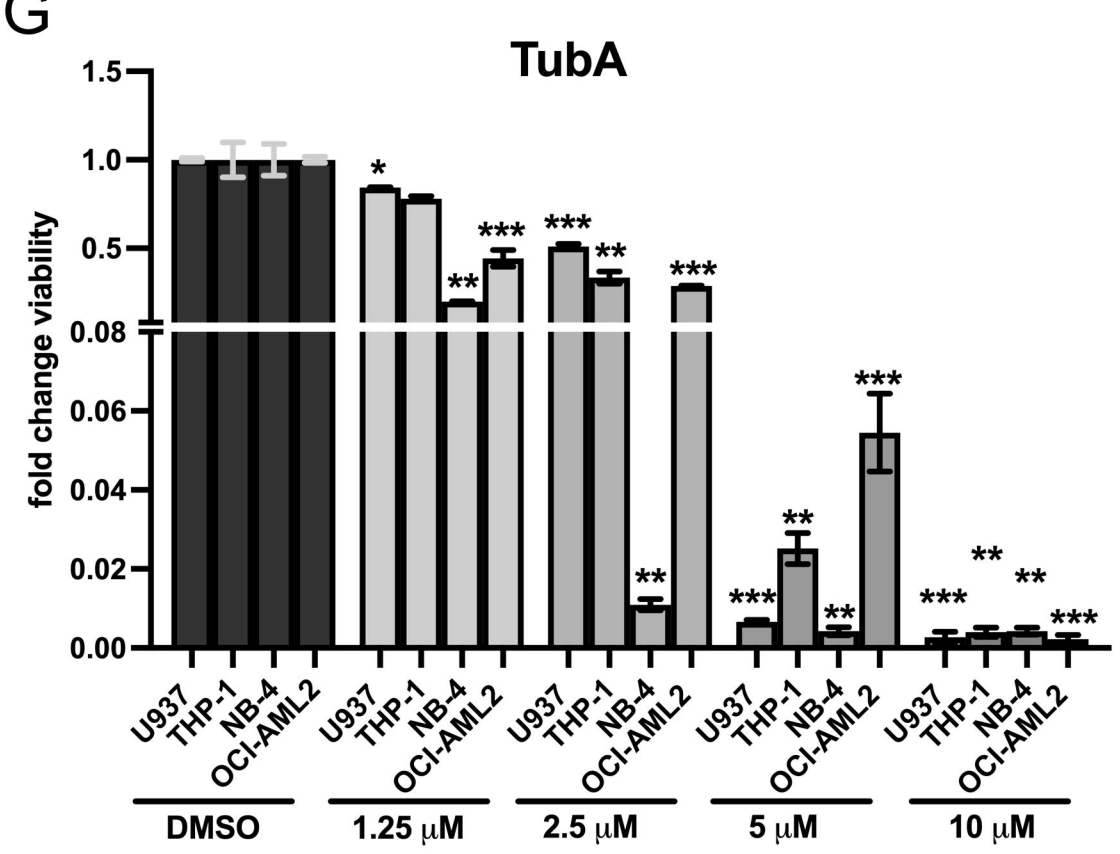

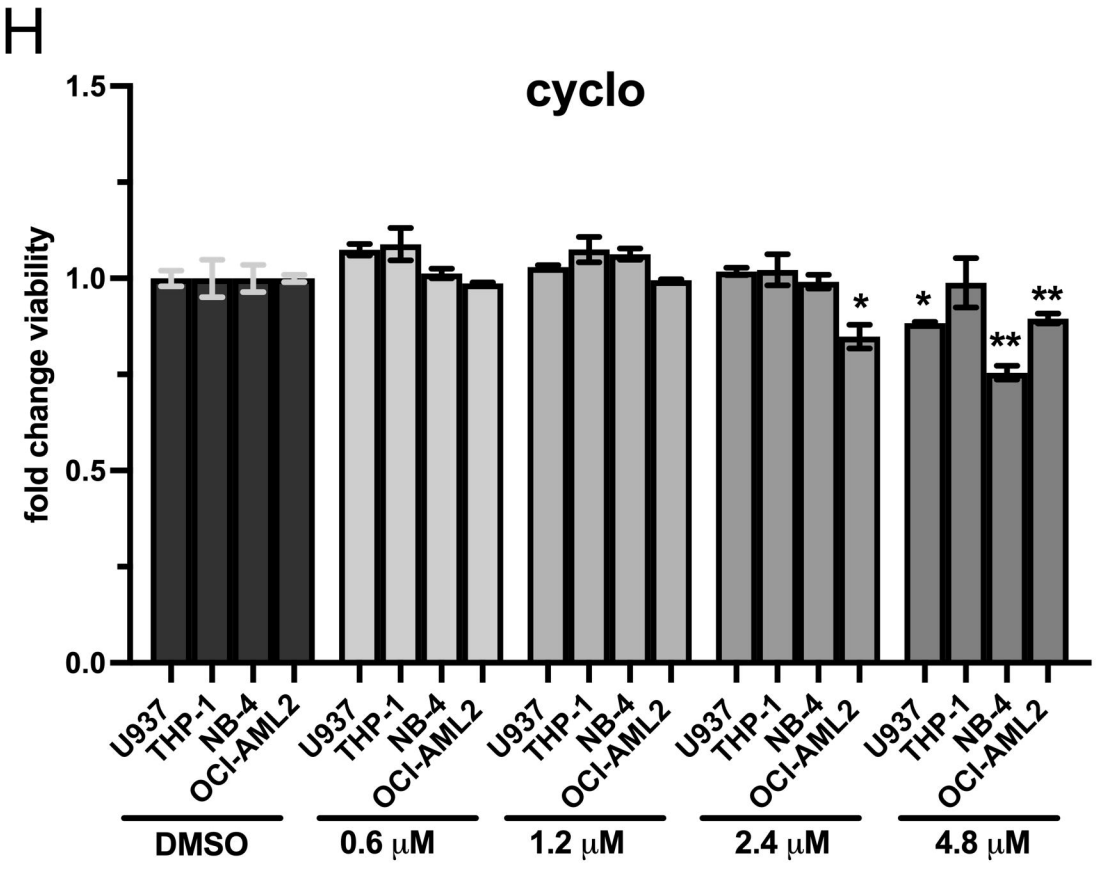

Figure 5

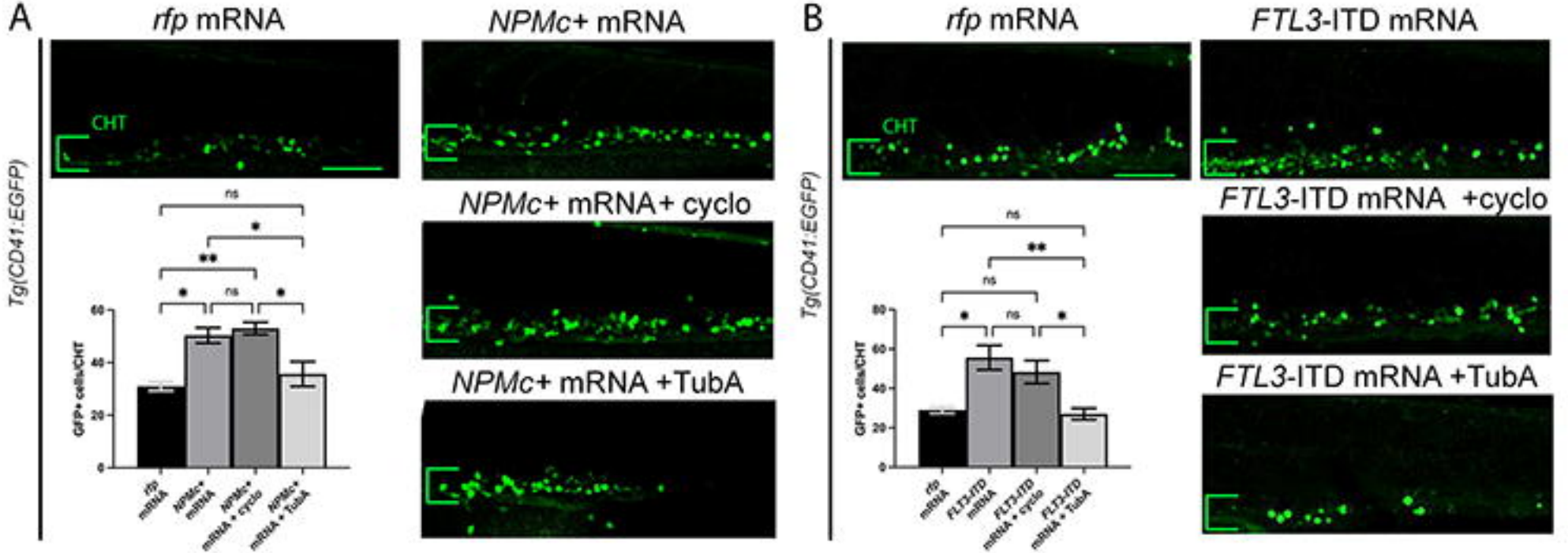
A
rfp mRNA
NPMc+ mRNA
NPMc+ mRNA+ cyclo
NPMc+ mRNA +TubA
CHT
Tg(CD41:EGFP)
GFP+ cells/CHT
ns
*
**
rfp mRNA
NPMc+ mRNA
NPMc+ mRNA + cyclo
NPMc+ mRNA + TubA
B
rfp mRNA
FTL3-ITD mRNA
FTL3-ITD mRNA +cyclo
FTL3-ITD mRNA +TubA
FLT3-ITD mRNA
FLT3-ITD mRNA + cyclo
FLT3-ITD mRNA + TubA

Figure 6

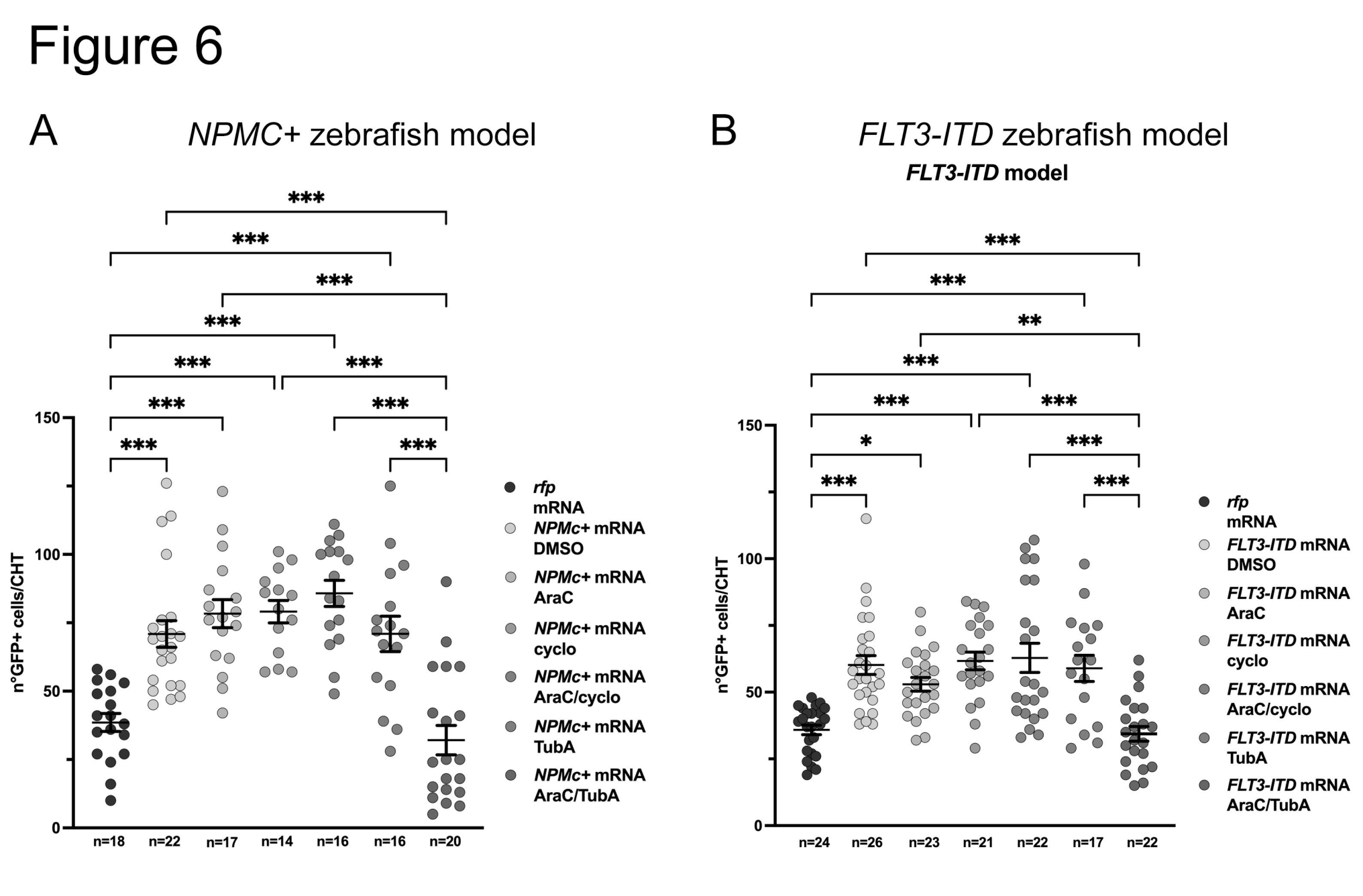
A
NPMC+ zebrafish model
n°GFP+ cells/CHT
150
100
50
0
n=18
n=22
n=17
n=14
n=16
n=16
n=20
***
rfp mRNA
NPMc+ mRNA DMSO
NPMc+ mRNA AraC
NPMc+ mRNA cyclo
NPMc+ mRNA AraC/cyclo
NPMc+ mRNA TubA
NPMc+ mRNA AraC/TubA
B
FLT3-ITD zebrafish model
FLT3-ITD model
n°GFP+ cells/CHT
150
100
50
0
n=24
n=26
n=23
n=21
n=22
n=17
n=22
***
**
*
rfp mRNA
FLT3-ITD mRNA DMSO
FLT3-ITD mRNA AraC
FLT3-ITD mRNA cyclo
FLT3-ITD mRNA AraC/cyclo
FLT3-ITD mRNA TubA
FLT3-ITD mRNA AraC/TubA

TITLE: Targeting *Hedgehog* and *HDAC6* in acute myeloid leukemia using *in vitro* and zebrafish models

RUNNING TITLE: Hedgehog and HDAC6 inhibition in AML

AUTHORS: Alex Pezzotta[1], Ilaria Gentile[1], Donatella Genovese[2], Maria Grazia Totaro[3], Cristina Battaglia[1], Anskar Leung Yu Hung[4], Monica Fumagalli[5], Matteo Parma[5], Gianni Cazzaniga[6], Grazia Fazio[6], Myriam Alcalay[2,7], Anna Marozzi[1], Anna Pistocchi[1]

AFFILIATIONS:

1 Dipartimento di Biotecnologie Mediche e Medicina Traslazionale, Università degli Studi di Milano, Milano, Italy

2 Dipartimento di Oncologia Sperimentale, Istituto Europeo di Oncologia IRCCS, Milano, Italy

3 IFOM (FIRC institute of molecular oncology), Milano, Italy.

4 Department of Medicine, LSK Faculty of Medicine, Hong Kong, China

5 Hospital San Gerardo, Clinica Ematologica e Centro Trapianti di Midollo Osseo, Monza, Italy

6 Centro Ricerca Tettamanti, Clinica Pediatrica Università di Milano-Bicocca, Centro Maria Letizia Verga, Monza, Italy

7 Dipartimento di Oncologia ed Emato-Oncologia, Università degli Studi di Milano, Milano, Italy

CORRESPONDING AUTHOR:

Anna Pistocchi, Department of Medical Biotechnology and Translational Medicine

University of Milan, LITA - Via Fratelli Cervi, 93 - 20090 Segrate (MI) Italy

tel: +39 0250330442

Email: anna.pistocchi@unimi.it

SUPPLEMENTARY MATERIALS

Patients

Patients were previously characterized for specific molecular aberrancies, such as mutations for *NPM1* and *FLT3-ITD*, in addition to translocations t(9;22), t(8;21) and inv(16), in accordance to

specific clinical protocol requirements. Patients enrolled belong to different French–American–British (FAB) classification systems (FABs), excluding M3, therefore all patients were negative for translocation t(15;17). Bone marrow of healthy individuals were collected as controls for gene expression assays, upon appropriate Informed Consent ASG-MA-052A approved on May 8th 2012 by Azienda San Gerardo (ASG). Clinical features have been reported in our previous study[1]. Human material and derived data has been used in accordance with the Declaration of Helsinki.

Animals

Zebrafish embryos were raised and maintained under standard condition according to the national guidelines (Italian decree March 4, 2014, n. 26). Embryos from AB and *Tg(CD41:GFP)* strains [2] were collected by natural spawning, staged according to the reference guidelines [3] and raised at 28° C in E3 medium fish water (instant ocean, 0.1% methylene blue in petri dishes). From the stage of 24 hours post-fertilization (hpf) 0.003% 1-phenyl-2-thiourea (PTU, Sigma-Aldrich, Saint Louis, MO) was added to prevent pigmentation. Before manipulations, embryos were dechorionated, and anesthetized with 0.016% tricaine (ethyl 3-aminobenzoate methanesulfonate salt; Sigma-Aldrich).

Reverse transcription and real-time quantitative techniques (RT-qPCR) in human samples, cell lines and zebrafish

Total RNA was isolated from human samples, cell lines and whole zebrafish embryos using TRIZOL reagents (Life Technologies, Carlsbad, CA, USA) following the manufacturer's instructions. After DNaseI RNase-free (Roche Diagnostics, Basel, Switzerland) treatment to avoid possible genomic contamination, 1 μg of RNA was used as template for the synthesis of cDNA using the "GoScript™" Reverse Transcription system (Promega, Madison, Wisconsin USA). Quantitative real-time polymerase reactions (Real-time qPCR) were carried out in a total volume of 10 μl containing iQ SYBR Green Super Mix (Promega, Madison, WI, USA) using the 384-well QuantStudio™ 5 Real-Time PCR System (Applied Biosystem, Whaltam, MA, USA). Genes of interest were normalized to *rpl8* and *beta-actin* for zebrafish and to *GAPDH* and *GUS* for human AML samples and cell lines.

Primers used for qPCR analyses in human and zebrafish samples are listed in the **Supplementary Table S2**.

Fluorescence activated cell sorting (FACS) analyses

Embryos dissociation was obtained as described [4]. Fluorescence-activated cell sorting (FACS) analyses were performed as described in the Supplementary Materials. FACS analysis were performed on *Tg(CD41:GFP)* zebrafish embryos at 2.5 dpf as previously described [1]. Flow cytometry acquisitions were performed using Attune NxT (Thermofisher). Analyses were done with Kaluza software from Beckman Coulter. Embryos of the wild-type AB strain were used to set the gate and exclude auto-fluorescence of cells. The gate for GFP low/high cells was set on control *Tg(CD41:GFP)* embryos to distinguish a GFPlow population representing around 0.2% of total cells, as previously reported [1], and applied to all categories analyzed.

Immunofluorescence staining and image processing

PTU-treated embryos belonging from the *Tg(CD41:GFP)* embryos were fixed overnight in 4% paraformaldehyde (Sigma-Aldrich) in Phosphate Buffer Saline (PBS) at 4 °C. After 2 hours in blocking solution at room temperature embryos were incubated with the primary antibodies mouse anti-GFP (1:1000, Sigma-Aldrich) and rabbit anti-3PH (1:200, Sigma-Aldrich) and secondary antibody was Alexa Fluor 488-conjugated goat anti-mouse IgG 1:400 (A11008, Invitrogen Life Technologies, Carlsbad, CA, USA) and Alexa 546-conjugated goat anti-rabbit IgG 1:400 (A11001 and A11010, InvitrogenLife Technologies). Staining was evaluated detecting GFP and/or 3PH fluorescence through confocal analyses (A1 HD25/A1R HD25 instrument, Nikon FRET-FLIM) provided by the UniTech nolimits NOxsz<LIMITS service (UNIMI department). For the count of proliferating hematopoietic stem and progenitor cells (HSPCs), confocal images have been analyzed by ImageJ software. We selected the caudal hematopoietic tissue as region of interest (ROI) and set

a common threshold for all the experimental group. The number of proliferating cells was obtained by the ratio HSPCs positive for the 3PH staining/total number of HSPCs.

Chemical treatments in AML cell lines

OCI-AML2, U937, THP-1, and NB4 cell lines were originally obtained from ATCC/DSMZ repositories and since stored at the internal cell line bank at the Department of Experimental Oncology, IEO. Cell lines undergo regular authentication and mycoplasma testing. Cells were seeded at 10,000 cells/well in 96-well plates in 100 µl of growth medium and allowed to grow for 72 h prior to treatment commencement. Cyclopamine (cyclo) and TubastatinA (TubA) were dissolved in DMSO, diluted in the appropriate culture medium and added into plates, as indicated. The concentration range of both compounds has been determined based on published data and ranged between 0.6 µM and 4.8 µM for cyclo [5] and 1.25 µM to 10 µM for TubA [6].72 hours later, CellTiter-Glo assay (Promega) was performed as indicated in the manufacturer's instructions and read on GloMax (Promega) plate reader. Cells treated with DMSO (0.2% in appropriate medium) were used as a control.

Western blotting analyses

For zebrafish, at least 30 hpf anesthetized zebrafish embryos were used for protein extraction after chemical removal of the yolk with deyolking solution to avoid yolk protein contamination. Proteins were collected and prepared using 2 µl/embryo of RIPA buffer (50 mM Tris-HCl pH 7.4, 1% NP-40, 150 mM NaCl, 0.25% sodium deoxycholate, 1mM EDTA, 1mM PMSF, protease inhibitors Roche). The lysate concentration was determined according to the manufacturer's instructions of the Quantum Micro BCA protein assay kit (Euroclone, Pero, MI, Italy). Electrophoresis analyses were done loading 40 µg of proteins onto a 7.5% polyacrylamide gels. After the transfer, PVDF membranes were treated with blocking solution at room temperature for 1 hour prior to incubation with the primary antibodies: Vinculin (anti mouse 1:6000, Sigma-Aldrich), total α-tubulin (anti rabbit 1:5000; Sigma-Aldrich)

and ac-alpha-Tubulin (anti mouse 1:1000; Sigma-Aldrich). After incubation with the HRP-conjugated secondary antibodies for 1h at room temperature (mouse Santa Cruz Biotechnology, Dallas, TX, USA, rabbit Thermofisher, Waltham, MS, USA), the protein bands were detected using ECL detection systems (Cyangen, Bologna, Italy). Imaging acquisition has been done with the Alliance MINI HD9 AUTO Western Blot Imaging System (UVItec Limited, Cambridge, UK) and analyzed with the related software. Images were processed using the Adobe Photoshop (Microsoft Windows; macOS) software.

SUPPLEMENTARY FIGURE AND LEGENDS

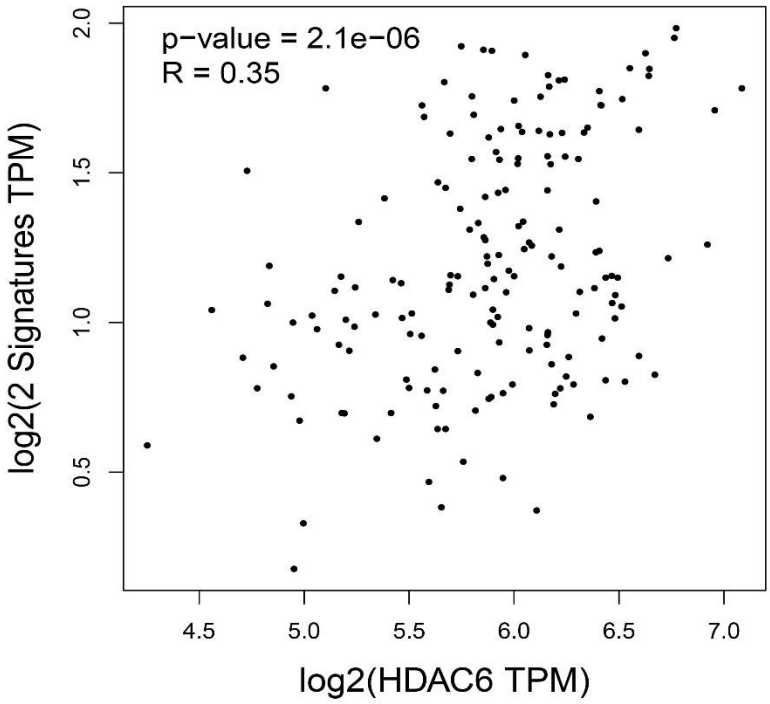

Suppl. Fig. 1 GEPIA2: *Hh*, *HDAC6* and *MDRs* in LALM dataset. Correlation analyses between the expression levels of *HDAC6* (HDAC6 TPM) and *GLI1* and *PTCH1* (2 signature TPM). Spearman correlation. ***p<0.001. LALM: Acute Myeloid Leukemia; TPM: transcript per millions.

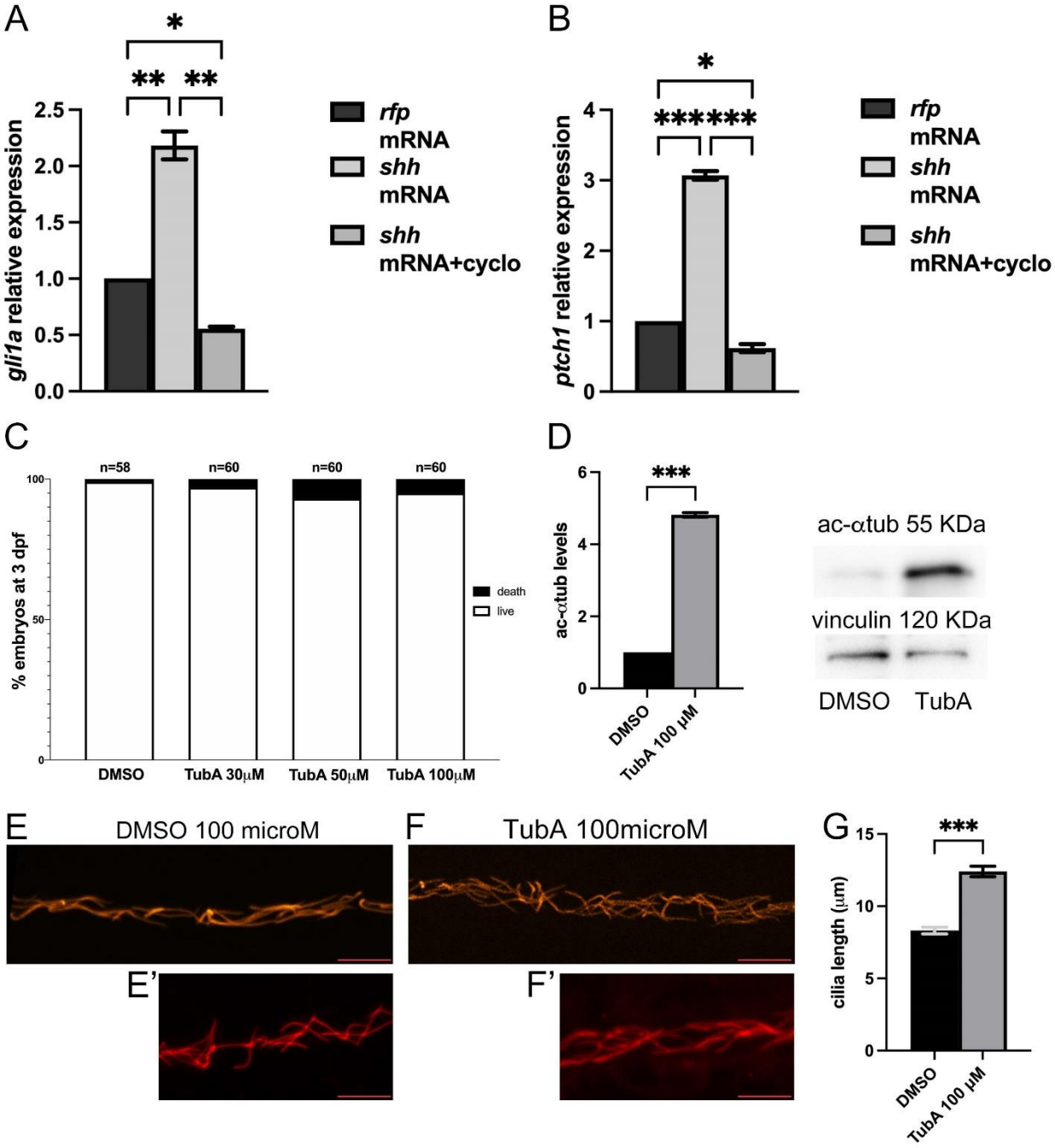

Suppl. Fig. 2 Validation of the efficacy of *Hh* and HDAC6 inhibition in zebrafish embryos trough cyclo and TubA administration respectively. A-B) Real-time qPCR analyses of the *Hh* target genes (**A**) *gli1*a, (**B**) *ptch1* in controls (*rfp*-mRNA), *Hh* overexpressed (*shh*-mRNA injected), and cyclo treated embryos. **C-G)** TubA treatments (**C**) Survival/lethality of embryos treated with different doses of TubA, **(D)** Western blotting analyses for the HDAC6 target acetylated-α tubulin **(**ac-α tubulin) in DMSO and TubA treated embryos. **(E-F')** Confocal images of the pronephric region of 2.5 dpf embryos stained for ac-α tubulin in embryos treated with DMSO or TubA and (**G)** cilia length measurement. ONE-way ANOVA with Tukey post hoc correction (**A**-**B**). Unpaired T-test with

Welch correction (**D**,**G**). ***p<0.001; **p<0.01; *p<0.05; ns not significant. Results are presented as mean ± SEM. Scale bar indicates 100 µm. cyclo: cyclopamine; TubA: TubastatinA.

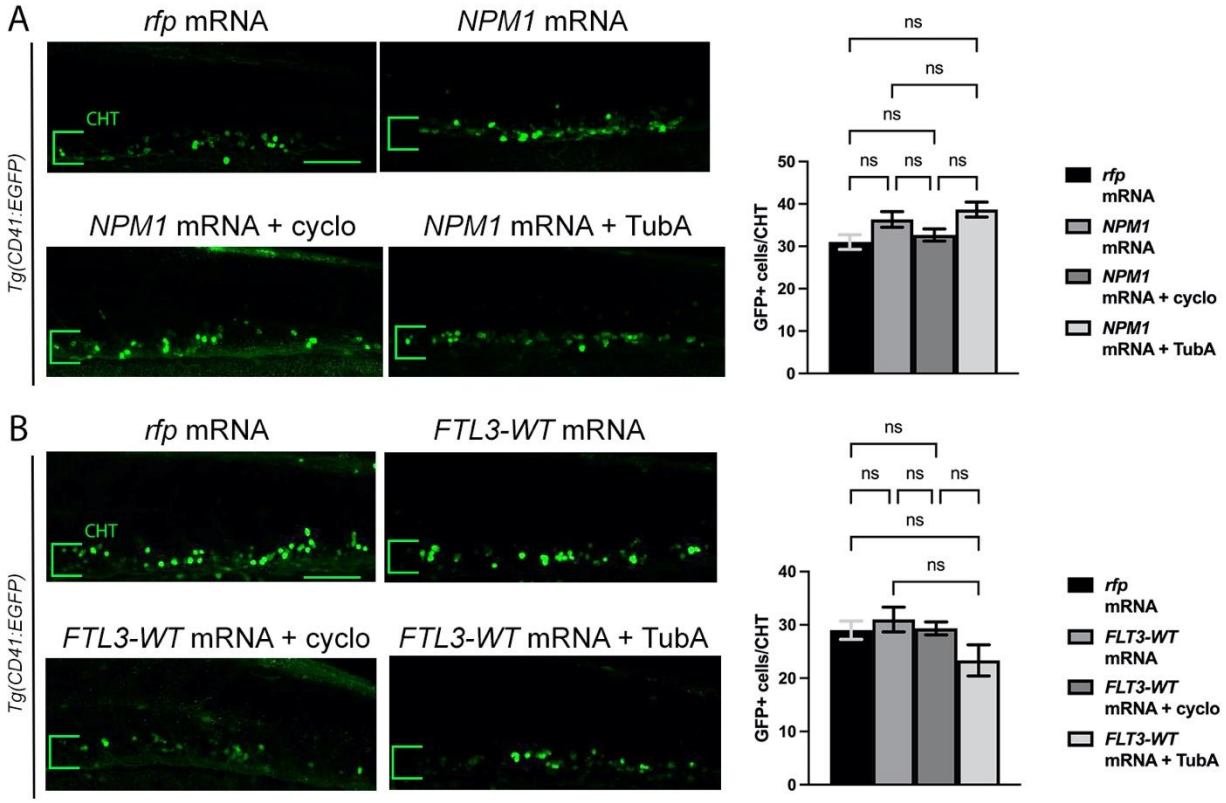

Suppl. Fig. 3: *Hh* and HDAC6 inhibition in the *NPM1* and *FLT3* zebrafish embryos. A-B) Confocal images of the caudal hematopoietic tissue (CHT) of the *Tg(CD41:GFP)* zebrafish embryos at 2.5 dpf (N=3), with the forced expression of the human (**A**) *NPM1* or (**B**) *FLT3* mRNA treated with cyclo or TubA. Histograms represents the number of HSPC-GFP positive cells. cyclo: cyclopamine; TubA: TubastatinA. ONE-way ANOVA with Tukey post hoc correction. ***p<0.001; **p<0.01; *p<0.05; ns not significant. Results are presented as mean ± SEM. Scale bar indicates 100 µm.

Supplementary Table S1 Clinical Features of patients' cohort

Supplementary Table S1. Clinical Features of patients' cohort.

	AGE AT ONSET	KARYOTYPE	FAB CLASSIFICATION	NPM	FLT3-ITD	CEBPA	ckit	JAK2	t(9;22)	t(8;21)	inv(16)
1	47	46,XX,t(10;11)(p11;p15)[20]	M0	NEG	NEG	nk	nk	nk	NEG	NEG	NEG
2	49	46,XY[20]	M0/M1	NEG	NEG	NEG	nk	nk	NEG	NEG	NEG
3	48	46,XX[20]	M1	NEG	NEG	NEG	nk	nk	NEG	NEG	NEG
4	70	45,X,-Y,t(8;21)(q22;q22)[5]/46,XY[5]	M2	NEG	NEG	nk	NEG	nk	NEG	POS	NEG
5	72	47,XY,+mar[10]/46,XY[10]	M2	NEG	NEG	nk	nk	nk	NEG	NEG	NEG
6	47	45-46,XY,del(3)(q?22q?26),der(4)t(?1;4)(p36;p16),add(11)(p14),-12,del(12)(p11),add(21)(q22)[cp13]/46,XY[7]	nk	NEG	NEG	nk	nk	nk	nk	NEG	NEG
7	37	43,XY,?del(2)(q?33),-4,der(6)t(?4;6)(q?22;q21),i(11)(q10),-17,-18[19]/46,XY[2]	M1	NEG	NEG	nk	nk	nk	NEG	nk	nk
8	59	46,XY[20]		NEG	POS	nk	nk	nk	NEG	NEG	NEG
9	33	46,XY[15]	M1	NEG	POS	nk	nk	nk	NEG	NEG	NEG
10	30	46,XY[20]	M5	NEG	POS	nk	nk	nk	nk	NEG	NEG
11	20	46,XY,t(8;21)(q22;q22)[21]/46,XY[1]	nk	NEG	POS	nk	NEG	nk	nk	POS	NEG
12	58	46,XY,inv(16)(p13q22)[20]	M4	NEG	POS	nk	nk	nk	nk	NEG	POS
13	76	nk	M5	NEG	POS	nk	POS ex17	nk	nk	NEG	NEG
14	78	46,XX[27]	M4	NEG	POS	nk	nk	nk	nk	NEG	NEG
15	53	46,XY[22]	M4	NEG	POS	nk	nk	nk	nk	NEG	NEG
16	64	46,XX[20]	M5	NEG	POS	nk	nk	nk	nk	NEG	NEG
17	75	46,XY[26]	M4	NEG	POS	nk	nk	nk	nk	NEG	NEG
18	39	46,XY[20]	M1	POS (A)	NEG	nk	nk	nk	NEG	NEG	NEG
19	47	46,XX[20]	M5	POS (A)	NEG	nk	nk	NEG	NEG	NEG	NEG
20	58	46,XY/47,XY,+8[7/10]	nk	POS (QM)	NEG	nk	nk	nk	nk	NEG	NEG
21	50	46,XX[20]	M4	POS (A)	NEG	nk	nk	nk	nk	NEG	NEG
22	77	46,XY[20]	nk	POS (A)	NEG	nk	nk	nk	nk	NEG	NEG
23	54	46,XX,t(9;22)(q34;q11)[14]/46,XX[6]	M4	POS (A)	NEG	nk	nk	NEG	POS	NEG	NEG
24	60	46,XX[6]	nk	POS	NEG	nk	nk	nk	nk	NEG	NEG
25	62	46,XX[25]	M5	POS (A)	NEG ITD/POS D835/D836	nk	nk	nk	nk	NEG	NEG
26	58	46,XX[20]	nk	POS (A)	NEG	nk	nk	nk	nk	NEG	NEG
27	48	46,XX[20]	M4	POS (A)	POS	nk	nk	nk	NEG	NEG	NEG
28	51	46,XX[20]	M5	POS (A)	POS	nk	nk	nk	NEG	NEG	NEG
29	68	46,XX[20]	M4	POS (A)	POS ITD/POS D835/D836	nk	nk	nk	NEG	NEG	NEG
30	46	46,XY[20]	M2	POS	POS	nk	nk	nk	NEG	NEG	NEG
31	39	46,XX[22]	M1	POS (A)	POS	nk	nk	nk	nk	NEG	NEG
32	58	46,XY	M5	POS (A)	POS	nk	nk	nk	nk	NEG	NEG
33	35	46,XY,?r(18)(?)[16]/47,idem,+8[3]/46,XY[1]	nk	POS (B)	POS	nk	nk	nk	nk	NEG	NEG
34	58	46,XY[24]	M1	POS (A)	POS	nk	nk	nk	nk	NEG	NEG
35	70	46,XY[20]	M5	POS (A)	POS	nk	nk	nk	nk	NEG	NEG
36	12	46,XY[24]	nk	POS (A)	POS	nk	nk	nk	NEG	NEG	NEG

Supplementary Table S2 Primers list

Primer	Sequence (5' – 3')
GLI1 HS f FF	AGT ACA TGC TGG TGG TTC AC
GLI1 HS RR	AGG TTT TCGA GGC GTGA GTA
PTCH1 HS FF	AGG TGC TAA TGT CCT GAC CA
PTCH1 HS RR	CCA CTG CCT GTT GTA CAT GT
HDAC6 HS FF	CTG GCT TGG TGT TGG ATG AG
HDAC6 HS RR	CTC CTG GAT CAG TTG CTC C
ABCC1 HS FF	ATG CAG AGG AGA ACG GGG T
ABCC1 HS RR	CCT GCA CTG TCC GTC ACC
ASXL1 HS FF	TCA CGC TCA AGA AGG ATG CC
ASXL1 HS RR	CCC ACA GCT CTC CAC ATC AG
GAPDH HS FF	CAA CGA CCA CTT TGT CAA GC
GAPDH HS RR	CTG TGA GGA GGG GAG ATT CA

GUS HS FF	CGC CCT GCC TAT CTG TAT TC
GUS HS RR	TCC CCA CAG GGA GTG TGT AG
gli1a zf FF	ACA CAC TGA AAT CTC AGC CG
gli1a zf RR	GTC ATT ATT ATT GGC GCT CC
ptch1 zf FF	GGA GAA ACT CTG GGT AGA AG
ptch1 zf RR	CCT GAC GAG GCG TCT GTA TC
asxl1 zf FF	GTC GCT CTT CAC AGT CAG GG
asxl1 zf RR	CGT GTT CAC CGT TGA CCT TG
abcc1 zf FF	CGT GAG GAG ACA CAA CTG AG
abcc1 zf RR	AGT TGC AGT ACA CAG CCC TG
hdac6 zf FF	GCA GAG ACA CCT AAC CGT TC
hdac6 zf RR	CCA GCA GCC TCC AGA ACT AA
cmyb zf FF	GAC ACA AAG CTG CCC AGT TC
cmyb zf RR	GCT CTT CCG TCT TCC CAC AA
rpl8 zf FF	CTC CGT CTT CAA AGC CAA TG
rpl8 zf RR	TCC TTC ACG ATC CCC TTG AT
beta-actin zf FF	GCA CGA GAG ATC TTC ACT CC
beta-actin zf RR	GCA GCG ATT TCC TCA TCC AT

REFERENCES

1. Mazzola M, Deflorian G, Pezzotta A, et al. NIPBL: a new player in myeloid cells differentiation. *Haematol. pii haematol.2018.200899. doi 10.3324/haematol.2018.200899. [Epub ahead print]*. 2019;

2. Lin HF, Traver D, Zhu H, et al. Analysis of thrombocyte development in CD41-GFP transgenic zebrafish. *Blood*. 2005;106(12):3803–3810.

3. Kimmel CB, Ballard WW, Kimmel SR, Ullmann B, Schilling TF. Stages of embryonic development of the zebrafish. *Dev. Dyn.* 1995;203(3):253–310.

4. Bresciani E, Broadbridge E LP. An efficient dissociation protocol for generation of single cell suspension from zebrafish embryos and larvae. *MethodsX*. 2018;10(5):1287–1290.

5. Kawahara T, Kawaguchi-Ihara N, Okuhashi Y, et al. Cyclopamine and quercetin suppress the growth of leukemia and lymphoma cells. *Anticancer Res.* 2009;

6. Inks ES, Josey BJ, Jesinkey SR, Chou CJ. A novel class of small molecule inhibitors of HDAC6. *ACS Chem. Biol.* 2012;

DISSEMINATION OF RESULTS

We have disseminated the results of this project participating at national conferences to promote their divulgation to the scientific community. For instance, the work has been discussed in an oral session at the Zebrafish Italian Meeting that will take place in Naples on 9-11th February 2022. On this occasion I had the opportunity to meet with experts obtaining new stimuli for future studies related to my PhD project.

According to the European Code of Conduct for Research Integrity, we have submitted our work, to a peer-review open access journal in the hematological field. We aim to share our results with experts in the field of acute myeloid leukemia, and the whole scientific community.

short summary of the work/breve riassunto del lavoro

English version: When altered, different molecular mechanisms drive the development of acute myeloid leukemia (AML). As the mechanisms governing hematopoiesis are conserved, in our research we used AML patients' samples, the zebrafish model system and human leukemic cell lines to gain insight into the role of the hedgehog (*Hh*) signaling pathway and the histone deacetylase HDAC6 in leukemia. We found that they were overexpressed and positively correlated in AML patients and in human AML cell lines. Their forced expression in the zebrafish model determines the proliferation of hematopoietic and progenitor stem cells (HSPCs), a situation that mimic the augmented number of leukemic cells in AML patients. We found that zebrafish HSPCs present, as human blood cells, the primary cilium, a structure that when formed, blocks cell proliferation. We demonstrated that the specific HDAC6 inhibition reduced the number of zebrafish HSPCs and AML cell viability. We speculated that HDAC6 might stabilize the PC on cell surface therefore blocking cell proliferation. We also demonstrated that HDAC6 inhibition might be used in combination with the standard chemotherapic agents, identifying the HDAC6 inhibition as an attractive strategy for the treatment of AML patients.

Italian version: Quando alterati, diversi meccanismi molecolari guidano lo sviluppo della leucemia mieloide acuta (AML). Poiché i meccanismi che regolano l'emopoiesi sono conservati, nella nostra ricerca abbiamo utilizzato campioni di pazienti affetti da AML, il sistema modello zebrafish e linee cellulari leucemiche umane per comprendere il ruolo della via di segnalazione di hedgehog (*Hh*) e dell'istone deacetilasi HDAC6 nella leucemia.

Abbiamo osservato che la loro aumentata espressione correla positivamente nei pazienti con AML e nelle linee cellulari leucemiche. In zebrafish, la loro overespressione determina la proliferazione dei progenitori e cellule staminali ematopoietiche (HSPC), una situazione che ricapitola l'aumentato numero di cellule leucemiche nei pazienti AML. Abbiamo scoperto che le HSPCs di zebrafish presentano, come quelle umane, il cilium primario, una struttura che, una volta formata, blocca la proliferazione cellulare. Abbiamo dimostrato che l'inibizione specifica di HDAC6 riduce il numero di HSPC in zebrafish e la vitalità delle cellule AML, ipotizzando che l'inibizione di HDAC6 potrebbe stabilizzare il PC sulla superficie cellulare bloccando così la proliferazione cellulare. Abbiamo anche dimostrato che l'inibizione di HDAC6 può essere utilizzata in combinazione con gli agenti chemioterapici standard. Questo consentirebbe di ridurre il dosaggio dei chemioterapici e quindi diminuire gli effetti avversi.